EVALUATION OF ASPHALT ADDITIVES FOR IMPROVED CRACKING AND RUTTING RESISTANCE OF ASPHALT PAVING MIXTURES

By

CHUANG-TSAIR SHIH

A DISSERTATION PRESENTED TO THE GRADUATE SCHOOL
OF THE UNIVERSITY OF FLORIDA IN PARTIAL FULFILLMENT
OF THE REQUIREMENTS FOR THE DEGREE OF
DOCTOR OF PHILOSOPHY

UNIVERSITY OF FLORIDA

1996

ACKNOWLEDGMENTS

It is very fortunate for the author to have had Dr. Mang Tia as advisor and chairman of the supervisory committee. Without his support, guidance and continuous encouragement, this work would not have been possible. Special thanks go to Dr. Byron E. Ruth, who has kindly served as the cochairman of his supervisory committee, for his technical advice and humor. Sincere thanks are given to Dr. Reynaldo Roque for his detailed advice through the challenging stages of this study. Special appreciation is expressed to Dr. David Bloomquist for his patient guidance on the projects since the early stage of the study. Thanks are given to Dr. Mark C. K. Yang for serving on the author's supervisory committee and having given of his expertise and time.

Thanks are extended to the Florida Department of Transportation (FDOT) for providing financial support, and to the FDOT personnel, particularly T. Dillow, G. Lopp, G. Schiller, A. Turner and P. Upshaw. The author would like to thank E. Dobson, D. Richardson, and B. Studstill, and to all the other students and friends, Shin-Che Huang, Chui-Te Chiu, Ming-Gin Lee, Jua-Rong Chou, Dai Lu, Xiaofang Wang, Tu-Ming Leung, A. M. Agosta, W. Buttlar, T. Safer, S. Qargha and G. Jonnson for their help.

Finally, the author is deeply indebted to his parents and sisters for their love, encouragement and support throughout his studies.

TABLE OF CONTENTS

LIST OF TABLES

LIST OF FIGURES

Abstract of Dissertation Presented to the Graduate School
of the University of Florida in Partial Fulfillment of the
Requirements for Degree of Doctor of Philosophy

EVALUATION OF ASPHALT ADDITIVES FOR IMPROVED CRACKING AND RUTTING RESISTANCE OF ASPHALT PAVING MIXTURES

By

Chuang-Tsair Shih

December 1996

Chairman: Mang Tia
Cochairman: Byron E. Ruth
Major Department: Civil Engineering

A laboratory investigation was conducted to evaluate the effects of a few asphalt additives on the cracking and rutting resistance of asphalt paving mixtures that might be considered for use under Florida conditions. The five types of additives evaluated in this study include (1) gilsonite, (2) ground tire rubber (GTR), (3) styrene-butadiene rubber (SBR), (4) ethylene vinyl acetate (EVA) and (5) styrene ethylene butylene styrene (SEBS). These additives were blended with an AC-5, AC-10, AC-20 and AC-30. These modified and unmodified asphalts were subjected to the thin film oven test (TFOT) to simulate the short-term aging effect that occurs in the hot-mixing process, and followed by the California tilt oven (CTO) and SHRP pressure aging vessel (PAV) processes to

simulate the additional aging of the asphalt binders in the field. All these asphalts and asphalt blends were evaluated by various rheological and chemical tests.

The five modified asphalt blends, and unmodified AC-20 and AC-30 were also used to make Florida type S-I structural course mixtures. These mixtures were compacted by the gyratory testing machine (GTM) at different compaction levels and aged according to the SHRP proposed long term oven aging (LTOA) procedure. These aged and unaged asphalt mixtures were evaluated by resilient modulus, indirect tensile strength and indirect tensile creep tests. Asphalt residues were recovered from the broken samples and evaluated by various rheological tests.

The test results indicate that the addition of the five types of modifiers is beneficial for the improvement of rutting resistance of the pavement. The addition of GTR and SBR is beneficial to the cracking resistance of asphalt pavement materials at low temperatures. The SBR modified asphalt mixtures show better rut resistance as compared with those of GTR and SEBS modified mixtures. The GTR and SBR modified asphalt mixtures have lower resilient modulus than that of the unmodified mixtures at low temperatures.

CHAPTER 1
INTRODUCTION

1.1 Background

In recent years, increasing truck traffic has been widely recognized as a serious threat to the durability of pavements. The Federal Highway Administration reported that the truck traffic mileage has doubled in the last fifteen years [1]. Some pavement failures are often attributed to the deficiencies in the asphalt cement. Rutting, for example, can be caused by inadequate binder stiffness at high pavement service temperatures. Cracking is thought to be a low temperature problem that occurs when the binder becomes too brittle to withstand thermal or load-induced strains. One of the promising methods to improve asphalt performance at both low and high service temperatures is through using additives. Among different additives which have been tried, polymers show excellent versatility in modifying the structural and adhesive properties of asphalt. Polymer modified asphalts are being specified in several states for heavily stressed pavements which might become rutted in the summer or undergo cracking in the winter. Unfortunately the role of modifiers is not widely understood and it is very difficult to evaluate modified asphalts by using conventional binder tests. Specifications based on conventional test methods for asphalt cements have not always resulted in failure-free pavements. The Strategic Highway Research Program (SHRP) has dedicated a large portion of its resources to

develop new test methods and specifications which are to reflect the anticipated performance of the binders and mixtures on the highway. There is a need to evaluate the applicability of these SHRP performance-related tests and criteria to conventional and modified asphalt binders for use in pavements under Florida conditions.

1.2 Study Objectives

The main objectives of this research are as follow:

1. To evaluate the effects of a few asphalt additives, that might be considered for use in Florida, on the cracking and rutting resistance of asphalt paving mixtures under Florida conditions.
2. To determine the optimal combination of asphalt cements and additives for improved rutting and cracking resistance under Florida conditions.
3. To evaluate the applicability of the proposed SHRP performance-related tests and criteria for conventional and modified asphalt binders under Florida conditions.

CHAPTER 2
LITERATURE REVIEW

2.1 Distresses In Asphalt Concrete Pavements

The major types of pavement surface defects and their possible causes are summarized in Table 2.1. These types of pavement distress develop interactively with each other at different stages of a pavement's life. The short range cracking, commonly referred to as premature cracking, is usually caused by poor construction, poor mix design, unsuitable climate during construction or opening for traffic too early. Middle range cracking is initiated under the combination of traffic loading, environment and asphalt age hardening. Long range failures (such as alligator cracking at wheelpaths, and rutting due to shear failures of the subgrade) are often the result of material fatigue due to repeated traffic loading and cyclic environmental changes [1].

Once initiated, cracking progresses rapidly under traffic and allows water to ingress into the underlying layers. The presence of water reduces the shear strength of unbound materials and weakens pavement support. This, accompanied by stress concentrations at crack tips, results in further cracking and deterioration of pavement layers which may be accelerated by the cyclic action of traffic and environment. Starting from cracked areas, spalling and potholes may develop, which constitutes a major hazard to vehicular traffic. Deterioration can continue until complete disintegration of the

Table 2.1 Pavement Distress and Possible Causes in Asphalt Concrete Pavements [1]

Type of Distress	Main Possible Causes
Cracking	
- Alligator (in wheel path)	- Fatigue
- Longitudinal	- Traffic + Environment
- Transverse	- Thrmal + Aging
- Block	- Combined effects
- Tearing (in friction course)	- Layer slippage (horizontal force)
- Premature	- Poor construction / Early trafficking
Disintegration	
- Ravelling	- Age hardening
- Potholes	- Severe cracking / Ravelling
- Edgebreak	- Water / Moisture
Permanent Deformation	
- Rutting	- Poor mix / construction Heavy trucks Weakened base
- Shoving	- Poor mix / construction Horizontal force Weak support
- Depression	- Weakened support Poor mix / construction Heavy trucks + High temperature
- Roughness	- Combined distress
- Skid resistance (wear)	- Traffic volume / Aggregate type
Layer slippage	Horizontal loading / Cyclic climate

pavement surface occurs. If no maintenance action is undertaken, deterioration of the pavement can excessively reduce serviceability and incur greater costs for users and subsequent reconstruction [2].

2.2 Mechanisms of Primary Pavement Distress

2.2.1 Mechanism of Low Temperature Cracking

Low temperature cracking is associated with the volumetric contraction that occurs as a material experiences a temperature drop. A material will shorten as the temperature drops if it is unrestrained. If a material is restrained, it will develop a thermal stress that can produce cracking, as is the case for asphalt concrete in a pavement structure. Asphalt concrete can be considered to act as a viscoelastic material at warm temperatures. When the temperature drops in a high temperature range, thermal stresses can develop in asphalt concrete and will dissipate gradually through stress relaxation. However, at a low temperature, the asphalt concrete behaves more like an elastic material and the thermal stresses cannot dissipate as rapidly and cracking can occur [3].

Low temperature cracking usually starts in the transverse direction at regular intervals. Initially, these intervals are relatively large. Further cracking then occurs in the middle of each previous interval until the length of the segment reduces sufficiently so that the effect of cumulative friction can no longer induce tensile strains greater than the tensile strength of the asphalt concrete [2].

2.2.2 Mechanism of Thermal Fatigue Cracking

Daily temperature cycles that occur throughout the year produce tensile stress cycling, which can eventually fail the asphalt concrete by fatigue. Pavement temperature

range is a major factor affecting thermal fatigue. A parameter which would be used to evaluate the potential for fatigue failure is the ratio of applied stress to strength. The closer this ratio is to unity, the more rapidly damage would accumulate.

The characteristic of the asphalt cement is the most important factor with respect to thermal fatigue failure of a mix. Sugawara and Moriyoshi [4] found that fatigue failures were observed when the minimum temperature was set close to the fracture temperature. In the harder asphalt cements, fatigue-type failures were observed at a lower number of thermal cycles compared with softer asphalt cements.

2.2.3 Mechanism of Rutting

Permanent deformation or unrecoverable deformation in flexible pavements includes rutting, shoving, heaving, and depressions. Rutting and shoving are considered to be the major types of permanent deformation encountered in practice. Rutting is defined as accumulated permanent deformation of pavement layers in the wheelpaths accompanied by small upheavals to the sides which results from the repeated application of heavy wheel loads [5]. It is caused by a combination of densification (decrease in volume and hence increase in density) and shear deformation and can occur in any one or more of the pavement layers as well as in the subgrade. Hofstra and Klomp [6] explained that shear deformation rather than densification was the primary rutting mechanism. The importance of placing materials at high densities in order to minimize shear deformation was emphasized. The deformation through the asphalt-concrete layer was greatest near the loaded surface and gradually decreased at lower levels because rutting was caused by plastic flow.

Eisenmann and Hilmer [7] pointed out the following development of rutting :

1. In the initial stage of trafficking, the increase of irreversible deformation below the tires was distinctly greater than the increase in the upheaval zones so the traffic compaction had an important influence on rutting.
2. After the initial stage, the volume decrement beneath the tires was approximately equal to the volume increment in the adjacent upheaval zones. This was an indication that compaction under traffic was completed for the most part and that further rutting was caused essentially by displacement with constancy of volume. This phase was considered to be representative of the deformation behavior for the greater part of the lifetime of a pavement.

Measurements at the AASHO Road Test [8] indicated that the surface rut depth reached a limiting value for asphalt-concrete thicknesses of approximately 10 inches. Thicker layers did not exhibit additional rutting. These results strongly suggest that most pavement rutting is confined to the asphalt-concrete layer if there are reasonably stiff supporting materials.

2.3 Factors Contributing to Pavement Distress

2.3.1 Factors Affecting Low Temperature Cracking and Thermal Fatigue Cracking

Factors that influence low temperature and thermal fatigue cracking in pavements can be categorized as material, environment and pavement structure. The degree of the cracking is a function of all variables as well as the interrelationship between these factors.

2.3.1.1 Material

It is believed that the consistency (i.e. viscosity) and the temperature susceptibility of an asphalt cement at low temperatures are the most important factors affecting low temperature cracking. An asphalt cement of lower viscosity would produce a lower rate of increase in stiffness with decreasing temperature and would have a lower potential for low temperature cracking [9]. Changes in asphalt cement content within a reasonable range about the optimum do not have a significant influence on low temperature cracking performance of the mix.

In general, aggregates that have high abrasion resistance, low freeze-thaw loss and low absorption show a little variation in low temperature strengths. Absorptive aggregates reduce low temperature strength because the asphalt cement remaining in the mixture for bonding is less than it would be in a mixture with non-absorptive aggregates. The gradation of the aggregates has little influence on the low temperature strength even though the mix is designed to provide reasonable rutting resistance. The degree of compaction in terms of air voids content is not a significant factor to influence low temperature cracking resistance of the mix.

2.3.1.2 Environment

When the pavement temperature is low, there is a higher potential for thermal cracking. The pavement surface temperature is related to the ambient air temperature, solar radiation and the wind speed. The low-temperature cracks mostly occured when the temperature decreases to a level below the glass transition temperature of the asphalt binder and is maintained at this level for a period of time. The greater the rate of cooling,

the greater the tendency for thermal cracking. Evidence indicates that pavements may crack in the fall or spring when the pavement structure is subjected to the greatest temperature differential between day and night. When the pavement becomes older, the chance for occurrence of thermal cracking is greater due to the increase in stiffness of the asphalt cement with age. However, the aging characteristics of the mix can be influenced by the air void content.

2.3.1.3 Pavement Structure

Field evidence shows that thermal cracks are more closely spaced for narrow pavements compared to wider pavements. As the pavement ages and the secondary and tertiary cracks develop, the differences in crack spacing are not apparent. Field data indicate that, in general, the thicker the asphalt concrete layer, the lower the incidence of thermal cracking. The use of a prime coat on an untreated aggregate base course layer apparently reduces the occurrence of low temperature cracking because the asphalt concrete layer is bonded to an underlying granular base which has a lower coefficient of thermal contraction. The percentage of aggregates finer than the No.200 sieve for the base course gradation may have a minor influence on low temperature cracking. The frequency of low temperature cracking is usually greater for pavements on sandy subgrades as compared with those on cohesive soils [3].

2.3.2 Factors Affecting Rutting

Factors that influence rutting (the permanent deformation) in pavements can be categorized as aggregate, binder, mixture and test/field condition. The degree of rutting developed is dependent upon the interactive effects of these variables with each other.

2.3.2.1 Aggregate

Available evidence indicate that a dense-graded gradation is desirable to mitigate the effects of rutting owing to fewer voids and more contact points between particles compared with open or gap-graded mixtures after proper compaction. Brown and Pell [10] concluded that gap-graded mixture exhibited more deformation than a continuously-graded mixture because of less aggregate interlock in the gap-graded mixture. Furthermore, from the aggregate interlock point of view, gap-graded mixtures may be even more susceptible to rutting at higher temperatures.

The surface texture and shape of the aggregate also plays an extremely important role on rutting resistance. A rough surface texture is required for the selection of aggregates in mix, especially in thicker asphalt-bound layers and hotter climates. Uge and van de Loo [11] reported that mixtures made from angular aggregates (obtained by crushing) deformed to a minor extent and were more stable than mixtures having the same composition and grading but made from rounded aggregates (river gravel).

With increased tire pressures, axle loads, and load repetitions, there has been an increase of interest to use large-stone mixtures. Davis [12] has reported that some asphalt pavements constructed with soft asphalts, high volume concentrations of aggregates, low air-void contents, and large maximum aggregate size (1½ in. or larger) exhibited good rutting resistance. Besides, the use of larger maximum aggregate size (about two-thirds of layer thickness) would be beneficial in reducing the rutting propensity of mixtures subjected to high tire pressures.

2.3.2.2 Binder

Mahboub and Little [13] reported that less viscous asphalts made the mixture less stiff and therefore more susceptible to irrecoverable deformations (i.e., rutting based on the uniaxial creep testing). Monismith, Epps, and Finn [14] made similar observations and recommended harder (more viscous) asphalt cements in thicker pavements and hotter climates. Several researchers have tried to improve rutting performance by using modifiers (polymers, microfillers, etc.) to increase the viscosity of the asphalt binder at high temperatures without the negative effect at low temperatures. The test results indicated the use of modifiers did improve the resistance to permanent deformation at high temperatures [15].

2.3.2.3 Mixture

The Marshall or Hveem method is generally used as a preliminary design tool to determine an adequate asphalt content. Monismith, Epps, and Finn [14] recommended that the mixture have an asphalt content such that the air void content would be approximately 4 percent. However, an absolute minimum of 3 percent air voids is to be used to prevent problems of instability and permanent deformation. These criteria must necessarily be associated with mixtures of "adequate" stability resulting from the use of high quality aggregates.

Mahboub and Little [13] indicated that higher asphalt contents producing lower air voids increased the rutting potential. As a result, the increase in asphalt content is equivalent to the introduction of lubricants between aggregate particles. This

phenomenon results in the mixture with a higher asphalt content to be more susceptible to permanent deformation.

Cooper, Brown, and Pooley [16] explained that good resistance to permanent deformation requires low voids in the mineral aggregate (VMA) and that the desirable grading for minimum VMA can be determined using dry aggregate tests. However, the lowest theoretical VMA could be undesirable as it may not allow sufficient voids in the aggregate for enough binder to ensure satisfactory compaction without the mixture becoming overfilled. In the field, a low air void content is generally achieved with higher compactive energy.

The degree of compaction is used as one of the primary quality parameters of the placed mixture. The compaction is much more crucial as the design has a low asphalt content and intends to deliver a high rutting resistance. The well-designed, well-produced mixture performs better (better durability and mechanical properties) when it is well-compacted [17].

Compaction is also a critical factor in preparing specimens for laboratory evaluation. The purpose of the laboratory compaction process is to simulate, as closely as possible, the actual compaction that is produced in the field. The AAMAS study [18] used five different compaction devices to fabricate laboratory specimens to compare with field cores on properties. The investigators ranked compaction devices in terms of their abilities to consistently simulate the engineering properties of field cores as follows:

1. Texas gyratory-shear compactor,

2. California kneading compactor and mobile steel wheel simulator,

3. Arizona vibratory/kneading compactor, and

4. Marshall hammer.

Field densities from in-service pavements, under traffic for several years, were consistently higher than laboratory densities of freshly prepared mixtures. Therefore, it is very important that the laboratory compaction method and compaction effort must produce specimens representative of pavements after conditioning by traffic loading. Studies [15,19] found that the kneading compaction produces specimens with essentially the same characteristics as traffic compacted specimens.

2.3.2.4 Test/Field Conditions

Temperature has been found to have a significant effect on rutting, especially in hot summers [17]. Researchers have recognized the need to conduct laboratory tests at temperature within the high temperature range of those encountered in the field. Bonnot [20] selected a test temperature of 60°C for wearing-course asphalt concrete and 50°C for base courses. Similarly, Mahboub and Little [13] conservatively selected the hottest pavement profile to represent critical conditions. Other assumptions about the accumulation of permanent deformation in Texas pavements included the following:

1. Permanent deformation occurs daily over the time interval from 7:30 a.m. to 5:30 p.m.,
2. Permanent deformation occurs only in the period from April to October, inclusive, and
3. Permanent deformation can be ignored at temperatures below 50°F (10°C).

Normally a mixture is designed for a given intensity and distribution of traffic based on past correlations with field performance. However, the accelearated rutting can occur when the distribution of traffic changes, such as increases in the proportion of heavy trucks, even if the pavement has been originally well designed and constructed. In general, the causes of early rutting in pavements are attributed to heavier-than-expected loads (i.e., up to 80,000-pound axle loads as compared to 20,000-pound axle loads used for design), higher tire pressures and loading conditions beyond those for which the available methodology was applicable [21].

2.4 Improvement of Pavement Performance by Using Modified Binders

2.4.1 Classification of Modifiers

Pavement failures related to asphalt cements are usually caused by one of the following problems: the binder stiffness is too low to resist the permanent deformation at high temperatures; the mixture is unable to withstand moisture related debonding of binder and aggregate; or the binder becomes too brittle at low temperatures to resist cracking which is caused by some combination of thermal stresses, repeated loading, low temperature physical hardening or oxidative aging. In many circumstances, it may not be effective to change the mix design, aggregate types or other approaches in order to solve the problems in the field. Therefore, polymeric and other additives have been incorporated into asphalt binders [22]. The definition of asphalt additives from Haas et al. [23] is as follow:

> An asphalt cement additive is a material which would normally be added to and/or mixed with the asphalt before mix production, or during mix production, to

improve the properties and/or performance of the resulting binder and/or the mix, or where an aged binder is involved, as in recycling, to improve or restore the original properties of the aged binder [23, p.21].

Most of the known asphalt additives available in today's market have been categorized by generic name as listed in Table 2.2 [24]. However, the purpose of modification is to have a set of properties making it possible to define a composite "ideal" binder for the manufacture of bituminous mixes with highly improved performance. Such a binder should have a very low thermal sensitivity throughout the pavement service temperature range, but a rather high sensitivity outside of this range. Its resistance to permanent deformation, as well as its tensile and fatigue strength, should be high. In addition, aging resistance should be high, both during placement as well as in service. Such modifications in binder properties should lead to a modification in the properties of asphalt mixes towards a reduction in plastic deformation at high temperature, better low temperature performance and better performance in service under heavy loads and repeated loading [25].

One of the commonly used additives is the polymeric material (polymer). A polymer is a large molecule that is formed from approximately hundreds to thousands of small molecules (monomers) held together by chemical bonds along the molecules to form a linear or branched chains or a three-dimensional polymer network called polymerization. In general, polymers can be categorized into three distinct groups: thermoplastics, thermosets and elastomers (rubbers) as shown in Table 2.3 [26].

Table 2.2 Asphalt Additives Currently Being Used or Tested in Pavements [24]

Types	Examples
Polymers	Styrene Butadiene Rubber (SBR) Styrene Butadiene Styrene (SBS) Styrene Ethylene Butylene Styrene (SEBS) Ethylene Vinyl Acetate (EVA) Polypropylene Crumb Tire Rubber
Extenders	Sulfur Fillers
Mineral Fillers	Carbon Black Hydrated Lime Fly Ash Silica Fines Baghouse Fines
Natural Asphalts	Trinidad Gilsonite
Antistripping Agents	Amidoamines Imidazolines Polyamines Hydrated Lime Organo-metallics
Antioxidants	Diethyldithio Carbamates Carbon Black Hydrated Lime Phenols
Hydrocarbons	Tall Oil Aromatics Naphthenics Paraffinics/Wax Vacuum Gas Oil Petroleum/Plastic Resins Asphaltenes
Fibers	Polypropylene Polyester Glass

Table 2.3 Classification of Polymeric Materials [26]

Polymer Types	Examples
Thermoplastics	Polyethylene (PE) Polypropylene (PP) Polybutylene (PBl) Polystyrene (PS) Polyester Ethylene Vinyl Acetate (EVA) Styrene-Butadiene-Styrene (SBS) Styrene-Ethylene-Butylene-Styrene (SEBS)
Elastomers	Natural rubber Polybutadiene Polyvinyl Chloride Styrene-Butadiene Rubber (SBR)
Thermosets	Ground tire rubber Epoxy

2.4.2 Effects of Modifiers on Asphalt Mixtures

2.4.2.1 Gilsonite

Gilsonite is a pure natural hydrocarbon found in the Utah Basin of eastern Utah by Sam Gilson in 1885. It is a natural, black and hard asphalt which has a low penetration (0 to 3 at 77°F) and high R&B softening point (250°F to 350°F) [26]. Study [24] indicated that the use of Gilsonite in mixes improved properties at high termperature. However, it did not show the improvement of properties at low temperature due to the increase of the binder viscosity.

2.4.2.2 Thermoplastic

Thermoplastic is a linear or branched polymer which melts upon heating [27]. In simple terms, a thermoplastic polymer is a material that is solid, and possesses significant elasticity at room temperature and turns into a viscous liquid-like material at higher temperatures, the change being reversible [28]. Ethylene Vinyl Acetate (EVA), Styrene-Butadiene-Styrene (SBS) and Styrene-Ethylene-Butylene-Styrene (SEBS) are some of those polymers.

SBS modified binders behave as cross-linked rubbers below approximately 100°C. They add substantially to the strength of modified bitumen at high pavement temperatures. The long polybutadiene chains contribute to the flexibility of the binder at very low temperatures. The elastomeric lattice in the bitumen provides the desired properties of elasticity, plasticity and elongation. Therefore, when SBS modified binders are applied in wearing courses, these binders improve the adhesion to aggregate, the chip

retention (initial and long term), the fatigue resistance, the rutting resistance, low temperature flexibility and resistance to bleeding [29].

Collins and Mikols [30] used SBS and SEBS as modifiers to upgrade binder systems in surface dressing applications, and found that the addition of SBS and SEBS or combination of these polymers to asphalt binders can provide reduced penetration, increased ring and ball softening points, improved low temperature ductility, increased toughness and tenacity, and increased viscosity at higher service temperatures.

EVA-copolymers are compatible with bitumens, as both the vinyl acetate content and molecular mass can be altered to suit different types of bitumen. The vinyl acetate content, which can vary between a few percent and more than fifty percent, determines the mechanical properties of the binder and the compatibility of the binder with the polymer. High vinyl acetate contents give low strength properties, good compatibility, soft blends and great tenacity, and vice versa. At high vinyl acetate contents, the modified blend has properties similar to those of elastomeric polymers [29]. Verhaeghe et al. [29] reported that modification of the binder with EVA improves the compressive strength of asphalt mixes and their resistance to rutting by comparison with those of unmodified asphalt mixes. The addition of SBR and SBS also improves their resistance to plastic deformation, but to a lesser extent. However, the modification with SBR or SBS has a significant bearing on improved fatigue resistance.

2.4.2.3 Elastomer

Elastomers are lightly cross-linked polymers which can be defined as materials capable of fairly large elastic deformations [27]. However, they exhibit a marked

tendency to retain their shape when subjected to the reaction of chemical interchain linking (or chemical cross-linking) referred to as vulcanization [31]. Some examples are natural rubber and Styrene-Butadiene Rubber (SBR).

SBR was developed in Germany under the name "BUNA-S" and in North America, during World War II, as "GR-S" (government rubber-styrene) [28]. SBR is an elastomeric polymer which is added in latex form to a base bitumen under agitation. At high service temperatures (50°C to 60°C), the behavior of the SBR-modified binder is characterized by greatly increased viscosities and shear rates by comparison with those of unmodified binders. This is indicative of greater stiffness of the binder for long loading times (or low frequencies). This improvement is important in order to resist mix tenderness and to prevent rutting in asphalt. At low service temperatures (below 10°C), the presence of the elastomer improves the elastic characteristics of the binder without increasing its stiffness, in contrast to what happens in the case of bitumens with lower penetration values. The modification of a bitumen with SBR may thus result in a substantially improved fatigue life by reducing flexural fatigue cracking [29,32]. Armijo [33] also reported that the use of SBR improves the physical properties related to the rutting problem of Montana asphalts.

2.4.2.4 Thermoset

Thermosets are rigid, tightly cross-linked polymers which degrade rather than melt upon the application of heat [27]. Once formed, the polymer cannot be returned to a plastic state by heating. In other words, they cannot be swollen, nor melted and they retain the shape of the molds in which they were manufactured. When they are subjected

to the reaction of chemical interchain linking (or chemical cross-linking) referred to as vulcanization, then they become swellable and deformable [29]. A typical example is the ground tire rubber.

Ground tire rubber blended to asphalt cement has been called asphalt-rubber for years. When granulated tire rubber and asphalt are mixed at high temperatures (135°C-200°C), rubber particles may swell to at least twice their original volume. Swelling has been postulated to occur as a result of both physical and chemical interactions between rubber particles and asphalt, and an increase in viscosity of the asphalt-rubber mixture. The use of asphalt-rubber materials has been increasing during the past decade as they have proven useful in various pavement maintenance applications including binders for asphalt concrete, low modulus stress absorbing membranes and stress absorbing membrane interlayers, and crack and joint sealers for both asphalt and portland cement concrete pavements [24,34]. Many studies [35,36,37,38,39] have reported that the asphalt-rubber can lower the temperature susceptibility, reduce the penetration, increase the viscosity and the softening point, and improve the resistance to age hardening. Due to those features, the resistance to plastic deformation, rutting, at high service temperatures will increase, and the resistance to cracking will decrease at low temperatures.

CHAPTER 3
RESEARCH PROGRAM AND INSTRUMENTATION

3.1 Laboratory Testing Program on Asphalt Cements

3.1.1 Materials Tested

Five types of modifiers which appeared promising in improving the properties of asphalt mixtures at low and high temperatures were selected for this study. These five modifiers were:

1. Gilsonite
2. Ground Tire Rubber (GTR)
3. Styrene-Butadiene Rubber (SBR)
4. Ethylene Vinyl Acetate (EVA)
5. Styrene Ethylene Butylene Styrene (SEBS)

Four types of asphalt cements, namely AC-5, AC-10, AC-20 and AC-30, were used in this study. Gilsonite was blended with the AC-5 and AC-10 using addition levels of 5%, 10% and 15% by weight of the asphalt. GTR was blended at levels of 5%, 10% and 15% with the AC-20 and AC-30. SEBS was added to the AC-20 at levels of 3% and 5%. The SBR- and EVA-modified asphalt binders were blended by the suppliers. SBR was blended with AC-20 at levels of 1.5%, 3% and 4.5%. In addition, 3% of SBR was also mixed with the AC-30. EVA was blended with AC-10 and AC-20 at 4% level.

Table 3.1 lists these 24 unmodified and modified binders. The following tests were run on the 24 original asphalt blends:

(1) Brookfield rheometer tests at 140°F and 275°F.

(2) Schweyer rheometer tests at 41°F and 77°F.

(3) Penetration at 77°F.

(4) Fraass breaking point test

(5) SHRP bending beam rheometer test at 0°C and -12°C

(6) SHRP dynamic shear rheometer test at 10 rad/sec

(7) SHRP direct tension test at -12°C

(8) IR spectral analysis

Table 3.1 List of Modified Asphalt Binders Tested

Asphalt Type	Abbreviation	Asphalt Type	Abbreviation
AC-5	A	AC-20	C
+ 5% Gilsonite	AGI5	+ 5% GTR	CGT5
+ 10% Gilsonite	AGI10	+ 10% GTR	CGT10
+ 15% Gilsonite	AGI15	+ 15% GTR	CGT15
		+ 4% EVA	CEV4
		+ 1.5% SBR	CSB15
		+ 3.0% SBR	CSB30
		+ 4.5% SBR	CSB45
		+ 3% SEBS	CSE3
		+ 5% SEBS	CSE5
AC-10	B	AC-30	D
+ 5% Gilsonite	BGI5	+ 5% GTR	DGT5
+ 10% Gilsonite	BGI10	+ 10% GTR	DGT10
+ 15% Gilsonite	BGI15	+ 15% GTR	DGT15
+ 4% EVA	BEV4	+ 3% SBR	DSB3

In this test series, there were a total of 24 different binders to be tested for evaluation of the effects of the modifiers on the temperature susceptibility of asphalt binders. Figure 3.1 shows the flow chart for this subtask.

3.1.2 Brookfield Rheometer Test

A Brookfield Digital Rheometer Model DV-III System was used in this research study and is illustrated in Figure 3.2. The Brookfield Digital Rheometer Model DV-III System consists of a rotational viscometer with a viscosity range of 0.8 - 320,000 poises, a thermosel system with programmable temperature controller and a computer software Rheocalc version 1.2, which is used to read, store, and analyze data.

The Brookfield viscometer consists of a synchronous drive motor with multiple-speed transmission, a spindle of a known size (area), and a digital readout with control keys. The synchronous drive motor powers the spindle through a calibrated spiral spring. The spring is wound as torque increases. The torque in the spring is measured by a RVDT (rotary variable displacement transducer) and is read out on the digital display or on the computer using the Rheocalc Software.

The spindles of the viscometer are cylindrical in shape and each has a specified shearing area. The submerged spindle is resisted from rotating by the viscous nature of the asphalt binder being tested. The selection of proper spindle is based on the viscosity range of the asphalt binder being tested.

The Brookfield Rheocalc Software is used to input parameters such as spindle number and to set the rotational speed of the viscometer. The output parameters from the

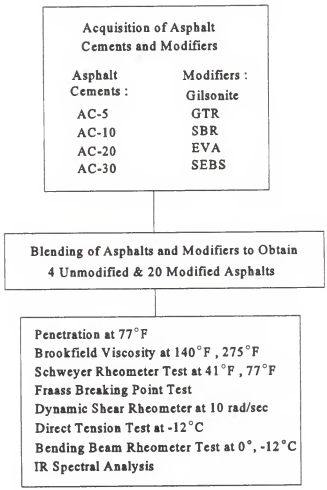

Figure 3.1 Flow Chart of Activities of Subtask I

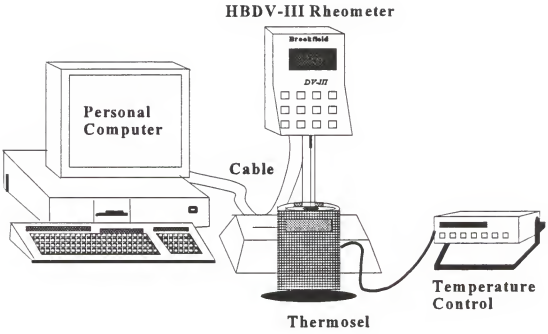

Figure 3.2 Brookfield Rheometer Reading and Controlling System

computer software include (1) applied torque, (2) rotational speed, (3) viscosity, (4) temperature, and (5) shear rate.

The torque required to maintain a cylindrical spindle at a constant rotational speed while immersed in an asphalt binder sample at a constant temperature is used to calculate the shear stress, and the viscosity of the tested binder [40].

3.1.3 Cannon Schweyer Constant Stress Rheometer

A Cannon Schweyer constant stress rheometer as shown in Figure 3.3 was used to measure the rheological properties of asphalt blends at lower temperature such as 25°C and lower. A comprehensive review on the theoretical background of the Schweyer constant stress rheometer and the application of rheological concepts proposed by H. E. Schweyer has been presented in a paper by Tia and Ruth [41]. The rheometer consists of a gas-operated pneumatic cylinder which applied a specified force to the plunger in the sample tube. The movement of the plunger was measured by a LVDT and the output voltage was digitized and acquired by a data acquisition and analysis system, which was operated on an IBM PC-compatible computer. The sample tube is inserted into an insulated aluminum block where the temperature is cooled or heated to the desired testing temperature through the refrigeration unit with the combination of an electrical wire heater.

The shear stress and shear rate at an applied pressure can be calculated from the movement of the plunger and dimensions of the tube, based on the steady-state laminar flow of a power law fluid in a capillary tube. The shear susceptibility is obtained and

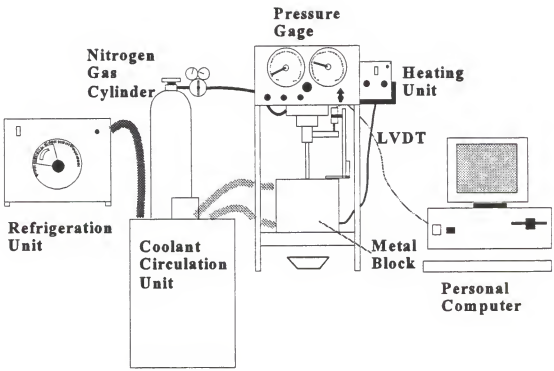

Figure 3.3 Cannon Schweyer Rheometer System

used to compute the constant power viscosity ($\eta_{j=100}$) at 100 W/m^3. This is the viscosity when the shear stress times the shear rate equals 100 W/m^3.

3.1.4 Fraass Breaking Point Test

A Fraass breaking point tester as shown in Figure 3.4 was used to characterize the property of bitumens at low temperatures (as low as -38°C). In this test, a film of asphalt is placed on a thin metal plate which is fixed between plate hinges at the bottom of the bending apparatus. The temperature is controlled by adding solid carbon dioxide (dry ice) to the acetone bath cylinder at a steady decreasing rate of 1°C per minute. The rotating handle at the top of the bending apparatus is turned at a rate of one revolution per second for 11 turns and then unwound at the same rate during the test. The thin metal plate with a film of asphalt is flexed at increasing lower temperatures until the first crack is observed and recorded. It has been observed that the Fraass breaking point is usually 16-19°C above the theoretical cracking temperature. This is due to the much higher strain rate applied to the asphalt in Fraass breaking point test [42].

3.1.5 SHRP Bending Beam Rheometer

The Bending Beam Rheometer (BBR) was used to measure the low temperature stiffness properties of the asphalt binders. The BBR uses a simply-supported (three-point loading) beam under a creep load to measure the stiffness of the asphalt binder. A creep load is used to simulate the stresses that gradually build up in an asphalt pavement when the air temperature drops. The SHRP bending beam rheometer test is described in AASHTO TP1 [43].

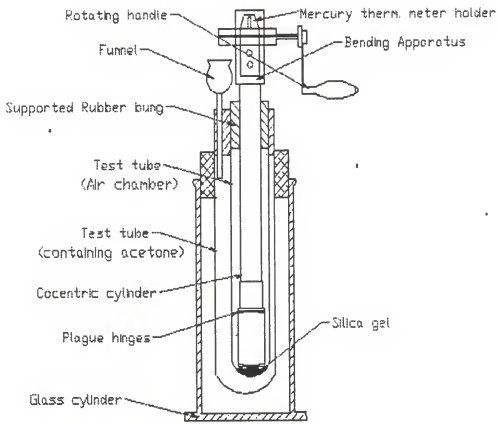

Figure 3.4 Fraass Breaking Point Tester

A Cannon Instruments bending beam rheometer was used in this research study and is illustrated in Figure 3.5. The Cannon bending beam rheometer test system consists of a loading frame, a controlled temperature fluid bath, and a computer controlled automatic data acquisition system.

The BBR uses a blunt-nosed loading shaft to apply a midpoint load to the asphalt binder test beam which is supported at both ends. A load cell is mounted on the loading shaft which is enclosed in an air bearing to eliminate any frictional resistance encountered when loading the asphalt binder test beam. A Linear Variable Differential Transducer (LVDT) is mounted axially above the loading shaft to monitor deflections. The load is applied to the asphalt binder test beam by air pressure, and regulators are used to adjust the load applied through the loading shaft.

The bending beam rheometer test loads an asphalt beam for four minutes with a constant load and measures the deflection at the center of the beam continuously throughout the test. From the continuous deflection data, the time dependent flexural creep stiffness, "S(t)" are calculated. The slope of the logarithm of stiffness versus the logarithm of time plot at a time of 60 seconds is determined and is called the "m" value [44].

3.1.6 SHRP Dynamic Shear Rheometer

Dynamic Shear Rheometer (DSR) was used to measure the elastic and viscous properties of the asphalt binders at intermediate and high temperatures. The SHRP Dynamic Shear Rheometer test is described in AASHTO TP5 [45]. A Bohlin

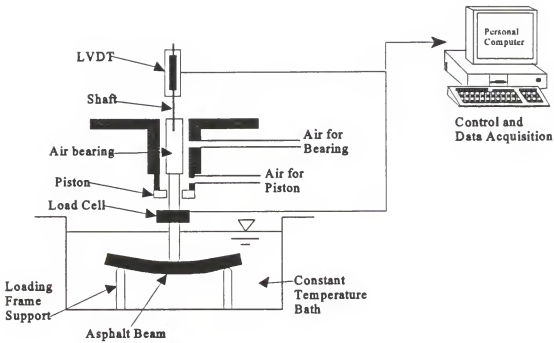

Figure 3.5 Bending Beam Rheometer

Instruments Dynamic Shear Rheometer Test System as illustrated in Figure 3.6 was used in this research study.

The Bohlin dynamic shear rheometer test system consists of a personal computer with Bohlin rheometer software, a temperature control unit and a Bohlin DSR where the sample is placed and tested. Before the test, an asphalt binder sample is placed between a spindle and a fixed baseplate. The spindle is oscillated back and forth in a constant stress or constant strain mode during the test. When this oscillation occurs, the resulting stresses and strains are recorded. The relationship between the applied stress and resulting strain is based on the assumption that the asphalt binder sample tested is in the linear viscoelastic region. It provides information necessary to compute the complex shear modulus, G^*, and the phase angle, δ [44].

3.1.7 SHRP Direct Tension Tester

The direct tension test (DTT) measures the low temperature strain at failure or ultimate tensile strain and stress at failure of an asphalt binder pulled at a constant rate of elongation. The SHRP direct tension test is described in AASHTO TP3 [46]. A Satec Model ACT1 Direct Tension Tabletop Test System was used in this research study and is illustrated in Figure 3.7. The Satec Model ACT1 Direct Tension Tabletop Test System consists of a displacement-controlled testing machine, an elongation measuring system and an environmental testing chamber. The direct tension test is performed at relatively low temperatures ranging from 0° to -36° C which is the temperature range where an asphalt binder usually exhibits brittle or brittle-ductile failure. The direct tension test determines the tensile strain at failure, is a measure of the amount of elongation that an

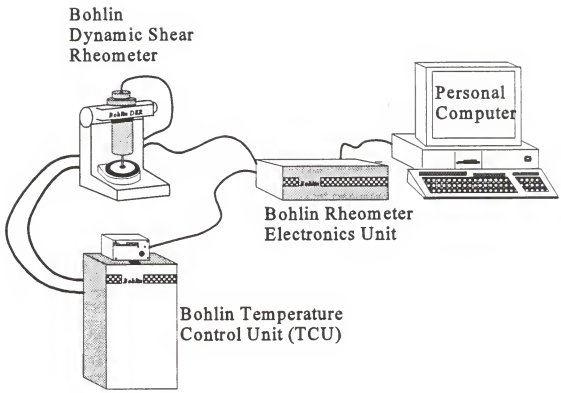

Figure 3.6 Bohlin Dynamic Shear Rheometer Test System

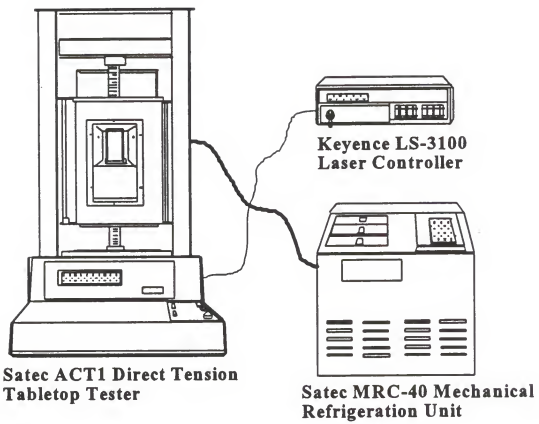

Figure 3.7 Direct Tension Tester

asphalt binder can sustain without cracking. This strain at failure is used as a criterion for specifying the low temperature properties of an asphalt binder in the SHRP asphalt binder specifications [44].

3.1.8 Infrared Spectral Analysis

Infrared spectroscopy is an analytical method where the infrared radiation is passed through the sample and the amount of the radiation absorbed (or transmitted) by the sample is measured. The Perkin-Elmer Model 1600 Fourier Transformation Infrared (FTIR) spectrophotometer as shown in Figure 3.8 was used in this study. It consists of three major parts: an optical system, a sample compartment, and a dedicated computer. The computer controls the optical components, collects and stores data, performs computations on the data and displays the absorption spectra.

The optical system illustrated in Figure 3.8 shows the optical path in the spectrophotometer [47]. The IR beam begins at the source coils. A fixed toroidal mirror collimate the beam from the source and directs it to the interferometer. The beam from a helium neon laser follows the IR beam through the interferometer. The system uses the laser beam to track the distance the moving mirror travels (optical path difference) and to determine when to take a data point.

The sample compartment is located at the front of the instrument, to the left of center. The single infrared beam enters the compartment from the left, behind the sample slide holder. After passing through the sample, it exits at the right, to enter the detector area. Liquid samples are examined for their spectral characteristics in sealed cells. These cells for handling solutions vary in thickness from 0.1 mm to 1.0 mm, the thickness

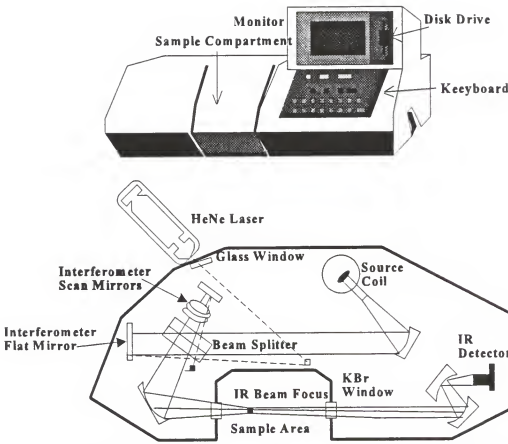

Figure 3.8 The Fourier Transformation Infrared Spectrophotometer

representing the path length through the film of solution held between two crystal windows. The increase in path length results in higher absorbance values and a higher signal-to-noise ratio. The crystal windows are generally made of optical grade sodium chloride (NaCl) or potassium bromide (KBr). The Spectra Tech 1.0 mm NaCl sealed cells were used in the FTIR tests. Solutions of asphalt in tetrahydrofuran (THF) at 5 % (W/V) were injected (by using a syringe) into the cell for test.

3.2 Investigation on Aging of Asphalt Cements

3.2.1 Materials Tested

The 24 asphalt binders as listed in Table 3.1 were used in this test series to evaluate the effects of TFOT (Thin Film Oven Test) as described in ASTM D1754, CTO (California Tilt Oven test) and PAV (Pressure Aging Vessel test) processes on the characteristics of the modified asphalts binders. The 20 modified asphalt blends and the 4 unmodified control (AC-5, AC-10, AC-20 and AC-30) asphalts were subjected to the following aging processes:

(1) TFOT at 163°C.

(2) TFOT at 185°C.

(3) CTO at 111°C for 72 hours.

(4) CTO at 111°C for 168 hours.

(5) PAV at 100°C for 20 hours.

(6) PAV at 100°C for 40 hours.

The following tests were performed on the 144 (24×6) asphalt residues from the TFO, CTO and PAV tests:

(1) Brookfield rheometer tests at 140°F.

(2) Schweyer rheometer tests at 41°F and 77°F.

(3) Penetration at 77°F.

(4) Fraass breaking point test

(5) SHRP bending beam rheometer test at 0°C and -12°C

(6) SHRP dynamic shear rheometer test

(7) SHRP direct tension test

(8) IR spectral analysis

Figure 3.9 shows the summary of the testing program for this subtask.

3.2.2 California Tilt Oven

A Rolling Thin Film Oven (RTFOT, ASTM D2872) as shown in Figure 3.10 was used in this study. The bottle carriage assembly rotates at a rate of 15 ± 0.2 rpm. The air flow was set at a rate of 4000 ± 200 ml/minute. In the process of California Tilt Oven [48], the oven was positioned so that the horizontal axes of the glass containers is tilted by 1° higher in the front of the oven as shown in Figure 3.10. The RTFOT bottles with 35 g samples were heated at the temperature of 111°C. After the process, the RTFOT bottles were covered with the aluminum foil and put into a 160 °C oven for 20 minutes in order to obtain sufficient fluidity to pour the aged residues out of the bottles.

3.2.3 Pressure Aging Vessel

The SHRP proposed Pressure Aging Vessel (PAV) which is the SHRP Product 1003 was used in this study. The method was designed to simulate the in-service

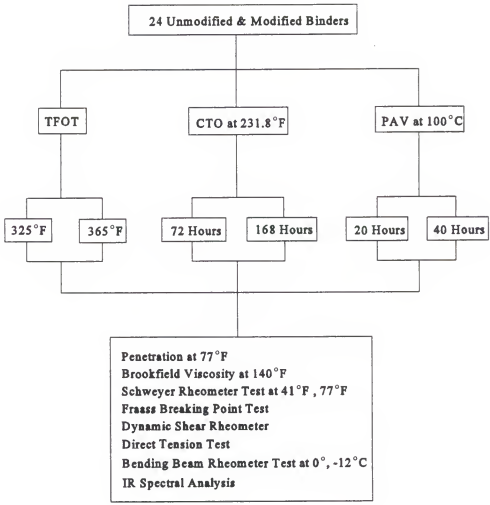

Figure 3.9 Flow Chart of Activities of Subtask II

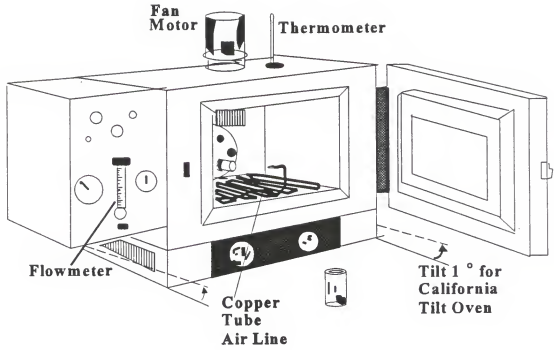

Figure 3.10 Rolling Thin Film Oven

oxidative aging that occurs in asphalt binders during pavement service after five to ten years. Figure 3.11 displays the PAV test system which consists of a pressure vessel, pressure controlling devices, temperature controlling devices, pressure and temperature measuring devices, and a temperature readout device. The system was operated under a pressure of 300 psi for 20 hours at 100°C following the SHRP proposed procedures as detailed in AASHTO Designation PP1 [49].

3.3 Laboratory Testing Program on Asphalt Mixture

3.3.1 Materials Tested

Seven of the 24 binders in subtask I were selected to be used in preparing Florida S-I mixtures. These seven binders included AC-20, AC-20+15%GTR, AC-20+3%SBR, AC-20+3%SEBS, AC-30+10%GTR and AC-30+3%SBR along with the reference AC-30.

Each of these seven binders was mixed with a washed aggregate blend with a controlled gradation and at a fixed binder content of 6.5% to produce mixtures. The aggregates used in the mixture were blended in the proportions of 20% #67 stone, 25% #89 stone, 35% screening, 18% sand and 2% mineral filler. The blended aggregates were washed, separated into different size groups and dried. These sized aggregates were re-combined to produce aggregate blends of controlled gradation. Table 3.2 shows the aggregate types, blends used, and job mix formula.

These mixtures were compacted into Marshall size specimens by using the Gyratory Testing Machine (GTM) for age hardening and subsequent testing. For each type of asphalt mix, there were nine specimens compacted by GTM at 18 revolutions

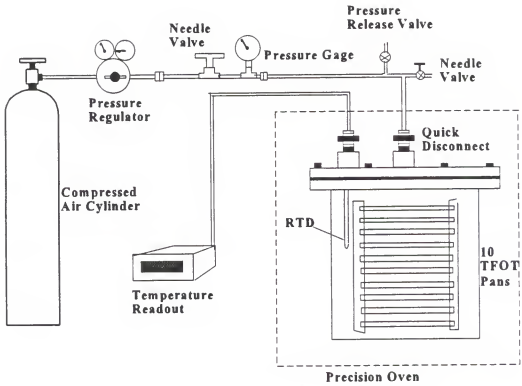

Figure 3.11 Pressure Aging Vessel Test System

Table 3.2 Source of Aggregates and Job Mix Formula for Dense-graded Mixes

Number	Aggregate Type	Producer	Pit Number
1	#67 Limestone	Florida Mining & Materials	08-005
2	#89 Limestone (S1-B)	Florida Mining & Materials	08-005
3	Screening	Florida Mining & Materials	08-005
4	Canal Auth. Sand		
5	Mineral Filler	Whitehearst Construction	

Aggre-gate	#67 Stone	#89 Stone	Screen-ing	Sand	Mineral Filler	Bulk Specific Gravity	Job Mix Formula	FDOT S-I Spec.
Blend	20%	25%	35%	18%	2%			
Sieve (Percentage Passing)								
3/4"	100	100	100	100	100	-	100	100
1/2"	72.2	100	100	100	100	2.375	99	88-100
3/8"	25.0	89.5	100	100	100	2.379	90	75-93
No.4	4.7	14.7	97.3	100	100	2.345	63	47-75
No.10	1.0	1.0	61.2	100	100	2.298	47	31-53
No.40	0.5	0.4	16.0	72.8	100	2.333	35	19-35
No.80	0.4	0.2	2.3	15.0	99.1	2.655	13	7-21
No.200	0.0	0.0	0.0	0.0	85.8	2.784	4	2-6

using a gyratory angle of 3 degree, 100 psi of ram pressure and 9 psi of air roller pressure. Three of nine specimens were used as unaged specimens and compacted by applying 18 GTM revolutions at 135-149°C to simulate the initial field compaction. Another three specimens were densified by applying an additional 50 GTM revolutions at 60°C at the same settings after the initial compaction to simulate the condition after two years of traffic. The rest of three specimens were densified by applying an additional 300 GTM revolutions at 60°C after the initial compaction to simulate the ultimate condition in the pavement. Those specimens were then evaluated in the AASHTO indirect tensile creep test which was proposed by Roque and Buttlar [51-53]. In addition, two more beams were fabricated for rut test using the Georgia Loaded Wheel Tester.

For each of the seven types of asphalt mixes, two samples of loose mixtures were evaluated by the Rice test (ASTM D2041). Three more specimens made and aged in accordance with the SHRP proposed long term oven aging process at 85°C for 5 days [50]. Those aged specimens were evaluated by the AASHTO indirect tensile creep test and then the binders were extracted for the penetration and Brookfield viscosity tests. Figure 3.12 shows the testing program on the asphalt mixtures.

3.3.2 Diametral Resilient Modulus Test

The test set-up for the SHRP Indirect Tensile Test at Low Temperatures (ITLT) as shown in Figure 3.13 was used to run the diametral resilient modulus test. The resilient modulus is defined as the ratio of the applied stress to the recoverable strain when a repeated dynamic load is applied. The resilient modulus test is performed in a load-control mode and by applying a repeated haversine waveform load to the specimen for a

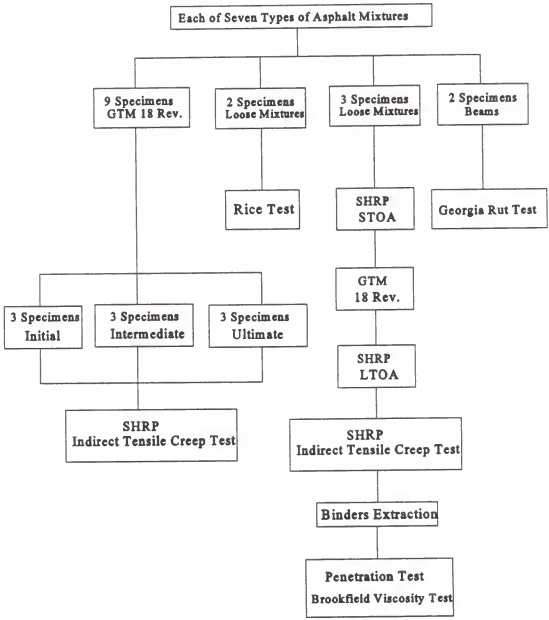

Figure 3.12 Flow Chart of Activities of Subtassk III

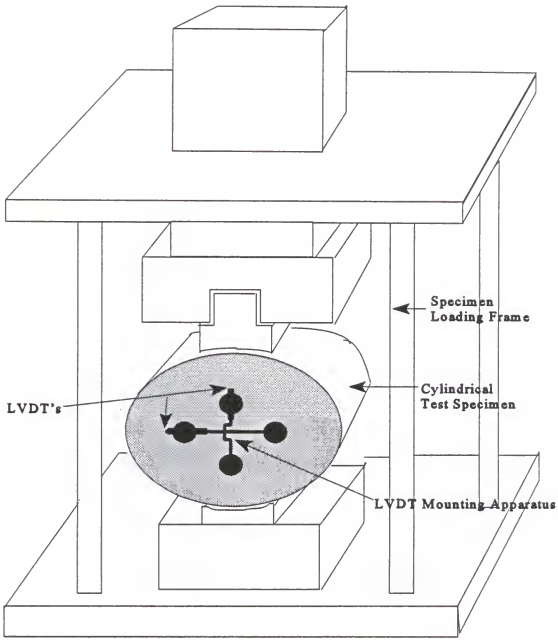

Figure 3.13 Indirect Tensile Testing Device

period of 0.1 second. Before the test, the load was chosen to keep horizontal strains in the linear viscoelastic range which is typically below a horizontal strain of 350 microstrains. The load selected is applied vertically in the vertical diametral plane of a cylindrical specimen of asphalt mixture during the test. Poisson's ratio is essential for accurate determination of the resilient modulus in this test method, along with stress level, specimen dimensions, and the time-dependent horizontal deflection. The resilient modulus can be determined by using equations which were developed based upon three-dimensional finite element analysis by Roque and Buttlar [51-53]. The procedure for resilient modulus test are summarized as follows:

(1) Four brass gage points are affixed with epoxy to each trimmed smooth face of the specimen. Test samples are stored in a conditional chamber hooked up with the dehumidifier at a constant relative humidity of 60 percent for 3 days before testing. Specimens were cooled at the test temperature for 3 hours before the test.

(2) LVDTs (Linear Variable Differential Transducers) are mounted and centered on the specimen to the gage points for the measurement of the horizontal and vertical deflections. The required range and resolution of measurements were ±0.1 inch and $\pm 10 \times 10^{-6}$ inch, respectively.

(3) A constant pre-loading of 10 to 30 pounds was applied to the test specimens to ensure proper contact with the loading heads before test loads were applied. The specimen is then tested by applying a repeated haversine waveform load for five seconds at five cycles of loading and unloading. The data acquistion system records the loads and deflections.

(4) The test will be repeated when the horizontal strains are not between 150 and 350 microstrains during the test. It is required for specimens to recover for a minimum of 3 minutes before reloading at a different level.

A computer program, which was written by R. Roque and X. Wang, was used to analyze these loads and deflections to determine the instantaneous and total resilient moduli and Poisson's ratio. The procedure for analysis of resilient modulus and Poisson's ratio are summarized as follows:

(1) Find the instantaneous and total recoverable horizontal and vertical deformations (ΔH_I, ΔH_T, ΔV_I and ΔV_T) as shown in Figure 3.14.

(2) Obtain the ratio of horizontal to vertical deformations, X/Y.

(3) Compute resilient moduli and Poisson's ratio by the following equations:

$$MR_I = \frac{P\ GL}{\Delta H_I\ t\ D\ C_{cmpl}}$$

$$MR_T = \frac{P\ GL}{\Delta H_T\ t\ D\ C_{cmpl}}$$

$$v_I = -0.10 + 1.480\times(X/Y)_I^2 - 0.778\times(t/D)^2\times(X/Y)_I^2$$

$$v_T = -0.10 + 1.480\times(X/Y)_T^2 - 0.778\times(t/D)^2\times(X/Y)_T^2$$

where,

ΔH_I = instantaneous recoverable horizontal deformation
ΔH_T = total recoverable horizontal deformation
ΔV_I = instantaneous recoverable vertical deformation

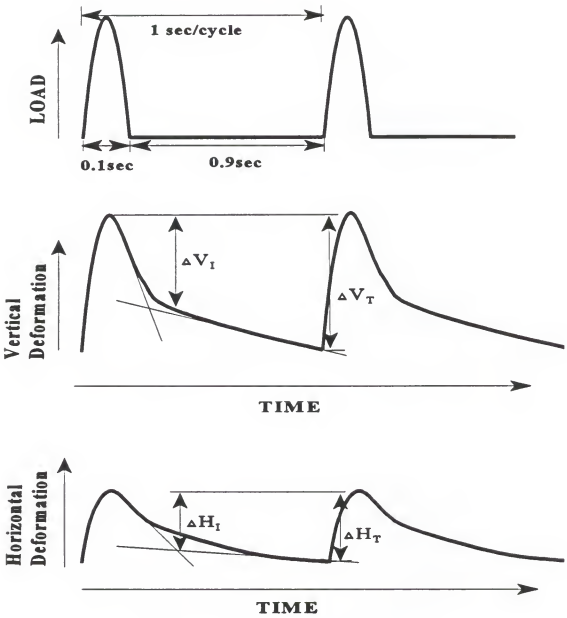

Note:

ΔH_I = Instantaneous recoverable horizontal deformation
ΔH_T = Total recoverable horizontal deformation
ΔV_I = Instantaneous recoverable vertical deformation
ΔV_T = Total recoverable vertical deformation

Figure 3.14 Typical Load, Deformation versus Time Relationships in a Repeated-Load Indirect Tension Test

ΔV_T = total recoverable vertical deformation
t, D, P = thickness, diameter, and maximum load of specimen
MR_I = instantaneous resilient modulus, GPa
MR_T = total resilient modulus, GPa
v_I = instantaneous resilient Poisson's ratio
v_T = total resilient Poisson's ratio
GL = gage length, inch
$(X/Y)_I$ = ratio of the instantaneous horizontal to vertical deformations
$(X/Y)_T$ = ratio of the total horizontal to vertical deformations
$C_{cmpl} = 0.6354 \times (X/Y)^{-1} - 0.332$

3.3.3 Indirect Tensile Creep Test

The SHRP Indirect Tensile Test at Low Temperatures (ITLT) was used to measure the creep properties of the mixtures. The creep test was conducted in a load-control mode and involved applying a static load and then holding it constant throughout the test. The load in the test was selected to keep horizontal strains in the linear viscoelastic range which is below a horizontal strain of 500 microstrains. The development and evaluation of the method, and test procedures were presented by Buttlar and Roque [52] and in the AASHTO Provisional Standard TP9 [54]. The general procedure for tensile creep test consists of the following steps:

(1) The preparation of test specimens are same as that for the resilient modulus test.

(2) The mounting and centering LVDT are same as that for resilient modulus test.

(3) The pre-loading job is same as that for resilient modulus test. The specimen is then tested by applying a static load and then holding it constant for 1000 seconds. The four displacements and the creep load were recorded in three stages during the test. They are recorded at a rate of 10 Hz for the first 10

seconds, at 1 Hz for the next 290 seconds, and at 0.2 Hz for the remaining 700 seconds of the creep test.

(4) The test is repeated when the horizontal strains are not between 40 and 120 microstrains at t = 30 seconds for a 1000-second creep test. Specimens must recover for a minimum of 3 minutes before reloading at a different level.

A computer program, which was written by R. Roque and W. Buttlar, was used to analyze these load and deflection data to calculate creep compliance and Poisson's ratio. The creep compliance and Poisson's ratio are calculated as follows:

(1) Find the thickness, diameter and maximum load for each set of 3 samples.

(2) Compute normalized horizontal and vertical deformations ($\Delta H_{(NORM)}$, and $\Delta V_{(NORM)}$) for each of the 6 specimen faces (3 specimens, 2 faces per specimen).

$$\Delta H_{(NORM)} = \Delta H \times C_{NORM}; \qquad \Delta V_{(NORM)} = \Delta V \times C_{NORM};$$

$$C_{NORM} = \frac{t_i \, D_i \, P_i}{t_{avg} \, D_{avg} \, P_{avg}}$$

where,

$\Delta H_{(NORM)}$ = normalized horizontal deformation
$\Delta V_{(NORM)}$ = normalized vertical deformation
C_{NORM} = normalized factor
t_i, D_i, P_i = thickness, diameter, and maximum load of specimen i (i=1 to 3)
t_{avg}, D_{avg}, P_{avg} = average thickness, diameter, and maximum load of three replicate specimens

(3) Obtain the average normalized horizontal and vertical deformations, ΔH_{avg} and ΔV_{avg}, at halfway (500 sec) creep loading period for each of the 6 specimen faces.

(4) Obtain the trimmed mean of the average normalized horizontal and vertical deformations by numerically ranking the 6 ΔH_{avg} and ΔV_{avg} values and averaging the 4 middle values. Thus, the highest and lowest values of the average normalized horizontal and vertical deformations are not included in the trimmed mean.

(5) Obtain the ratio of horizontal to vertical deformations, X/Y, which is equal to the ratio of trimmed mean of the average normalized horizontal to vertical deformations.

(6) Compute creep compliance and Poisson's ratio by the following equations:

$$D(t) = \frac{\Delta H_{avg}\ t_{avg}\ D_{avg}\ C_{cmpl}}{P_{avg}\ GL}$$

$$v = -0.10 + 1.480\times(X/Y)^2 - 0.778\times(t_{avg}/D_{avg})^2\times(X/Y)^2$$

where,

D(t) = creep compliance at time t, 1/psi
v = resilient Poisson's ratio
GL = gage length, inch
ΔH_{avg} = trimmed mean of the average normalized horizontal deformation
(X/Y) = ratio of the average normalized horizontal to vertical deformations
$C_{cmpl} = 0.6354\times(X/Y)^{-1} - 0.332$

3.3.4 Indirect Tensile Strength Test

The indirect tensile strength is the maximum tensile stress that a specimen can tolerate before fracture. This property can be used for prediction of thermal cracking potential and characterization of the asphalt concrete resistance to the tensile stress failure. The test procedure for determining the indirect tensile strength of the mixture is described in the AASHTO Provisional TP9 [54]. The tensile strength test was set up after accomplishing the tensile creep test by changing load-control mode to displacement-control mode. A loading rate of 0.5-inch per minute for 4-inch-diameter specimens was used in this study. The horizontal and vertical deformations, and the applied load were gathered at the rate of 20 Hz in the test. The maximum tensile strength were calculated as:

$$S_t = \frac{2\ P\ (C_{sx})}{\pi\ b\ D}$$

where,

C_{sx}	=	0.948 - 0.01114*(b/D) - 0.2693*(v) + 1.436*(b/D)(v)
S_t	=	maximum indirect tensile strength, psi
P	=	failure load at first crack, lbf
b	=	specimen thickness, inches
D	=	specimen diameter, inches
v	=	Poisson's ratio

3.3.5 Loaded Wheel Test

The Loaded Wheel Tester (LWT) is a simple laboratory testing device which was designed to determine the rutting resistance of asphalt concrete paving mixtures. The

principle of the LWT is to simulate the stress conditions resulting from repeated, moving wheel loads as they occur in actual pavements. Figure 3.15 shows a schematic view of the Georgia Loaded Wheel Tester which was used in this research study and was the first model manufactured after the prototype LWT developed by Dr. James Lai at Georgia Tech [55,56].

The test specimens are 3" (width) ×1.5" (height) ×15" (length) asphalt concrete beams and fabricated to match the field produced mixtures with a target air void content to simulate a typical initial density achieved in the field. The materials are heated to 300°F, mixed, then returned to the oven prior to compaction. Compaction is achieved by static loading across the top of the beam to 60,000 lbs., then releasing the load. This process is repeated four times. On the fifth application, the load is held at 60,000 lbs. for six minutes.

The compacted beams are removed from the molds the next day and allowed to cure at room temperature for seven days. During the curing period, the bulk density and the air void content for each beam are determined. Prior to testing, each beam is placed in the preheating chamber at 105°F for 24 hours.

The test beams are rigidly confined on the sides and ends with angle brackets. A stiff pressurized hose at 100 psi mounted along the top of the beam acts as a tire to transfer the load from the wheel of the moving chassis to the beam. Steel weights of 122 lbs are bolted to the chassis which is driven by the motor / gear-box assembly through the articulated arms. One loading cycle consists of a forward and return pass of the loaded chassis. The entire LWT assembly is housed in a heated and insulated temperature

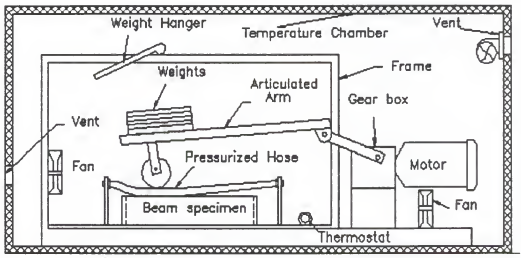

Figure 3.15 Loaded Wheel Tester

chamber which serves to maintain the test at a relatively constant temperature of 105°F. Small fans are placed within the chamber to circulate the air. However, some fluctuation in temperature occur due to heat generated by the drive motor and heat loss during rut measurements. Temperature is monitored with a thermometer embedded in a dummy specimen placed in the LWT. Rut depth measurements are recorded with a dial gauge and reference template at set cycle intervals as well as the temperature.

3.3.6 Asphalt Extraction and Recovery Methods

Asphalt binders were extracted and recovered after the mixtures were performed by the indirect tensile strength test at -10°C. The asphalt extraction was performed after the mixtures were heated and crushed into small pieces. The extraction method used in this study was the reflux method as described in ASTM D2172 Method B [57]. The extracted solutions then were centrifuged at a force of higher than 770 times gravity for at least 30 minutes accordance to ASTM D1856 [58] to eliminate mineral matter. The final procedure after the centrifugation of the solutions was the asphalt recovery. The recovery apparatus used was the Buchi Rotavapor and the recovery method was according to the "Standard Test Method for Recovery of Asphalt from Solution Using the Rotavapor Apparatus, Draft 9" [59].

CHAPTER 4
RESULTS OF BINDERS TESTS

4.1 Statistical Model

Statistical analysis using the ANOVA model was used to determine whether the effect of main factors and interactions of factors are significant. The effects of asphalt type and aging process were studied by means of this method. The test results from the binder tests were analyzed on the basis of a factorial experiment that included 24 types of asphalt and six types of aging process. Asphalt (α) and aging process (β) are regarded as fixed effects. The following linear model is assumed for any single response variable in the experiment :

$$Y_{ijk} = \mu + \alpha_i + \beta_j + (\alpha\beta)_{ij} + \epsilon_{ijk}$$

where

Y_{ijk} = the response of k^{th} replicate, j^{th} aging process, and i^{th} asphalt

μ = the overall mean

α_i = the main effect of i^{th} asphalt type

β_j = the main effect of j^{th} aging process

$\alpha\beta_{ij}$ = the interaction effect

ϵ_{ijk} = the experimental error

I = 1 to 24 for 24 asphalts

j= 1 to 6 for six aging processes

k= 1 to 2 for two replicates

SAS/STAT computer program was used to perform the analysis. A probability of Type I error (α) of 0.05 was used. Comparison of means was done by Duncan's multiple-range test at an α level of 0.05. However, some test data did not meet the assumption of homogeneity of variance as assumed by the ANOVA model, and the data had to be transformed to meet the requirement of homogeneity of variance. The usual approach for dealing with that kind of nonconstant variance is to apply a variance-stabilizing transformation and then to run the analysis of variance on the transformed data. If the data follows the log-normal distribution, then the logarithmic transformation is appropriate.

4.2 Effects of Modifiers on the High-Temperature Properties

4.2.1 Brookfield Viscosity

The Brookfield viscosity is measured in accordance with ASTM D4402 procedure at temperatures of 60°C and 135°C. The high temperature viscosity is measured in the SHRP specifications to ensure that the asphalt binder is fluid enough to be pumped in the mixing process. The Brookfield viscosity is measured on the unaged asphalt binders. According to the SHRP specifications, it must not exceed 30 poises at 135°C. The test result shows that AC-20+4.5% SBR does not meet the requirement among all 24 unaged binders. The viscosity of AC-20+4.5% SBR at 135°C is 70 poises.

The results of the Brookfield viscosity tests at 60°C on original and aged binders are given in Appendix A.1. The results of ANOVA and Duncan's grouping on the

Brookfield viscosity at 60°C of the original and PAV-20 hour-aged binders are shown in Table 4.1. It can be seen that all modifiers increase the viscosity of the binder in comparison to the unmodified binder. The effect of modifiers on the viscosity increases as the level of addition increases. Figure 4.1 shows the relationship between Brookfield viscosity at 60°C and level of Gilsonite added on an unaged AC-5. The results of regression analyses for the relationship between Brookfield viscosity and level of added modifier for all unaged and aged binders are shown in Table 4.2. It indicates that most of regression equations show a high goodness of fit as seen from the high R^2 values. The regression analyses on California-tilt-oven-aged binders show less consistency. This may be due to the process of sample collection from the RTFOT bottles which may result in the problem of residue inhomogeneity. The b1 in the regression equation indicates the increase rate of Brookfield viscosity due to the modifier added. The higher the b1, the more significant the effect of modifier. For unaged binders, SBR has the most effect on the Brookfield viscosity increase with b1 of 0.221, and is followed by EVA, SEBS and Gilsonite. The ground tire rubber (GTR) has the least effect among them with b1 of 0.059. Most of the modified binders have higher viscosity as compared with the control AC-30. The modified binder's viscosity at 60°C increases up to 529% for the original binders and 646% for the PAV-20 hour-aged binders as compared with that of the control AC-30. An increase in viscosity of the binders at a high pavement temperature usually means a higher resistance to rutting for the pavement material.

Table 4.1 Results of ANOVA and Duncan's Grouping on the Brookfield Viscosity of the Original and PAV-20 hour-aged Binders

Dependent Variable:Brookfield Viscosity [Model = $\mu + \alpha_i + \beta_j + (\alpha\beta)_{ij} + \epsilon_{ijk}$]

Source	DF	ANOVA SS	Mean Square	F Value	Pr > F
ASPHALT, α	23	74266446268	3228975925	578.84	0.0001
METHOD, β	1	70647886205	70647886205	12664.73	0.0001
INTERACTION, $\alpha\beta$	23	51297332007	2230318783	399.82	0.0001

R-Square= 0.998637

Duncan Grouping at Method = Original

Duncan Grouping	Mean	N	ASPHALT
A	23812	2	AC-10 + 15% Gilsonite
A			
B A	22443	2	AC-20 + 4.5% SBR
B			
B C	20605	2	AC-20 + 15% GTR
C			
D C	18507	2	AC-20 + 5% SEBS
D			
D	17407	2	AC-30 + 3%SBR
D			
D	16688	2	AC-30 + 15% GTR
D			
D	16200	2	AC-20 + 4% EVA
E	10709	2	AC-20 + 3.0% SBR
E			
F E	9779	2	AC-30 + 10% GTR
F E			
F E G	8334	2	AC-5 + 5 % Gilsonite
F E G			
F H E G	8137	2	AC-10 + 10% Gilsonote
F H G			
F H G	7812	2	AC-20 +3% SEBS
F H G			
F H I G	7683	2	AC-20 +10 % GTR
H I G			
J H I G	6055	2	AC-20 + 1.5 %SBR
J H I			
J H I K	5452	2	AC-10 +4% EVA
J L I K	5045	2	AC-20 + 5% GTR
J L K	4798	2	AC-30 +5% GTR
J L M K	3785	2	AC-30
J L M K	3515	2	AC-5 +10% Gilsonite
N L M K	3172	2	AC -10 +5 %Gilsonite
N L M	2526	2	AC-20
N M	1677	2	AC-5 +5% Gilsonite
N M	1181	2	AC-10
N	571	2	AC-5

Table 4.1 Continued

Duncan Grouping at Method = PAV 20 hours

Duncan Grouping	Mean	N	ASPHALT
A	241359	2	AC-10 + 15% Gilsonite
B	141953	2	AC-5 +15% Gilsonite
C	129256	2	AC-20 +5% GTR
D	104319	2	AC-30 +15% GTR
D	100555	2	AC-10 +10% Gilsonite
E	85971	2	AC-20 +4% EVA
F	72639	2	AC-20 +15% GTR
G F	67677	2	AC-20 +3% SEBS
G	65544	2	AC-30 +10% GTR
H	57608	2	AC-20 +4.5% SBR
I	50595	2	AC-30 +5% GTR
I	48963	2	AC-5 +10% Gilsonite
J I	44947	2	AC-20% +10%GTR
J I	44499	2	AC-10% +4%EVA
J I	43776	2	AC-30 +3% SBR
J I	43482	2	AC-20 +3.0% SBR
J	39645	2	AC-10 +5% Gilsonite
K	32338	2	AC-30
L K	28523	2	AC-20 +5% GTR
L K	27339	2	AC-20 +1.5%SBR
L M	22718	2	AC-20
N M	17011	2	AC-5 + 5%Gilsonite
N O	11599	2	AC-10
O	5710	2	AC-5

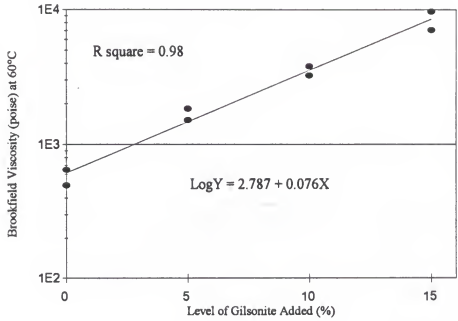

Figure 4.1 Relationship Between Brookfield Viscosity at 60°C and Level of Gilsonite Added on Unaged AC-5

Table 4.2 Summary of Results of Regression Analyses for the Relationship between Brookfield Viscosity and Level of Modifier Added

Regression Equation: Log(Brookfield Viscosity) = bo+b1 (Level of Modifier)

Condition	Asphalt type	AC-5	AC-10	AC-10	AC-20
	Added Modifier	Gilsonite	Gilsonite	EVA	EVA
Unaged	bo	2.786	3.063	3.067	3.398
	b1	0.076	0.087	0.159	0.203
	R^2	0.98	0.99	0.86	0.99
CTO 72 hrs	bo	4.057	4.262	4.252	4.372
	b1	0.065	0.025	0.156	0.152
	R^2	0.99	0.62	0.99	1.00
CTO 168 hrs	bo	4.690	4.657	4.628	4.568
	b1	0.031	0.033	0.103	0.128
	R^2	0.87	0.95	0.93	0.97
TFOT 163°C	bo	3.256	3.533	3.503	3.773
	b1	0.080	0.082	0.131	0.132
	R^2	1.00	0.99	0.97	1.00
TFOT 185°C	bo	3.624	3.714	3.766	4.074
	b1	0.084	0.093	0.216	0.217
	R^2	0.98	0.99	0.99	1.00
PAV 20hrs	bo	3.760	4.108	4.064	4.356
	b1	0.093	0.087	0.146	0.144
	R^2	1.00	0.99	0.99	1.00
PAV 40hrs	bo	4.160	4.424	4.417	4.820
	b1	0.093	0.088	0.151	0.145
	R^2	1.00	1.00	0.98	0.99

Table 4.2 Continued

Condition	Asphalt type	AC-20	AC-30	AC-20	AC-30	AC-20
	Added Modifier	GTR	GTR	SBR	SBR	SEBS
Unaged	bo	3.386	3.531	3.424	3.578	3.391
	b1	0.059	0.045	0.207	0.221	0.173
	R^2	0.97	0.97	0.98	1.00	0.99
CTO 72 hrs	bo	4.399	4.510	4.430	4.553	4.369
	b1	0.008	0.003	0.088	0.045	0.085
	R^2	0.36	0.12	0.61	0.96	0.99
CTO 168 hrs	bo	4.562	4.875	4.628	4.905	4.569
	b1	0.014	0.006	0.073	-0.002	0.084
	R^2	0.81	0.25	0.69	0.02	0.75
TFOT 163°C	bo	3.746	3.907	3.736	3.916	3.830
	b1	0.043	0.040	0.149	0.100	0.119
	R^2	0.99	0.99	0.93	1.00	0.85
TFOT 185°C	bo	4.080	4.198	4.083	4.196	4.113
	b1	0.047	0.052	0.177	0.168	0.074
	R^2	0.99	0.99	0.88	0.99	0.72
PAV 20hrs	bo	4.324	4.515	4.336	4.508	4.362
	b1	0.034	0.033	0.094	0.044	0.152
	R^2	0.97	0.98	0.96	0.84	1.00
PAV 40hrs	bo	4.822	4.918	4.831	4.920	4.818
	b1	0.039	0.050	0.180	-0.001	0.186
	R^2	0.98	0.99	1.00	0.10	1.00

4.2.2 Results of Dynamic Shear Rheometer Test

In SHRP testing for specification purposes, a standard testing frequency of 10 radians/second (1.59 Hertz) is specified. This frequency was used because it corresponds to a loading time of 0.1 seconds which simulates the effects of traffic loading. The Bohlin Rheometer was used in the constant stress mode to measure the complex shear modulus (G*) and phase angle (δ) of the binders. The results of the dynamic shear rheometer tests on the original and aged binders are given in Appendix A.2 and A.3. The results of ANOVA and Duncan's grouping on the complex shear modulus at 60°C and 10 rad/sec of the original binders and TFOT-163°C-aged binders are shown in Table 4.3. The G* (complex shear modulus) represents the total resistance to deformation under load. It can be noted that all modifiers increase the complex shear modulus of the binder in comparison to the unmodified binder. The effect of modifiers on the complex shear modulus increases as the level of addition increases.

There is a relationship between the level of the addition and the increase of complex shear modulus. Figure 4.2 shows the relationship between complex shear modulus at 60°C at 10 rad/sec and level of Gilsonite added on an original AC-5. The results of regression analyses on the relationship between the complex shear modulus at 60°C and level of modifier added for the unaged and TFOT-163°C-aged binders are shown in Table 4.4. It indicates that all regression equations show a high goodness of fit. The b1 in the regression equation indicates the increase rate of G* due to the modifier added. For the unaged binders, SEBS has the most effect on the complex shear modulus increase with b1 of 0.114, and is followed by SBR, EVA and Gilsonite. The ground tire

Table 4.3 Results of ANOVA and Duncan's Grouping on the Complex Modulus at 60°C at 10 rad/sec of the Original and TFOT-163°C-aged Binders

Dependent Variable:Complex Modulus [Model = $\mu + \alpha_i + \beta_j + (\alpha\beta)_{ij} + \epsilon_{ijk}$]

Source	DF	ANOVA SS	Mean Square	F Value	Pr > F
ASPHALT, α	23	4981403159	216582746	106.53	0.0001
METHOD, β	1	1394786963	1394786963	686.07	0.0001
INTERACTION, $\alpha\beta$	23	654087970	28438607	13.99	0.0001

R-Square= 0.986310

Duncan Grouping at Method = Original

Duncan Grouping	Mean	N	ASPHALT
A	26407.4	2	AC-10 +15% Gilsonite
B	15169.7	2	AC-30 +15% GTR
C	13252.5	2	AC-20 +5% SEBS
C			
C	13001.5	2	AC-5 +15% Gilsonite
C			
C	12071.5	2	AC-20 +4.5% SBR
C			
C	11884.6	2	AC-20 +15% GTR
D	10428.3	2	AC-30 +10 %GTR
D			
E D	9199.5	2	AC-20 +4% EVA
E D			
E D	9126.2	2	AC-30 +5% GTR
E			
E	8883.4	2	AC-20 + 3.0% SBR
E			
E F	7919.1	2	AC-10 +10% Gilsonite
F			
G F	7408.4	2	C-20 + 10% GTR
G F			
G F H	6893.8	2	C-10 +4% EVA
G F H			
G F H	6815.5	2	AC-20 +3%SEBS
G F H			
G F H	6470.7	2	AC-30 +3%SBR
G H			
G I H	6061.8	2	AC-10 +5% Gilsonite
I H			
J I H	5819.4	2	AC-5 +10 % Gilsonite
J I H	5711.5	2	AC-20 + 1.5% SBR
J I			
J I K	4653.9	2	AC-30
J K			
J K	4324.0	2	AC-20 +5%GTR
L K	3522.3	2	AC-20
M L	2754.9	2	AC-5 5% Gilsonite
M L	2751.9	2	AC-10
M	1342.9	2	AC-5

Table 4.3 Continued

Duncan Grouping at Method = TFOT 163 °C

Duncan Grouping	Mean	N	ASPHALT
A	47084	2	AC-10 +15% Gilsonite
B	28498	2	AC-20 +4%EVA
B			
B	27002	2	AC-20 +5% SEBS
B			
C B	25510	2	AC-10 +10% Gilsonite
C			
C D	22590	2	AC-5 +5% Gilsonite
D			
E D	21286	2	AC-20 +4.5% SBR
E D			
E D	21252	2	AC-30 + 15 %GTR
E D			
E D	20092	2	AC-20 +15 % CGT15
E			
E F	17069	2	AC-30 + 10%GTR
F			
G F	15690	2	AC-20 +10%GTR
G F			
G F H	15002	2	AC-20 +3%SEBS
G F H			
G I F H	14235	2	AC-10 +4%EVA
G I F H			
G I F H	14108	2	AC-30 +5%GTR
G I H			
G I J H	12376	2	AC-30 +35 SBR
G I J H			
G I J H	12090	2	AC-5 +10% Gilsonit
G I J H			
K G I J H	11341	2	AC-20 +3.0% SBR
K I J H			
K I J H	11057	2	AC-20 +5%GTR
K I J H			
K I J H	10683	2	AC-20 +1.5%SBR
K I J			
K I J	10227	2	AC-10 +55 Gilsonite
K J			
K L J	9160	2	AC-30
K L			
K L M	7259	2	AC-20
L M			
L M N	5512	2	AC-5 +5% Gilsonite
M N			
M N	3701	2	AC-10
N	2014	2	AC-5

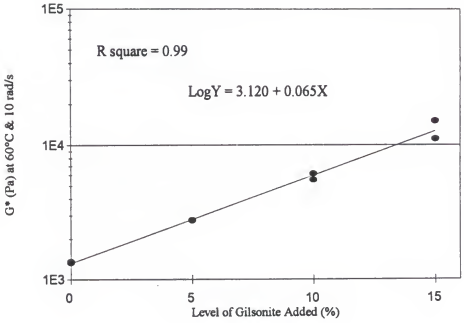

Figure 4.2 Relationship Between Complex Modulus at 60°C at 10 rad/sec and Level of Gilsonite Added on Unaged AC-5

Table 4.4 Summary of Results of Regression Analyses for the Relationship between Complex Modulus at 60°C and Level of Modifier Added

Regression Equation: Log (Complex Modulus) = bo + b1 (Level of Modifier)

Condition	Asphalt Type	AC-5	AC-10	AC10	AC-20
	Added Modifier	Gilsonite	Gilsonite	EVA	EVA
Unaged	bo	3.120	3.426	3.440	3.547
	b1	0.065	0.061	0.100	0.104
	R^2	0.99	0.94	1.00	0.99
TFOT 163°C	bo	3.347	3.608	3.568	3.860
	b1	0.070	0.074	0146	0.147
	R^2	0.99	0.99	1.00	0.97

Condition	Asphalt Type	AC-20	AC-30	AC-20	AC-30	AC-20
	Added Modifier	GTR	GTR	SBR	SBR	SEBS
Unaged	bo	3.509	3.717	3.564	3.668	3.531
	b1	0.036	0.032	0.120	0.048	0.114
	R^2	0.96	0.93	0.99	1.00	0.99
TFOT 163°C	bo	3.879	3.991	3.853	3.962	3.853
	b1	0.030	0.024	0.095	0.044	0.112
	R^2	0.98	0.95	0.90	0.93	0.94

rubber (GTR) has the least effect among them, with b1 of 0.032. The addition of modifier to AC-30 increased the G*-value at 60°C up to 567% for the original binders and 514% for the TFOT-163°C-aged binders. An increase in the complex shear modulus of the binders at a high pavement temperature usually means a higher resistance to rutting for the pavement material.

The results of ANOVA and Duncan's grouping on the phase angle of the original binders and TFOT-163°C-aged binders at 60°C and 10 rad/sec are shown in Table 4.5. The phase angle (δ) is an indicator of the relative amounts of recoverable and non-recoverable deformation. A material with higher δ (up to 90 degrees) acts like a viscous liquid. A material with lower δ (up to 0 degree) behaves like an elastic solid. It can be noted that all modifiers decrease the phase angle of the binder in comparison to the unmodified binder. The phase angle decreases as the concentration of modifier increases. The phase angle decreases after the binder ages -- that is, its elastic response becomes more prominent. The increase in elastic component, as reflected by a lower phase angle, should give the binder improved resistance to permanent deformation. All modifiers in this study are effective in improving the properties at high pavement temperatures by increasing the value of G* and by slightly reducing the value of sinδ or δ.

Figure 4.3 shows the relationship between complex modulus at 10 rad/sec and test temperature for the unaged Gilsonite modified AC-5 binders. The results of regression analyses on the relationship between the complex modulus and temperature are also shown in Table 4.6. It can be seen that the regression equations have a high goodness of

Table 4.5 Results of ANOVA and Duncan's Grouping on the Phase Angle at 60°C at 10 rad/sec of the Original Binders and TFOT-163°C-aged Binders

Dependent Variable:Phase Angle [Model = $\mu + \alpha_i + \beta_j + (\alpha\beta)_{ij} + \epsilon_{ijk}$]

Source	DF	ANOVA SS	Mean Square	F Value	Pr > F
ASPHALT, α	23	3551.956867	154.432907	53.16	0.0001
METHOD, β	1	446.225203	446.225203	153.61	0.0001
INTERACTION, $\alpha\beta$	23	52.365962	2.276781	0.78	0.7330

R-Square= 0.966722

Duncan Grouping at Method=Original

Duncan Grouping	Mean	N	ASPHALT
A	86.148	2	AC-5
B A	84.107	2	AC-10
B A			
B A	83.949	2	AC-20
B A			
B A	83.376	2	AC-5 +5%Gilsonite
B A			
B A	83.360	2	AC-30
B B C	80.648	2	AC-10 +5%Gilsonite
C			
D C	79.572	2	AC-20 +5%GTR
D C			
D C	79.354	2	AC-5 +10%Gilsonite
D C			
D C	78.954	2	AC-30 +3% SBR
D C			
D C E	78.579	2	AC-20 +1.5%SBR
D C E			
D C E	77.685	2	AC-20 +3% SEBS
D E			
D F E	76.571	2	AC-30 +5% GTR
D F E			
D G F E	75.895	2	AC-5 +15% Gilsonite
G F E			
G F E	75.001	2	AC-20 +10% Gilsonite
G F			
H G F	73.934	2	AC-20 +10%GTR
H G			
H G I	72.622	2	AC-20 +3.0% SBR
H I			
H I	71.411	2	AC-30 +10%GTR
H I			
H I J	70.659	2	AC-10 +15%Gilsonite
I J	69.692	2	AC-10 + BEV4
I J	69.600	2	AC-20 +4%EVA
I J	69.552	2	AC-20 +5% SEBS
K J	67.324	2	AC-20 4.5%SBR
K	65.843	2	AC-30 +15%Gilsonite
K	65.026	2	AC-20 +15%GTR

Table 4.5 Continued

Duncan Grouping at Method =TFOT 163°C

Duncan Grouping	Mean	N	ASPHALT
A	84.013	2	AC-5
A			
B A	81.920	2	AC-10
B			
B C	79.539	2	AC-20
B C			
B C	78.877	2	AC-30
B C			
B C	78.658	2	AC-5 + 5% Gilsonite
C			
D C	76.343	2	AC-10 + 5%Gilsonite
D C			
D C	75.517	2	AC-20 +1.5%SBR
D			
D E	73.655	2	AC-30 +3% SBR
D E			
D E	73.484	2	AC-5 +10%Gilsonite
D E			
D E	73.101	2	AC-20 +3%SEBS
D E			
D E	72.724	2	AC-20 +5%GTR
D E			
D E	72.532	2	AC-30 +5% GTR
E			
F E	70.021	2	AC-20 +3.0%SBR
F E			
F E	69.657	2	AC-10 +10% Gilsonite
F E			
F E G	69.375	2	AC-5 +15%Gilsonite
F G			
F H G	67.640	2	AC-10 +4% EVA
F H G			
F H G	67.622	2	AC-30 +10%GTR
F H G			
F H G	67.335	2	AC-20 +10%GTR
H G			
I H G	65.401	2	AC-20 +4.5%SBR
I H G			
I H G	65.196	2	AC-20 +5% SEBS
I H			
I H	65.105	2	AC-20 +4%EVA
I H			
I H J	64.568	2	AC-10 +15%Gilsonite
I J			
I J	62.280	2	AC-20 + 15%GTR
J	60.815	2	AC-30 +15% GTR

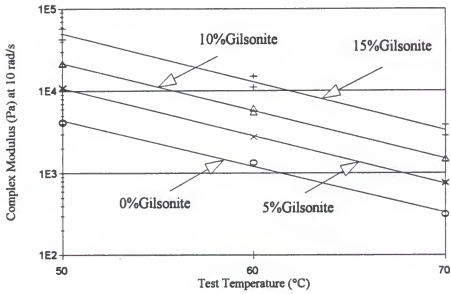

Figure 4.3 Relationship Between Complex Modulus at 10 rad/sec and Test Temperature for Unaged Gilsonite Modified AC-5 Binders

Table 4.6 Summary of Results of Regression Analyses on the Relationship between the Complex Modulus and Temperature

Regression Equation: Log (Complex Modulus) = bo + b1 (Temperature)

Asphalt Type	Unaged			TFOT 163°C		
	bo	b1	R Square	bo	b1	R Square
AC-5	6.248	-0.056	0.99	6.841	-0.059	1.00
AC-5+5%Gilsonite	6.915	-0.058	1.00	7.236	-0.058	1.00
AC-5+10%Gilsonite	7.237	-0.058	1.00	7.682	-0.060	1.00
AC-5+15%Gilsonite	7.630	-0.059	0.98	7.851	-0.058	1.00
AC-10	6.991	-0.059	1.00	7.112	-0.059	1.00
AC-10+5%Gilsonite	7.527	-0.062	1.00	7.592	-0.060	1.00
AC-10+10%Gilsonite	7.456	-0.059	1.00	7.869	-0.058	1.00
AC-10+15%Gilsonite	8.124	-0.062	1.00	8.160	-0.058	1.00
AC-10+4%EVA	6.491	-0.044	0.99	7.067	-0.048	1.00
AC-20	7.041	-0.058	1.00	7.586	-0.062	1.00
AC-20+5%GTR	6.868	-0.054	1.00	7.427	-0.057	1.00
AC-20+10%GTR	6.705	-0.047	1.00	7.275	-0.052	1.00
AC-20+15%GTR	6.438	-0.039	1.00	7.152	-0.048	1.00
AC-20+1.5%SBR	7.207	-0.058	1.00	7.432	-0.057	1.00
AC-20+3.0%SBR	7.152	-0.053	1.00	7.387	-0.056	1.00
AC-20+4.5%SBR	6.940	-0.048	1.00	7.257	-0.053	1.00
AC-20+3.0%SEBS	7.130	-0.055	1.00	7.668	-0.059	0.98
AC-20+5.0%SEBS	7.250	-0.052	1.00	7.769	-0.056	0.98
AC-20+4%EVA	6.482	-0.041	0.98	7.425	-0.049	0.97
AC-30	7.218	-0.059	1.00	7.435	-0.058	1.00
AC-30+5%GTR	7.488	-0.059	1.00	7.408	-0.055	1.00
AC-30+10%GTR	7.166	-0.053	1.00	7.416	-0.053	1.00
AC-30+15%GTR	7.108	-0.049	1.00	7.196	-0.048	1.00
AC-30+3.0%SBR	7.359	-0.059	1.00	7.383	-0.055	1.00

fit as seen from the high R^2 values. The regression lines are parallel shifted upward and downward with respect to one another.

4.3 Effects of Modifiers on the Intermediate-Temperature Properties

4.3.1 Penetration

The penetration test is an empirical test used to measure the consistency of asphalt cement. The results of the penetration tests at 25°C on the unaged and aged binders are given in Appendix A.4. The results of ANOVA and Duncan's grouping on the penetration at 25°C of the original and PAV-20 hour-aged binders are shown in Table 4.7. It can be seen that the penetrations of the gilsonite modified binders are lower than those of the base asphalt before aging and after aging. After the PAV aging, the penetrations of binders modified with a higher level of gilsonite are lower than those of the control AC-30. However, the ground tire rubber, SBR and SEBS modified binders generally have a lower penetration than the base asphalts before aging, and they generally have about the same or slight higher penetration as compared with the base asphalts after aging. Figure 4.4 displays the comparison of penetration at 25°C for the unaged and PAV-20 hour-aged ground tire rubber modified binders.

4.3.2 Results of Dynamic Shear Rheometer Test

The results of the dynamic shear rheometer tests on the PAV aged binders at intermediate temperatures are given in Appendices A.2 and A.3. The results of ANOVA and Duncan's grouping on the complex shear modulus at 20°C and 10 rad/sec of the PAV-20 hour-aged binders are shown in Table 4.8. The G*(complex shear modulus) represents the total resistance to deformation under load. It can be noted that all

Table 4.7 Results of ANOVA and Duncan's Grouping on the Penetration at 25°C of the Original Binders and PAV-20 hour-aged Binders

Dependent Variable:Penetration [Model = $\mu + \alpha_i + \beta_j + (\alpha\beta)_{ij} + \epsilon_{ijk}$]

Source	DF	ANOVA SS	Mean Square	F Value	Pr > F
ASPHALT, α	23	27146.40625	1180.27853	40.89	0.0001
METHOD, β	1	29786.26042	29786.26042	1031.93	0.0001
INTERACTION, $\alpha\beta$	23	11156.98958	485.08650	16.81	0.0001

R-Square=0.980058

Duncan Grouping at Method= Unaged

Duncan Grouping	Mean	N	ASPHALT
A	161.500	2	AC-5
B	110.000	2	AC-10
B	96.500	2	AC-5+5% Gilsonite
C	74.500	2	AC-20+4.5%SBR
C			
D C	72.500	2	AC-20
D C			
D C E	70.000	2	AC-10+4%EVA
D C E			
D F C E	62.500	2	AC-20+1.5%SBR
D F C E			
G D F C E	62.000	2	AC-10+5%Gilsonite
G D F C E			
G D F C E	61.000	2	AC-20+5%GTR
G D F C E			
G D F C E	59.500	2	AC-5+10%Gilsonite
G D F C E			
G D F C E	58.500	2	AC-20+3.0%SBR
G D F C E			
G D F C E	57.500	2	AC-20+10%GTR
G D F E			
G D F H E	56.500	2	AC-30+3.0%SBR
G D F H E			
G D F H E I	55.000	2	AC-30
G F H E I			
G J F H E I	52.500	2	AC-20+3.0%SEBS
G J F H I			
G J F H I	51.500	2	AC-20+15%GTR
G J F H I			
G J F H I	50.500	2	AC-20+4%EVA
G J F H I			
G J F H I	49.000	2	AC-30+5%GTR
G J F H I			
G J F H I	47.500	2	AC-30+10%GTR
G J H K I	44.000	2	AC-30+15%GTR
J H K I	39.500	2	AC-10+10%Gilsonite
J K I	37.500	2	AC-20+5.0%SEBS
J K	36.000	2	AC-5+15%Gilsonite
K	27.500	2	AC-10+15%Gilsonite

Table 4.7 Continued

Duncan Grouping at Method=PAV 20 hours

Duncan Grouping	Mean	N	ASPHALT
A	49.500	2	AC-5
B	43.000	2	AC-20+4.5%SBR
C	33.500	2	AC-10
C			
D C	33.000	2	AC-5+5% Gilsonite
D			
D E	30.500	2	AC-10+4%EVA
E			
E	30.000	2	AC-20+3.0%SEBS
E			
F E	28.000	2	AC-20+5.0%SEBS
F			
F G	27.000	2	AC-20+10%GTR
F G			
F G	27.000	2	AC-30+15%GTR
F G			
F G	26.500	2	AC-20+15%GTR
F G			
F G	26.500	2	AC-20+3.0%SBR
F G			
F G H	26.000	2	AC-20+1.5%SBR
F G H			
F G H	26.000	2	AC-30+10%GTR
F G H			
F G H	26.000	2	AC-20
G H			
I G H	25.000	2	AC-10+5%Gilsonite
I G H			
I G H	25.000	2	AC-20+5%GTR
I G H			
I G H	24.500	2	AC-30+5%GTR
I H			
I H	23.500	2	AC-30+3.0%SBR
I			
I	22.500	2	AC-20+4%EVA
I			
I	22.500	2	AC-30
I			
I	22.500	2	AC-5+10%Gilsonite
J	19.000	2	AC-10+10%Gilsonite
J	17.000	2	AC-5+15%Gilsonite
K	13.500	2	AC-10+15%Gilsonite

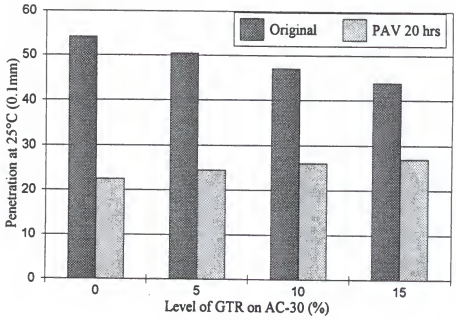

Figure 4.4 Comparison of Penetration at 25°C for Unaged and PAV-20 hour-aged Ground Tire Rubber Modified Binders

Table 4.8 Results of ANOVA and Duncan's Grouping of PAV-20 hour-aged Binders on the basis of Complex Modulus at 20°C at 10 rad/sec

Dependent Variable: Complex Modulus

Source	DF	ANOVA SS	Mean Square	F Value	Pr > F
Model	23	4.32423E+14	1.88010E+13	108.20	0.0001
Error	24	4.17036E+12	1.73765E+11		
Corrected Total	47	4.36593E+14			

R-Square= 0.990448

Duncan Grouping	Mean	N	ASPHALT
A	14141847	2	AC-10+15%Gilsonite
B	10166800	2	AC-5+15%Gilsonite
C	8805177	2	AC-20+5.0%SEBS
C	8729457	2	AC-10+10%Gilsonite
D	6012600	2	AC-5+10%Gilsonite
D			
E D	5715033	2	AC-10+5%Gilsonite
E			
E F	5002148	2	AC-30
F			
G F	4300000	2	AC-30+5%GTR
G F			
G F	4200000	2	AC-20+4%EVA
G			
G H	4024686	2	AC-20+3.0%SEBS
G H			
G H I	3977893	2	AC-30+3.0%SBR
G H I			
G J H I	3605400	2	AC-10+4%EVA
G J H I			
G J H I	3537300	2	AC-5+5% Gilsonite
G J H I			
K G J H I	3388802	2	AC-30+10%GTR
K J H I			
K L J H I	3217486	2	AC-10
K L J H I			
K L J H I	3156519	2	AC-30+15%GTR
K L J I			
K L J M I	3005051	2	AC-20
K L J M			
K L J M N	2700000	2	AC-20+5%GTR
K L M N			
K L O M N	2433085	2	AC-20+1.5%SBR
L O M N			
L O M N	2269058	2	AC-20+10%GTR
O M N			
O M N	2181911	2	AC-20+15%GTR
O N	1900000	2	AC-20+3.0%SBR
O	1700000	2	AC-20+4.5%SBR
O	1488200	2	AC-5

modifiers increase the complex shear modulus of the unaged binder. After PAV-20 hour-aging, some modifiers, such as SBR and GTR, show the effect of decreasing the modulus of the binder. The modified AC-20 binders (with 5% GTR, 10% GTR, 15% GTR, 1.5% SBR, 3% SBR and 4.5% SBR) have a complex modulus as low as that of an aged AC-5 after PAV. The modified AC-30 binders (with 5% GTR, 10% GTR, 15% GTR, and 3% SBR) have a complex modulus as low as that of an aged AC-10 or AC-20 after PAV process.

The results of ANOVA and Duncan's grouping on the phase angle at 20°C and 10 rad/sec of the PAV-20 hour-aged binders are shown in Table 4.9. It can be noted that most modifiers decrease the phase angle of the binder in comparison to the unmodified binder. The difference in phase angle among aged binders is not as significant as the difference in complex modulus.

Figure 4.5 shows the relationship between complex shear modulus at 20°C and 10 rad/sec and level of Gilsonite addition to AC-5 after PAV-20 hour-aging. The results of regression analyses for the relationship between complex shear modulus at 20°C and level of modifier addition for the PAV-20 hour-aged binders are shown in Table 4.10. All GTR- and SBR-modified binders have a negative b1 while the gilsonite-, EVA- and SEBS-modified binders have a positive b1. A reduction in the complex shear modulus of PAV-aged binders at an intermediate pavement temperature usually means a higher resistance to fatigue cracking for the pavement material.

The complex shear modulus increases as the temperature decreases. Figure 4.6 shows the relationship between complex modulus at 10 rad/sec and test temperature for

Table 4.9 Results of ANOVA and Duncan's Grouping of PAV-20 hour-aged Binders on the basis of Phase Angle at 20°C at 10 rad/sec

Dependent Variable: Phase Angle

Source	DF	ANOVA SS	Mean Square	F Value	Pr > F
Model	23	553.4726139	24.0640267	8.91	0.0001
Error	24	64.8342635	2.7014276		
Corrected Total	47	618.3068773			

R-Square= 0.895142

Duncan Grouping	Mean	N	ASPHALT
A	50.683	2	AC-5
B A	47.753	2	AC-10
B C	46.474	2	AC-20
B C D	46.049	2	AC-20+5%GTR
B C D			
B E C D	45.405	2	AC-30+3.0%SBR
B E C D			
F B E C D	45.192	2	AC-5+5% Gilsonite
F B E C D			
F B E C D G	44.977	2	AC-20+1.5%SBR
F B E C D G			
F B E C H D G	44.705	2	AC-20+10%GTR
F B E C H D G			
F B E C H D G	44.348	2	AC-30
F E C H D G			
F E C H D G	43.705	2	AC-30+3.0%SBR
F E C H D G			
F E C H D G	43.505	2	AC-20+15%GTR
F E C H D G			
F I E C H D G	42.855	2	AC-30+5%GTR
F I E H D G			
F I E J H D G	42.400	2	AC-20+4.5%SBR
F I E J H D G			
F I E J H D G	42.336	2	AC-20+3.0%SEBS
F I E J H D G			
F I E J H D G	42.305	2	AC-10+5%Gilsonite
F I E J H D G			
F I E J H D G	42.235	2	AC-10+4%EVA
F I E J H G			
F I E J H G	42.000	2	AC-30+10%GTR
F I J H G			
F I J H G	41.242	2	AC-5+10%Gilsonite
I J H G			
I J H G	41.000	2	AC-20+4%EVA
I J H	40.800	2	AC-30+15%GTR
I J K	39.030	2	AC-20+5.0%SEBS
J K	38.463	2	AC-10+10%Gilsonite
L K	37.051	2	AC-5+15%Gilsonite
L	34.782	2	AC-10+15%Gilsonite

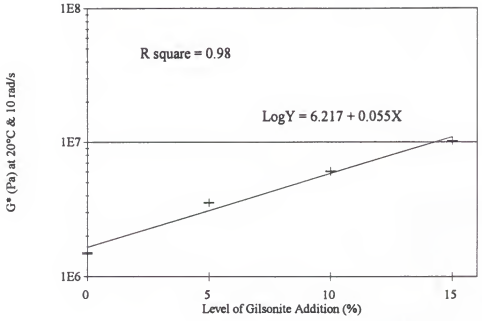

Figure 4.5 Relationship Between Complex Modulus at 20°C and 10 rad/sec and Level of Gilsonite Addition to PAV-20 hour-aged AC-5

Table 4.10 Summary of Results of Regression Analyses Relating the Complex Modulus at 20°C to the Level of Modifier Added for PAV-20 hour-aged Binders

Regression Equation: Log(Complex Modulus) = bo + b1 (Level of Modifier)

Asphalt type	AC-5	AC-10	AC-10	AC-20
Added Modifier	Gilsonite	Gilsonite	EVA	EVA
bo	6.217	6.522	6.508	6.478
b1	0.055	0.042	0.012	0.035
R^2	0.98	1.00	0.98	0.70

Asphalt type	AC-20	AC-30	AC-20	AC-30	AC-20
Added Modifier	GTR	GTR	SBR	SBR	SEBS
bo	6.473	6.694	6.471	6.699	6.435
b1	-0.010	-0.014	-0.058	-0.033	0.089
R^2	0.71	0.82	0.80	1.00	0.79

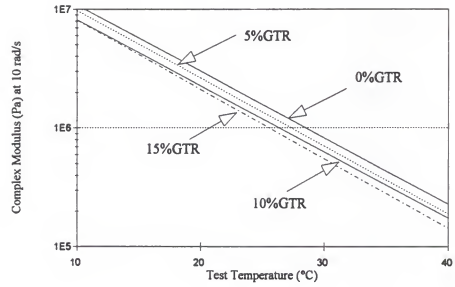

Figure 4.6 Relationship Between Complex Modulus at 10 rad/sec and Test Temperature on PAV-20 hour-aged GTR Modified AC-20 Binders

the PAV-20 hour-aged GTR-modified AC-20 binders. The results of regression analyses for relating the complex modulus to intermediate pavement service temperatures are also shown in Table 4.11. It can be seen that the regression equations have an excellent goodness of fit.

According to SHRP binder specifications, the parameter G*sinδ is an indicator of resistance to fatigue cracking and should not exceed a value of 5,000 kPa at a specified intermediate temperature, which is equal to 4°C plus the mean of the maximum and minimum pavement design temperatures. Table 4.12 shows the results of ANOVA and Duncan's grouping of PAV-20 hour-aged binders on the basis of G*sinδ at 20°C at 10 rad/sec. It can be seen that the addition of the ground tire rubber and SBR both result in a substantial decrease in the G*sinδ values of the asphalt binders after PAV-aging. The modified AC-20 binders (with 5% GTR, 10% GTR, 15% GTR, 1.5% SBR, 3% SBR and 4.5% SBR) have G*sinδ values as low as that of an aged AC-5 after PAV as seen from Table 4.12. The modified AC-30 binders (with 5% GTR, 10% GTR, 15% GTR, and 3% SBR) have G*sinδ values as low as that of aged AC-10 or AC-20 after PAV. Figure 4.7 displays the relationship between G*sinδ and temperature for PAV-20 hour-aged SBR modified AC-20 binders. At 10°C, only the binders modified with 3% and 4.5% of SBR can meet the maximum limit of 5,000 kPa. These modifiers show the potential to reduce fatigue cracking.

4.3.3 Results of Constant Stress Rheometer Test

The results of the constant power viscosity at 5°C and 25°C of the different binders before and after aging are given in Appendix A.5 and A.6. The results of

Table 4.11 Summary of Results of Regression Analyses for Relating the Complex Modulus at 10 rad/sec to Temperature for PAV-20 hour-aged Binders

Regression Equation: Log (Complex Modulus) = bo + b1 (Temperature)

Asphalt Type	bo	b1	R Square
AC-5	7.435	-0.064	1.00
AC-5+5% Gilsonite	7.661	-0.057	1.00
AC-5+10%Gilsonite	7.866	-0.055	1.00
AC-5+15%Gilsonite	8.064	-0.054	1.00
AC-10	7.619	-0.059	0.99
AC-10+5%Gilsonite	7.876	-0.057	1.00
AC-10+10%Gilsonite	7.966	-0.052	1.00
AC-10+15%Gilsonite	8.134	-0.051	0.99
AC-10+4%EVA	7.700	-0.058	1.00
AC-20	7.597	-0.056	1.00
AC-20+5%GTR	7.561	-0.057	0.99
AC-20+10%GTR	7.467	-0.056	1.00
AC-20+15%GTR	7.494	-0.058	1.00
AC-20+1.5%SBR	7.548	-0.059	0.99
AC-20+3.0%SBR	7.436	-0.058	0.99
AC-20+4.5%SBR	7.310	-0.055	0.99
AC-20+3.0%SEBS	7.662	-0.054	0.97
AC-20+5.0%SEBS	7.999	-0.054	1.00
AC-20+4%EVA	7.745	-0.056	0.99
AC-30	7.834	-0.058	1.00
AC-30+5%GTR	7.759	-0.057	0.99
AC-30+10%GTR	7.630	-0.055	0.99
AC-30+15%GTR	7.549	-0.054	1.00
AC-30+3.0%SBR	7.754	-0.058	1.00

Table 4.12 Results of ANOVA and Duncan's Grouping of PAV-20 hour-aged Binders on the Basis of G*sinδ at 20°C at 10 rad/sec

Dependent Variable: G*sinδ

Source	DF	ANOVA SS	Mean Square	F Value	Pr > F
Model	23	1.39145E+14	6.04980E+12	63.13	0.0001
Error	24	2.30001E+12	9.58339E+10		
Corrected Total	47	1.41445E+14			

R-Square= 0.983739

Means with the same letter are not significantly different.

Duncan Grouping	Mean	N	ASPHALT
A	8067253	2	AC-10+ 15% Gilsonite
B	6125676	2	AC-5+15% Gilsonite
C B	5545855	2	AC-20+5% SEBS
C	5429842	2	AC-10+10% Gilsonite
D	3963691	2	AC-5+10% Gilsonite
D	3846635	2	AC-10+5% Gilsonite
D			
E D	3496573	2	AC-30
E			
E F	2924166	2	AC-30+5% GTR
E F			
E F G	2832613	2	AC-30+3% SBR
F G			
H F G	2770693	2	AC-20+ 4% EVA
H F G			
H F G	2717921	2	AC-20+3% SEBS
H F G			
H I F G	2509609	2	AC-5+5% Gilsonite
H I F G			
J H I F G	2423351	2	AC-10+ 4% EVA
J H I F G			
J H I F G	2381751	2	AC-10
J H I F G			
J H I F G K	2265317	2	AC-30+10% GTR
J H I G K			
J H I L G K	2178837	2	AC-20
J H I L K			
J H I L K	2060494	2	AC-30+15% GTR
J I L K			
J M I L K	1943645	2	AC-20+5% GTR
J M L K			
J M L N K	1719752	2	AC-20+1.5% SBR
M L N K			
M L N K	1594879	2	AC-20+10% GTR
M L N			
M L N	1501015	2	AC-20+15% GTR
M N	1319697	2	AC-20+3.0% SBR
N	1152495	2	AC-20+4.5% SBR
N	1151330	2	AC-5

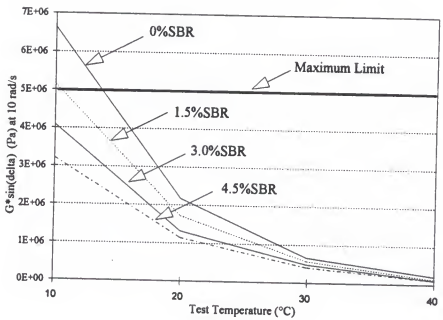

Figure 4.7 Plot of G*sin(delta) versus Temperature for PAV-20 hour-aged SBR Modified AC-20 Binders

ANOVA and Duncan's grouping of the PAV-40 hour-aged binders on the basis of constant power viscosity at 5°C and 25°C are shown in Table 4.13. It can be seen that there are no significant difference among the constant power viscosity at 25°C of the different binders after PAV-40 hour-aging except for the binders modified with 15% gilsonite. The binders with the highest level of modifier added usually have a higher viscosity at 5°C. These modified binders include AC-10+15% gilsonite, AC-20+15% GTR, AC-20+4.5% SBR, AC-20+5% SEBS, AC-20+ 4% EVA and AC-30+15% GTR. The constant power viscosity at 5°C of the modified AC-20 binders after the standard TFOT process at 185°C are plotted in Figure 4.8. These viscosity values are compared with a limit of 2×10^9 Pa.sec (2×10^{10} poises), which is usually used as the maximum allowable binder viscosity to avoid low temperature cracking of the asphalt mixture in service. As shown in Figure 4.8, five residues exhibit a viscosity value exceeding this limit. They are aged residues of AC-20 group with 10% GTR, 15% GTR, 3% SEBS, 5% SEBS and 4% EVA. However, the residues with three different concentrations of SBR are all within the limit. The SBR modifiers shows the potential to reduce cracking.

4.4 Effects of Modifiers on the Low-Temperature Properties

4.4.1 Fraass Breaking Point Test

The Fraass breaking point temperatures of the different binders before and after the CTO, TFOT and PAV processes are given in Appendix A.7. The results of ANOVA and Duncan's grouping of unaged and CTO-72 hour-aged binders on the basis of Fraass breaking point are shown in Table 4.14. Figure 4.9 displays the comparison of Fraass breaking point temperatures of the unaged and PAV-20 hour-aged AC-20 binders. The

Table 4.13 Results of ANOVA and Duncan's Grouping of PAV-40 hour-aged Binders at 5°C and 25°C on the Basis of Constant Power Viscosity

Dependent Variable:Constant Power Viscosity [Model = $\mu + \alpha_i + \beta_j + (\alpha\beta)_{ij} + \epsilon_{ijk}$]

Source	DF	ANOVA SS	Mean Square	F Value	Pr > F
ASPHALT, α	23	1.71640E+21	7.46262E+19	7.31	0.0001
METHOD, β	1	3.82803E+21	3.82803E+21	374.86	0.0001
INTERACTION, $\alpha\beta$	23	1.69941E+21	7.38874E+19	7.24	0.0001

R-Square= 0.936621

Duncan Grouping at Method= 5°C

Duncan Grouping	Mean	N	ASPHALT
A	2.99497E10	2	AC-30+15% GTR
B A	2.57079E10	2	AC-20+5% SEBS
B A	2.55931E10	2	AC-20+ 4% EVA
B A C	2.36164E10	2	AC-10+ 15% Gilsonite
B A C			
B A C	2.3222E10	2	AC-20+15% GTR
B A C			
B A C	2.27725E10	2	AC-20+4.5% SBR
B C			
B D C	1.87903E10	2	AC-30+10% GTR
D C			
E D C	1.45905E10	2	AC-20+10% GTR
E D C			
E D C	1.4577E10	2	AC-20+3.0% SBR
E D C			
E D C	1.44929E10	2	AC-30+5% GTR
E D			
E D F	1.21902E10	2	AC-20+3% SEBS
E D F			
E G D F	1.10622E10	2	AC-10+10% Gilsonite
E G D F			
E G D F	9622355108	2	AC-5+15% Gilsonite
E G D F			
E G D F	9181897245	2	AC-20+5% GTR
E G D F			
E G D F	9003291091	2	AC-20+1.5% SBR
E G F			
E G F	7303346477	2	AC-30
E G F			
E G F	6639684448	2	AC-10+ 4% EVA
E G F			
E G F	5724008561	2	AC-20
E G F			
E G F	5549505184	2	AC-30+3% SBR
E G F	5178352248	2	AC-10+5% Gilsonite
E G F	4278553841	2	AC-5+10% Gilsonite
G F	2277724218	2	AC-10
G F	1960595609	2	AC-5+5% Gilsonite
G	843529698	2	AC-5

Table 4.13 Continued

Duncan Grouping at Method= 25°C

Means with the same letter are not significantly different.

Duncan Grouping	Mean	N	ASPHALT
A	226407515	2	AC-10+ 15% Gilsonite
B	174575695	2	AC-5+15% Gilsonite
C	92815534	2	AC-20+5% SEBS
C			
D C	66453961	2	AC-10+10% Gilsonite
D C			
D C E	49934846	2	AC-20+ 4% EVA
D C E			
D C E	48038472	2	AC-20+3% SEBS
D C E			
D C E	43002186	2	AC-30+15% GTR
D C E			
D C E	42166477	2	AC-5+10% Gilsonite
D E			
D E	40586679	2	AC-20+15% GTR
D E			
D E	31071552	2	AC-20+10% GTR
D E			
D E	29860038	2	AC-30+10% GTR
D E			
D E	24410268	2	AC-10+ 4% EVA
D E			
D E	20736243	2	AC-30+5% GTR
D E			
D E	18924546	2	AC-20+4.5% SBR
D E			
D E	18171178	2	AC-10+5% Gilsonite
D E			
D E	17887731	2	AC-20+3.0% SBR
D E			
D E	16950537	2	AC-20+5% GTR
D E			
D E	15164308	2	AC-30
D E			
D E	14742000	2	AC-20
D E			
D E	12560119	2	AC-20+1.5% SBR
E			
E	7531450	2	AC-5+5% Gilsonite
E			
E	4878365	2	AC-30+3% SBR
E	3751442	2	AC-10
E	1560000	2	AC-5

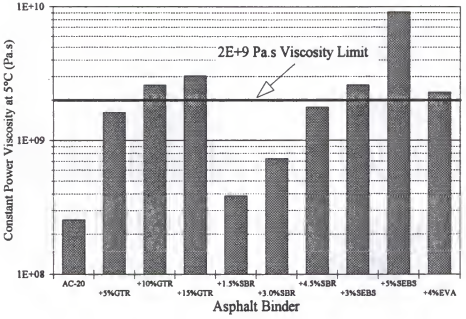

Figure 4.8 Comparison of Constant Power Viscosity at 5°C for TFOT-185C-aged Unmodified and Modified AC-20 Binders

Table 4.14 Results of ANOVA and Duncan's Grouping of Original and CTO-72 hour-aged Binders on the basis of Fraass Breaking Point

Dependent Variable:Fraass Breaking Point [Model = $\mu + \alpha_i + \beta_j + (\alpha\beta)_{ij} + \epsilon_{ijk}$]

Source	DF	ANOVA SS	Mean Square	F Value	Pr > F
ASPHALT, α	23	689.9348958	29.9971694	17.27	0.0001
METHOD, β	1	690.6901042	690.6901042	397.64	0.0001
INTERACTION, $\alpha\beta$	23	113.2473958	4.9237998	2.83	0.0012

R-Square=0.947139

Duncan Grouping at Method= Original

Duncan Grouping	Man	N	ASPHALT
A	5.500	2	AC-10+ 15% Gilsonite
B	-8.750	2	AC-5+15% Gilsonite
B			
C B	-9.000	2	AC-20+5% SEBS
C B			
C B D	-9.750	2	AC-10+10% Gilsonite
C B D			
C B D	-10.000	2	AC-20+3% SEBS
C B D			
C E B D	-10.250	2	AC-30
C E B D			
F C E B D	-10.500	2	AC-30+5% GTR
F C E B D			
F C E B D	-10.500	2	AC-30+3% SBR
F C E B D			
F C E B D	-10.750	2	AC-20+ 4% EVA
F C E B D			
F C E B D	-11.000	2	AC-20
F C E B D			
F C E B D	-11.000	2	AC-20+1.5% SBR
F C E B D			
F C E B D	-11.000	2	AC-5+10% Gilsonite
F C E B D			
F C E B D	-11.500	2	AC-10+5% Gilsonite
F C E B D			
F C E B D	-11.500	2	AC-30+10% GTR
F C E D			
F C E G D	-11.750	2	AC-20+5% GTR
F E G D			
F E G D	-12.000	2	AC-20+3.0% SBR
F H E G D	-12.500	2	AC-30+15% GTR
F H E G	-13.000	2	AC-10
F H E G	-13.000	2	AC-20+10% GTR
F H E G	-13.000	2	AC-5+5% Gilsonite
F H G	-13.250	2	AC-10+ 4% EVA
H G	-14.500	2	AC-20+15% GTR
H	-15.250	2	AC-5
I	-21.000	2	AC-20+4.5% SBR

Table 4.14 Continued

Duncan Grouping at Method= CTO-72 hour-aging

Means with the same letter are not significantly different.

Duncan Grouping	Mean	N	ASPHALT
A	-1.500	2	AC-10+ 15% Gilsonite
A			
A	-2.000	2	AC-5+15% Gilsonite
A			
B A	-2.500	2	AC-10+10% Gilsonite
B A			
B A C	-3.500	2	AC-30
B A C			
B A C	-3.500	2	AC-10+5% Gilsonite
B A C			
B D A C	-4.000	2	AC-5+10% Gilsonite
B D A C			
B D A C	-4.000	2	AC-10
B D A C			
B D A C	-4.000	2	AC-20
B D A C			
B D A C	-4.000	2	AC-20+ 4% EVA
B D A C			
B D A C	-4.000	2	AC-30+3% SBR
B D C			
B D E C	-5.500	2	AC-20+5% SEBS
D E C			
F D E C	-6.000	2	AC-10+ 4% EVA
F D E C			
G F D E C	-6.500	2	AC-30+5% GTR
G F D E C			
G F D E C	-6.500	2	AC-5+5% Gilsonite
G F D E			
G F D E	-7.000	2	AC-20+3% SEBS
G F E			
G F E H	-7.500	2	AC-20+5% GTR
G F E H			
G F E H	-8.000	2	AC-20+1.5% SBR
G F H			
G F I H	-9.000	2	AC-30+10% GTR
G F 1 H			
G F I H	-9.000	2	AC-20+10% GTR
G 1 H			
G I H	-9.500	2	AC-20+3.0% SBR
1 H	-10.500	2	AC-5
1 H	-10.500	2	AC-30+15% GTR
1	-11.500	2	AC-20+4.5% SBR
1	-11.500	2	AC-20+15% GTR

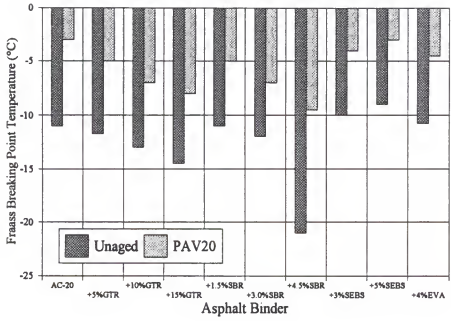

Figure 4.9 Comparison of Fraass Breaking Point Temperatures of Unaged and PAV-20 hour-aged AC-20 Binders

SBR modified binders can be seen to exhibit a significantly lower Fraass breaking temperature than the other binders while the gilsonite elevates the Fraass breaking temperature more as the concentration increases. After the severe CTO-72 hour-aging, some modified residues, such as AC-20+GTR, AC-20+SBR, AC-30+GTR, have a Fraass breaking temperature as low as that of an AC-5 residue as seen in Table 4.14. The modification with the ground tire rubber and SBR also tends to prevent the sudden rupture of the asphalt test specimen that usually happens in the other unmodified and modified asphalt test specimens, such as the gilsonite, EVA and SEBS modified binders.

4.4.2 Results of Bending Beam Rheometer Test

The creep stiffness and m-value at -12°C and -24°C of the PAV-20 hour-aged residues are given in Appendix A.8 and A.9. The results of ANOVA and Duncan's grouping of the creep stiffness at -12°C and -24°C of the PAV-20 hour-aged residues are shown in Table 4.15. It can be seen that the gilsonite modified binders usually have the highest stiffness and are followed by SEBS and EVA modified binders. After the severe PAV-20 hour-aging, some modified AC-20 and AC-30 residues, such as AC-20+GTR, AC-20+SBR, AC-30+GTR, have a creep stiffness as low as that of an AC-5 residue as seen in Table 4.15.

Current SHRP Binder Specifications require that the creep stiffness not exceed 300 MPa at a loading time of 60 seconds and a minimum m-value of 0.3 for PAV-aged asphalt binders at 10°C above the minimum pavement design temperature. The limiting stiffness temperature (below which low-temperature cracking would occur) is 10°C below the temperature at which the binder reaches this stiffness. Figure 4.10 displays the

Table 4.15 Results of ANOVA and Duncan's Grouping on the Creep Stiffness of PAV-20 hour-aged Binders at -12°C and -24°C

Dependent Variable: Creep Stiffness [Model = $\mu + \alpha_i + \beta_j + (\alpha\beta)_{ij} + \epsilon_{ijk}$]

Source	DF	ANOVA SS	Mean Square	F Value	Pr > F
ASPHALT, α	23	375289.772	16316.947	72.52	0.0001
METHOD, β	1	2093999.035	2093999.035	9306.51	0.0001
INTERACTION, $\alpha\beta$	23	112413.048	4887.524	21.72	0.0001

R-Square=0.995834

Duncan Grouping at Method= -12°C

Duncan Groupin			Mean	N	ASPHALT
	A		176.450	2	AC-10+ 15% Gilsonite
	B		130.400	2	AC-10+10% Gilsonite
	B				
C	B		121.350	2	AC-5+15% Gilsonite
C	B				
C	B		117.650	2	AC-30
C					
C			113.550	2	AC-20+ 4% EVA
C					
C			113.500	2	AC-20+5% SEBS
C					
C			111.350	2	AC-20+3% SEBS
	D		98.365	2	AC-10+5% Gilsonite
	D				
E	D		95.005	2	AC-30+3% SBR
E	D				
E	D	F	88.500	2	AC-20+1.5% SBR
E	D	F			
E	D	F	87.530	2	AC-20
E	D	F			
E G	D	F	85.365	2	AC-5+10% Gilsonite
E G		F			
E G	H	F	83.400	2	AC-20+3.0% SBR
G	H	F			
G	H	F	78.330	2	AC-30+5% GTR
G	H	F			
G	H	F	76.185	2	AC-20+5% GTR
G	H				
I G	H		71.935	2	AC-30+10% GTR
I	H		70.885	2	AC-10+ 4% EVA
I			61.800	2	AC-20+10% GTR
I			60.355	2	AC-20+4.5% SBR
I			59.420	2	AC-30+15% GTR
I	J		58.580	2	AC-5+5% Gilsonite
I	J		58.365	2	AC-10
K	J		46.065	2	AC-20+15% GTR
K			39.555	2	AC-5

Table 4.15 Continued

Duncan Grouping at Method= -24°C

Means with the same letter are not significantly different.

Duncan Grouping	Mean	N	ASPHALT
A	601.60	2	AC-10+ 15% Gilsonite
B	529.15	2	AC-10+10% Gilsonite
B			
B	514.51	2	AC-20+5% SEBS
B			
C B	500.35	2	AC-30
C B			
C B D	484.90	2	AC-30+3% SBR
C D			
C E D	462.70	2	AC-5+ 15% Gilsonite
E D			
F E D	444.40	2	AC-20
F E			
F E	434.15	2	AC-20+ 4% EVA
F			
F G	403.55	2	AC-30+5% GTR
F G			
F G	400.27	2	AC-20+3% SEBS
G			
H G	379.40	2	AC-5+10% Gilsonite
H G			
H G I	369.35	2	AC-20+3.0% SBR
H G I			
H G I	369.05	2	AC-20+1.5% SBR
H G I			
H G I	361.55	2	AC-10+5% Gilsonite
H I			
H J I	351.60	2	AC-30+10% GTR
H J I			
H K J I	337.25	2	AC-20+5% GTR
K J I			
L K J I	326.95	2	AC-10+ 4% EVA
L K J			
L K J M	310.35	2	AC-10
L K J M			
L K J M	309.00	2	AC-5+5% Gilsonite
L K M			
L K M	298.00	2	AC-20+4.5% SBR
L M			
L M	287.05	2	AC-30+15% GTR
N M	265.45	2	AC-20+10% GTR
N	229.15	2	AC-5
N	223.30	2	AC-20+15% GTR

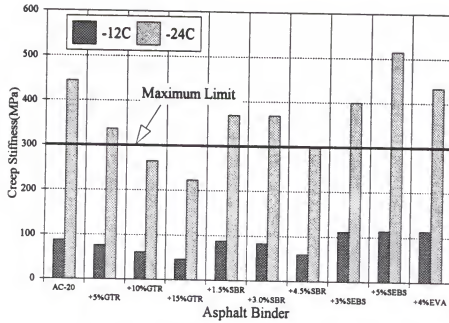

Figure 4.10 Comparison of Creep Stiffness at -12°C and -24°C for PAV-20 hour -aged AC-20 Binders

comparison of the creep stiffness at -12°C and -24°C of the PAV-20 hour-aged AC-20 binders at a loading time of 60 seconds. At -24°C, most of the modified AC-20 residues do not meet the maximum limit requirement, except for those modified with 10% GTR, 15% GTR and 4.5% SBR. If creep stiffness is too high, the binder will behave in a brittle manner, and cracking will be more likely.

Figure 4.11 shows the relationship between creep stiffness at -12°C at a loading time of 60 seconds and level of GTR added on AC-20 after PAV-20 hour-aged. The results of regression analyses on the relationship between the creep stiffness at -12°C and level of modifier added for PAV-20 hour-aged binders are shown in Table 4.16. The b1 in the regression equation indicates the increase or decrease rate of the creep stiffness due to the modifier added. The higher the b1 is, the more significant the effect of modifier is. All GTR and SBR modified AC-20 and AC-30 have a negative b1 while the gilsonite, EVA and SEBS-modified binders have a positive b1. A lower creep stiffness of PAV-aged binders at the low pavement service temperature usually means a higher resistance to cracking for the pavement material.

In the SHRP binder specification, the rate at which the binder stiffness changes with creep load at low temperatures is controlled using the m-value. A high m-value is desirable because this means that as the temperature changes and thermal stresses accumulate, the stiffness will decrease relatively fast. A relatively fast decrease in stiffness means that the binder will tend to shed stresses that would otherwise build up to a level where low temperature cracking would occur. An m-value greater than 0.3 is required by the SHRP binder specification. The results of ANOVA and Duncan's

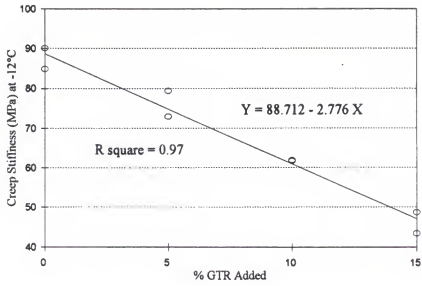

Figure 4.11 Relationship Between Creep Stiffness at -12°C and Level of GTR Added on PAV-20 hour-aged AC-20

Table 4.16 Summary of Results of Regression Analyses for the Relationship Between the Creep Stiffness at -12°C and the Level of Modifier Added

Regression Equation: Creep Stiffness = bo + b1 (Level of Modifier)

Asphalt Type	Added Modifier	bo	b1	R Square
AC-5	Gilsonite	35.39	5.44	0.98
AC-10	Gilsonite	57.95	7.73	0.97
AC-10	EVA	58.37	3.13	0.98
AC-20	EVA	87.53	6.51	0.92
AC-20	GTR	88.71	-2.78	0.97
AC-30	GTR	109.00	-3.62	0.92
AC-20	SBR	92.94	-5.78	0.66
AC-30	SBR	117.65	-7.55	0.80
AC-20	SEBS	89.70	5.41	0.81

grouping of PAV-20 hour-aged residues on the basis of m-value at -12°C and -24°C are shown in Table 4.17. It can be noted that the ground tire rubber modified binders have higher m-values among all modified binders, and are followed by the SBR modified binders. Figure 4.12 displays the comparison of m-value at -12°C and -24°C for PAV-20 hour-aged AC-20 binders. Among those PAV-aged binders that passed the stiffness requirement at -24°C, AC-20+ 15%GTR is the only one which passes the m-value requirement of 0.3.

4.4.3 Results of Direct Tension Test

As the temperature of a pavement decreases, it attempts to shrink. Restraint causes stresses to build up in the pavement. When these stresses exceed the strength of the binder, a crack occurs. Results [44, 46] have shown that if the binder can stretch to more than 1% of its original length during this shrinkage, cracks are less likely to occur. Therefore, the direct tension test is included in the SHRP specification. It is only applied to binders that have a creep stiffness between 300 and 600 MPa. If the creep stiffness is below 300 MPa, the direct tension test need not be performed, and the direct tension requirement does not apply. In this test, an asphalt sample is pulled at a very slow rate, which simulates the condition in the pavement as shrinkage occurs. The amount of strain that a sample can take before fracture is compared to the 1 percent minimum value required in the specification.

The results of the direct tension test at -12°C for PAV-20 hour-aged residues are given in Appendix A.10. Figure 4.13 shows the comparison of failure strain at -12°C for the PAV-20 hour-aged binders. It can be noted that some of the modified binders do not

Table 4.17 Results of ANOVA and Duncan's Grouping of PAV-20 hour-aged Binders on the Basis of m-value at -12°C and -24°C

Dependent Variable: m-value [Model = $\mu + \alpha_i + \beta_j + (\alpha\beta)_{ij} + \epsilon_{ijk}$]

Source	DF	ANOVA SS	Mean Square	F Value	Pr > F
ASPHALT, α	23	0.06229466	0.00270846	31.88	0.0001
METHOD, β	1	0.26156376	0.26156376	3078.35	0.0001
INTERACTION, αβ	23	0.00447299	0.00019448	2.29	0.0078

R-Square= 0.987731

Duncan Grouping at Method= -12°C

Duncan Grouping	Mean	N	ASPHALT
A	0.44150	2	AC-5
B	0.40600	2	AC-10
B			
C B	0.40100	2	AC-5+5% Gilsonite
C			
C D	0.38950	2	AC-20+15% GTR
D			
E D	0.38450	2	AC-30+15% GTR
E D			
E D F	0.38250	2	AC-20+10% GTR
E D F			
E D F	0.37950	2	AC-30+3% SBR
E D F			
E G D F	0.37700	2	AC-20
E G D F			
E G D F	0.37550	2	AC-20+5% GTR
E G D F			
E G D F	0.37400	2	AC-30+10% GTR
E G D F			
E G D F	0.37300	2	AC-20+1.5% SBR
E G D F			
E G D F	0.37300	2	AC-20+3.0% SBR
E G D F			
E G D F	0.37250	2	AC-20+4.5% SBR
E G F			
E G F	0.36950	2	AC-10+5% Gilsonite
E G F			
E G F	0.36750	2	AC-10+ 4% EVA
E G F			
E G F	0.36700	2	AC-5+10% Gilsonite
G F	0.36600	2	AC-30+5% GTR
G F	0.36500	2	AC-20+3% SEBS
G	0.35950	2	AC-30
H	0.33950	2	AC-10+10% Gilsonite
H	0.33600	2	AC-20+ 4% EVA
H	0.33500	2	AC-20+5% SEBS
H	0.33100	2	AC-5+15% Gilsonite
I	0.30650	2	AC-10+15% Gilsonite

Table 4.17 Continued

Duncan Grouping at Method= -24°C

Means with the same letter are not significantly different.

Duncan Grouping	Mean	N	ASPHALT
A	0.3235	2	AC-5
A			
B A	0.3015	2	AC-20+15% GTR
B			
B C	0.2995	2	AC-5+5% Gilsonite
B C			
B C D	0.2925	2	AC-10
B C D			
B E C D	0.2905	2	AC-20+5% GTR
B E C D			
B E C D	0.2865	2	AC-20+10% GTR
B E C D			
B E C D	0.2825	2	AC-10+ 4% EVA
B E C D			
B E C D	0.2825	2	AC-30+15% GTR
E C D			
F E C D	0.2745	2	AC-30+10% GTR
F E D			
F E D	0.2740	2	AC-30+3% SBR
F E D			
F E G D	0.2680	2	AC-20
F E G D			
F E G D	0.2670	2	AC-30+5% GTR
F E G			
F E G	0.2655	2	AC-5+10% Gilsonite
F G			
F G H	0.2555	2	AC-20+4.5% SBR
F G H			
F G H	0.2545	2	AC-20+ 4% EVA
F G H			
F G H	0.2520	2	AC-20+3% SEBS
F G H			
F G H	0.2495	2	AC-20+3.0% SBR
G H			
G H	0.2475	2	AC-20+1.5% SBR
G H			
I G H	0.2445	2	AC-30
I H			
I H	0.2385	2	AC-5+15% Gilsonite
I H			
I H	0.2375	2	AC-10+5% Gilsonite
I H	0.2360	2	AC-10+10% Gilsonite
I	0.2220	2	AC-20+5% SEBS
I	0.2210	2	AC-10+ 15% Gilsonite

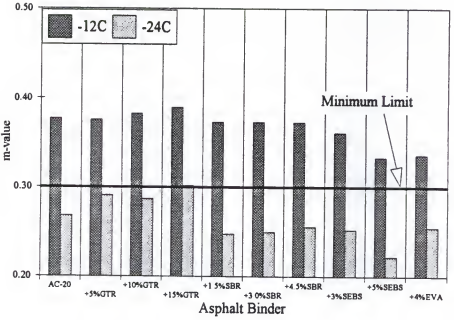

Figure 4.12 Comparison of m-value at -12°C and -24°C for PAV-20 hour-aged AC-20 Binders

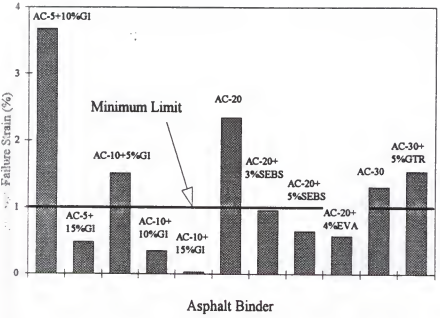

Figure 4.13 Comparison of Failure Strain at -12°C for PAV-20 hour-aged Binders

pass the requirement of 1 percent minimum strain. These include AC-5+ 15% GI (gilsonite), AC-10+10% GI, AC-10+15% GI, AC-20+SEBS and AC-20+EVA. However, all of the SBR and the ground tire rubber (GTR) modified binders pass the requirement and some of them have a failure strain of greater than five percent which is the limit of the direct tension tester used in this study.

4.5 Effects of Modifiers on Temperature Susceptibility

4.5.1 Penetration Viscosity Number

A conventional way to characterize the temperature susceptibility is by means of the penetration viscosity number (PVN) defined by the following equation [26]:

$$PVN_{(25-60)} = \frac{-1.5(\ 6.4890 - 1.59\ \log(\ P_{25}) - \log(\ V_{60}\ ))}{1.05 - 0.2234\ \log(\ P_{25})}$$

where

V_{60} = viscosity in poises at 60°C

P_{25} = penetration in 0.1 mm at 25°C

A high value of PVN would indicate a material that has a low temperature susceptibility. The results of the penetration viscosity number are given in Appendix A.11. The results of ANOVA and Duncan's grouping of the penetration viscosity number of the unaged and PAV-20 hour-aged binders are shown in Table 4.18. It can be seen that all of the modified binders show a significantly higher PVN as compared with the unmodified binders, and the PVN is higher as the concentration of modifiers increases. All the different aging methods have the same effect of increasing PVN. This

Table 4.18 Results of ANOVA and Duncan's Grouping of $PVN_{(25\text{-}60)}$ of Unaged and PAV-20 hour-aged Binders

Dependent Variable: $PVN_{(25\text{-}60)}$ [Model = $\mu + \alpha_i + \beta_j + (\alpha\beta)_{ij} + \epsilon_{ijk}$]

Source	DF	ANOVA SS	Mean Square	F Value	Pr > F
ASPHALT, α	23	27.38221250	1.19053098	29.16	0.0001
METHOD, β	1	9.15135000	9.15135000	224.17	0.0001
INTERACTION, αβ	23	5.49830000	0.23905652	5.86	0.0001

R-Square= 0.955457

Duncan Grouping at Method= Unaged

Duncan Grouping	Mean	N	ASPHALT
A	1.965	2	AC-20+4.5% SBR
B	1.225	2	AC-20+15% GTR
C B	1.195	2	AC-30+3% SBR
C B			
C B D	0.960	2	AC-20+ 4% EVA
C B D			
C E B D	0.800	2	AC-20+3.0% SBR
C E B D			
C E B D	0.760	2	AC-30+15% GTR
C E D			
C E F D	0.600	2	AC-20+5% SEBS
E F D			
G E F D	0.445	2	AC-20+10% GTR
G E F D			
H G E F D	0.370	2	AC-30+10% GTR
H G E F D			
H G E F D	0.360	2	AC-10+ 15% Gilsonite
H G E F D			
H G E F D I	0.350	2	AC-10+ 4% EVA
H G E F D I			
H G E F D I	0.340	2	AC-20+1.5% SBR
H G E F I			
H G E F J I	0.310	2	AC-20+3% SEBS
H G F J I			
H GK F J I	0.120	2	AC-20+5% GTR
H GK J I			
H GK L J I	-0.090	2	AC-10+10% Gilsonite
H K L J I			
H K L J I	-0.210	2	AC-5+15% Gilsonite
K L J I			
K L J I	-0.270	2	AC-30+5% GTR
K L J I	-0.275	2	AC-5+5% Gilsonite
K L J	-0.290	2	AC-5+10% Gilsonite
K L J	-0.310	2	AC-20
K L	-0.325	2	AC-30
K L	-0.330	2	AC-10+5% Gilsonite
K L	-0.445	2	AC-10
L	-0.610	2	AC-5

Table 4.18 Continued

Duncan Grouping at Method= PAV20

Means with the same letter are not significantly different.

Duncan Grouping	Mean	N	ASPHALT
A	1.905	2	AC-20+5% SEBS
A			
A	1.900	2	AC-20+4.5% SBR
B	1.655	2	AC-30+15% GTR
C	1.435	2	AC-20+3% SEBS
C			
D C	1.300	2	AC-20+15% GTR
D C			
D C	1.300	2	AC-10+ 15% Gilsonite
D			
D	1.195	2	AC-5+15% Gilsonite
D			
D	1.185	2	AC-20+ 4% EVA
D			
D	1.180	2	AC-30+10% GTR
D			
D E	1.080	2	AC-10+ 4% EVA
D E			
D E F	1.070	2	AC-10+10% Gilsonite
E F			
G E F	0.905	2	AC-20+10% GTR
G E F			
G E F	0.860	2	AC-30+5% GTR
G F			
G F	0.840	2	AC-20+3.0% SBR
G			
G	0.705	2	AC-5+10% Gilsonite
G			
G	0.675	2	AC-10+5% Gilsonite
G			
G	0.665	2	AC-30+3% SBR
H	0.405	2	AC-20+1.5% SBR
H			
H	0.380	2	AC-20+5% GTR
H			
H	0.340	2	AC-30
H			
H	0.330	2	AC-5+5% Gilsonite
H			
H	0.240	2	AC-20
I	0.000	2	AC-10
I			
I	-0.085	2	AC-5

implies that the temperature susceptibility of an asphalt reduces with hardening. The higher the degree of aging, the lower the temperature susceptibility would become. AC-20 + 4.5% SBR is the least temperature susceptible binder among all while all four unmodified binders remain the most temperature susceptible group of binder as seen in Table 4.18. Figure 4.14 displays the comparison of PVN of the unaged and PAV-20 hour-aged AC-20 binders. Among all modifiers, the SBR increases the PVN the most (i.e. lowers the temperature susceptibility the most).

4.5.2 Bitumen Test Data Chart

The Bitumen Test Data Chart (BTDC) is a diagram which consists of one horizontal scale for the temperature and two vertical scales for the penetration and viscosity, respectively. The consistency of an asphalt binder at different temperatures can be plotted on the BTDC to show its temperature susceptibility. The BTDC includes different physical property measurements (viscosity, penetration, Fraass temperature, and/or softening point) and, can predict the consistency of the material over a wide temperature range. The family of curves for the BTDC can show the effects of aging and modifier added on an asphalt binder over a wide temperature range.

Figures 4.15 and 4.16 show the BTDC for the unaged and PAV-aged gilsonite modified AC-5 binders, respectively. It indicates that the slope of the curve shifts upward as with the level of gilsonite addition increases. The temperature susceptibility of a binder is not changed with the addition of gilsonite. Figures 4.17 and 4.18 show the BTDCs for the unaged and PAV-aged ground tire rubber modified AC-20 Binders, respectively. It can be seen that the slope of the curve gradually levels off as the amount

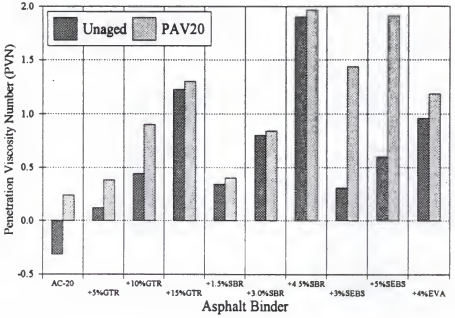

Figure 4.14 Comparison of Penetration Viscosity Number for Unaged and PAV-20 hour-aged AC-20 Binders

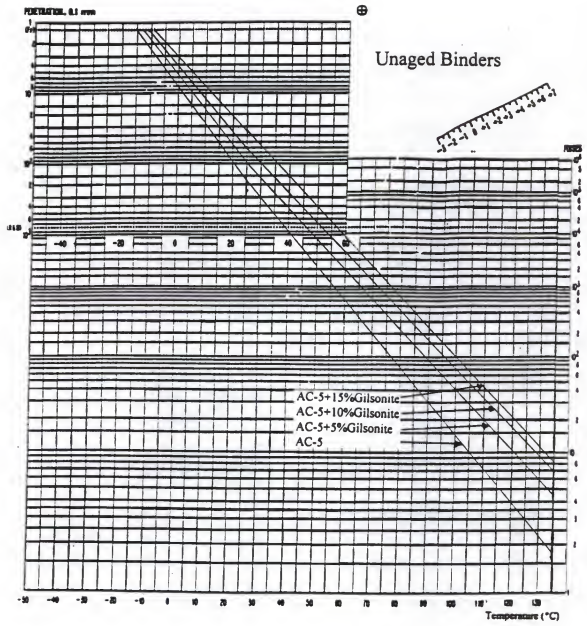

Figure 4.15 Bitumen Test Data Charts for Unaged Gilsonite Modified AC-5 Binders

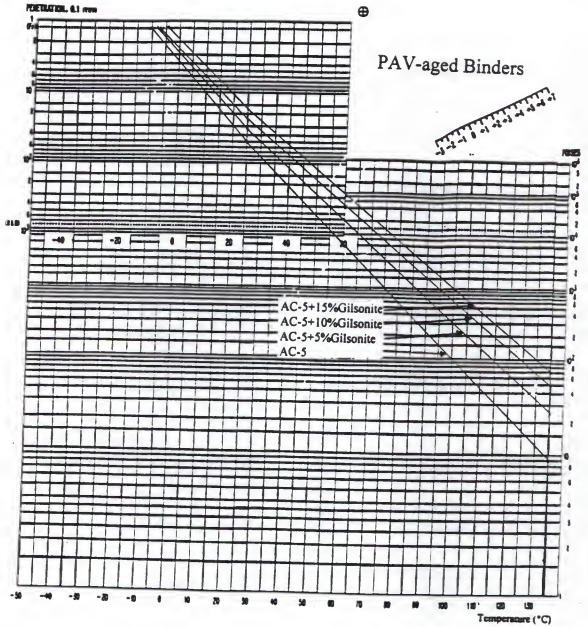

Figure 4.16 Bitumen Test Data Charts for PAV-20 hour-aged Gilsonite Modified AC-5 Binders

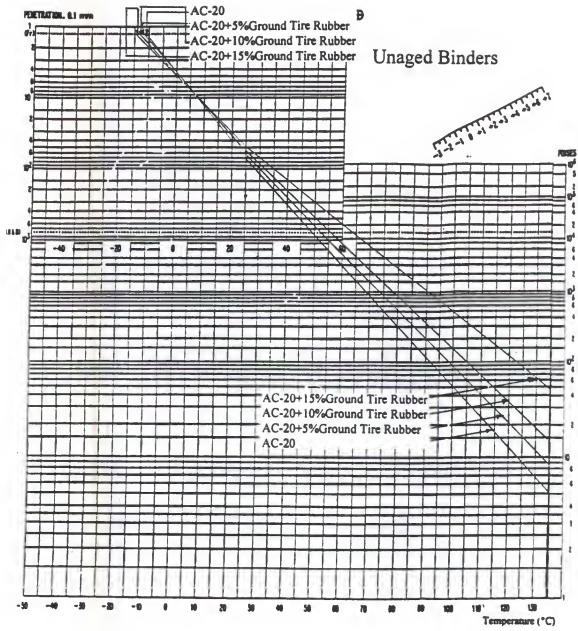

Figure 4.17 Bitumen Test Data Charts for Unaged Ground Tire Rubber Modified AC-20 Binders

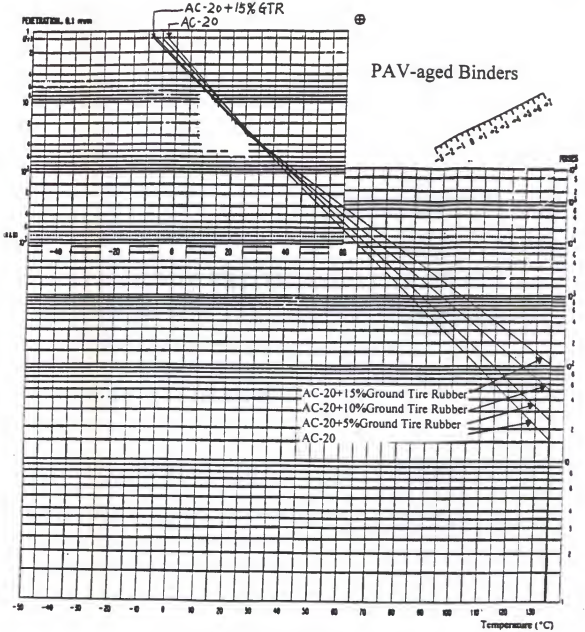

Figure 4.18 Bitumen Test Data Charts for PAV-20 hour-aged Ground Tire Rubber Modified AC-20 Binders

of ground tire rubber addition increases. The temperature susceptibility of a binder is changed with the addition of the ground tire rubber. The lines intersect at temperatures around 5°C and 30°C for the unaged and PAV-aged binders, respectively. The intersection of the lines is at the temperature at which all different binders have the same consistency. This temperture is increased with aging process which lowers the temperature susceptibility. Figure 4.19 displays the BTDCs for the unaged SBR modified AC-20 binders. It shows that the addition of SBR could lower the temperature susceptibility.

Figure 4.20 exhibits the BTDC for the unaged SEBS modified AC-20 binders. It can be noted that the addition of SEBS slightly decreases the temperature susceptibility of a binder. However, the effect of SEBS is not as significant as that of SBR and the ground tire rubber as seen from small differences in the slopes of the lines. Figures 4.21, 4.22 and 4.23 show the effects of different aging conditions on the temperature susceptibility for AC-5+15% gilsonite, AC-20 and AC-20+15% ground tire rubber, respectively. The slope of the curve for a gilsonite modified binder is decreased after aging. The slope of the curve for an AC-20 binder is slightly flattened after aging. However, the slope of the curve after aging for a ground tire rubber modified binder is nearly parallel with that of the unaged binder as seen in Figure 4.23. The temperature susceptibility of the binders modified with a high level of ground tire rubber addition is hardly changed with an aging process.

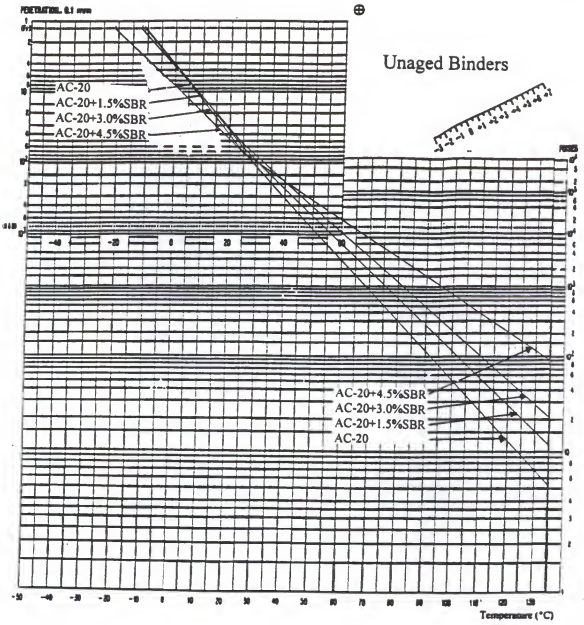

Figure 4.19 Bitumen Test Data Charts for Unaged SBR Modified AC-20 Binders

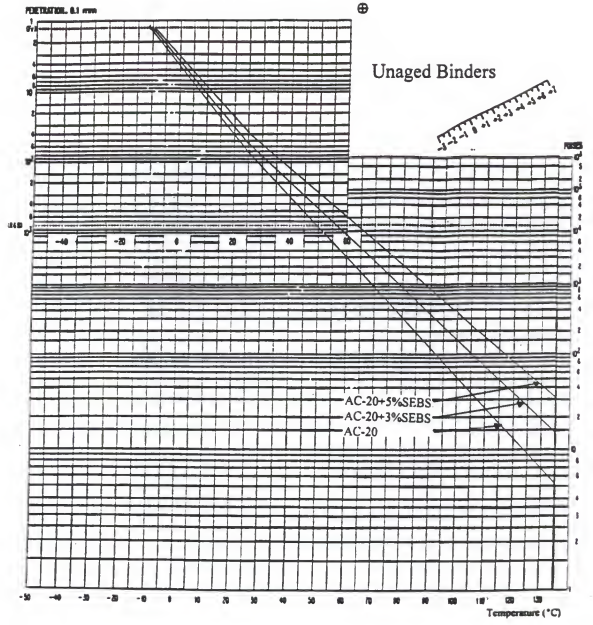

Figure 4.20 Bitumen Test Data Charts for Unaged SEBS Modified AC-20 Binders

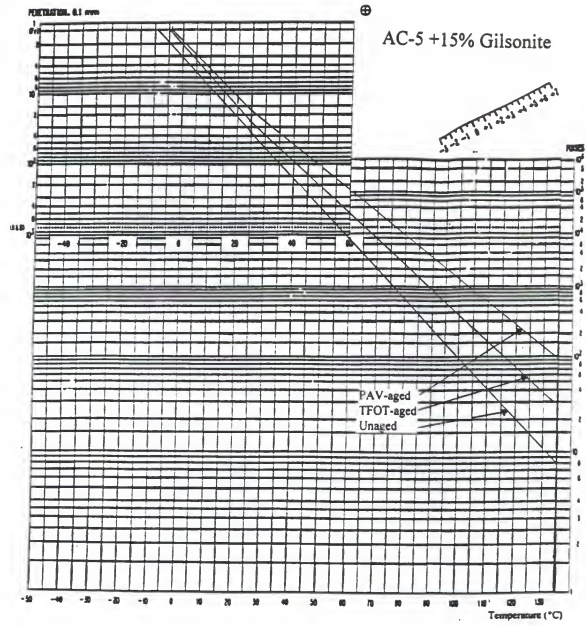

Figure 4.21 Bitumen Test Data Charts for AC-5+15% Gilsonite Binders

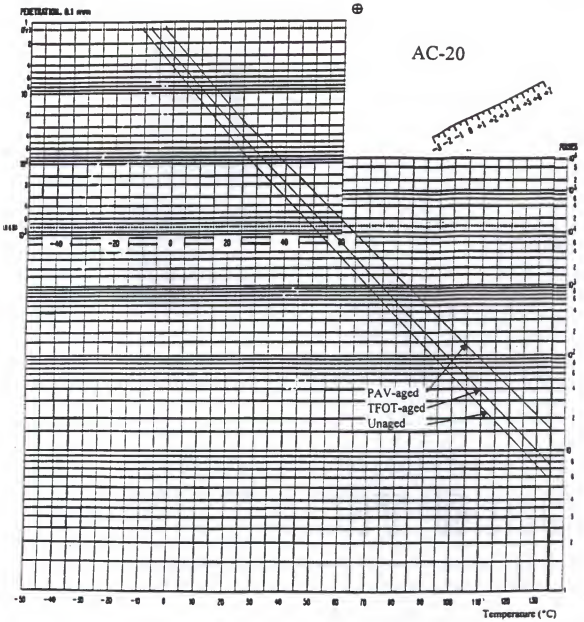

Figure 4.22 Bitumen Test Data Charts for AC-20 Binders

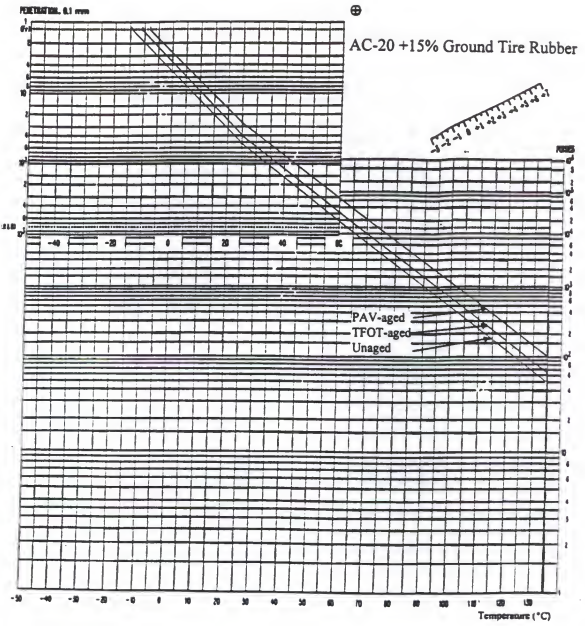

Figure 4.23 Bitumen Test Data Charts for AC-20+15% Ground Tire Rubber Binders

4.6 Effects of Modifiers on Aging Characteristics

4.6.1 Viscosity Aging Index

The severity of asphalt aging is often quantified by means of an aging index. The aging index is defined as the ratio of the viscosities after aging to the viscosities before aging. It is a measure of structuring from age hardening which is caused by a combination of oxidation and an increase in molecular interactions. The viscosity aging indices based on Brookfield viscosities are given in Appendix A.12. Among six different aging methods, the California tilt oven process for 168 hours (CTO168) or the pressure aging vessel process for 40 hours (PAV40) is the most severe aging method for binders while the thin film oven test process at 163 °C (TFOT163) is the least severe. AC-5 +10 % gilsonite and AC-5 + 15% gilsonite show consistently the highest aging indexes while AC-30 + 3% SBR, AC-20 + 15% ground tire rubber, AC-20 + 4% EVA and AC-20 + 4.5% SBR show consistently the lowest aging indexes. However, the aging indexes of AC-20 + SEBSs (3% and 5%) for the different aging methods are not consistent.

Figure 4.24 shows the comparison of aging index for AC-5 + gilsonite binders. It can be seen that the aging index for the CTO-168 hour aged residues decreases as the level of gilsonite increases. However, the aging indice for the PAV-40 hour aged residues increase as the concentration of gilsonite increases.

Figures 4.25 and 4.26 display the comparison of aging index for the modified AC-20 and AC-30 binders, respectively. It can be seen that the aging index generally decreases as the level of modifier increases. The ground tire rubber modified binders have the least severe aging following by SBR, EVA and then SEBS. The aging indexes

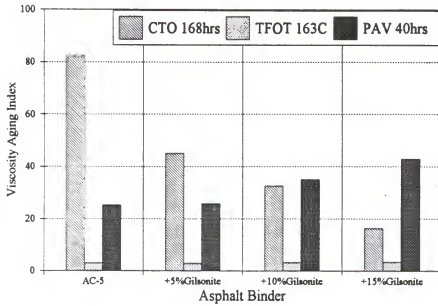

Figure 4.24 Comparison of Viscosity Aging Index for AC-5 + Gilsonite Binders

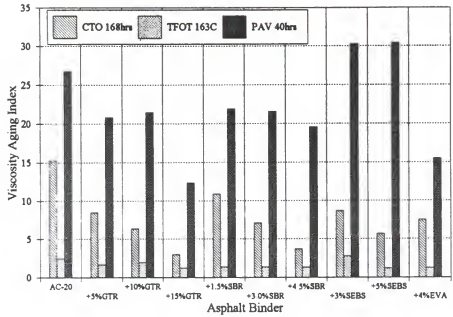

Figure 4.25 Comparison of Viscosity Aging Index for Modified AC-20 Binders

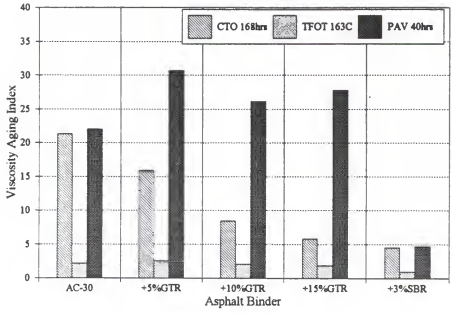

Figure 4.26 Comparison of Viscosity Aging Index for Modified AC-30 Binders

of the PAV-40 hour aged residues are not consistent with those of the CTO-168 hour aged residues. The inconsistency might be caused by the non-homogeneity of residues after the PAV process.

4.6.2 Carbonyl Ratio Index

The results of Infrared Spectral analysis in terms of carbonyl ratio are given in Appendix A.13. The carbonyl ratio index, which is the ratio of carbonyl ratio of the aged residue to the carbonyl ratio of original asphalt, was used to describe the aging severity. A higher value of carbonyl ratio index means a more severe aging condition. The carbonyl ratio index of the residues are listed in Table 4.19. Figures 4.27 and 4.28 show the comparison of carbonyl ratio index for AC-5 and AC-20 modified binders, respectively. It can be noted that all modifiers appear to reduce the aging potential of the asphalt binders in terms of caronyl ratio index. SBR shows the greatest effect on reducing the aging potential of the asphalts. However, the effect of modifier concentration does not show any consistent trend.

4.7 Summary of Findings

Based on the results of tests on asphalt binders in this testing program, the major findings are summarized as follows:

1. All modifiers increase the viscosity of the binders at 60°C in comparison with the unmodified binders. The effect of modifiers to the Brookfield viscosity increases as the level of addition increases. An increase in viscosity of the binders at a high pavement temperature usually means a higher resistance to rutting for the pavement material.

Table 4.19 Carbonyl Ratio Indexes of Asphalt Binders

Asphalt Type	CTO 72hrs	TFOT 163°C	PAV 20hrs
AC-5	1.88	1.21	1.56
AC-5+5% Gilsonite	1.66	1.16	1.39
AC-5+10% Gilsonite	1.40	1.10	1.24
AC-5+15% Gilsonite	1.26	1.12	1.30
AC-10	2.01	1.24	1.47
AC-10+5% Gilsonite	1.45	1.09	1.19
AC-10+10% Gilsonite	1.38	1.05	1.46
AC-10+ 15% Gilsonite	1.14	1.04	1.38
AC-10+ 4% EVA	1.48	1.14	1.69
AC-20	1.64	1.16	1.76
AC-20+5% GTR	1.48	1.07	1.62
AC-20+10% GTR	1.26	1.08	1.45
AC-20+15% GTR	1.53	0.97	1.43
AC-20+1.5% SBR	1.37	1.02	1.45
AC-20+3.0% SBR	1.27	1.07	1.29
AC-20+4.5% SBR	1.46	1.08	1.42
AC-20+3% SEBS	1.54	1.08	1.49
AC-20+5% SEBS	1.57	1.01	1.42
AC-20+ 4% EVA	1.37	1.16	1.42
AC-30	1.37	1.16	1.58
AC-30+5% GTR	1.65	1.08	1.44
AC-30+10% GTR	1.49	1.16	1.42
AC-30+15% GTR	1.43	1.22	1.52
AC-30+3% SBR	1.63	1.12	1.47

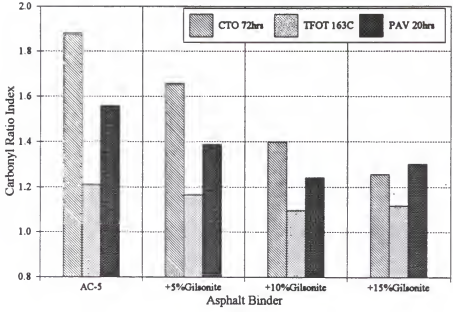

Figure 4.27 Comparison of Carbonyl Ratio Index for AC-5 Modified Binders

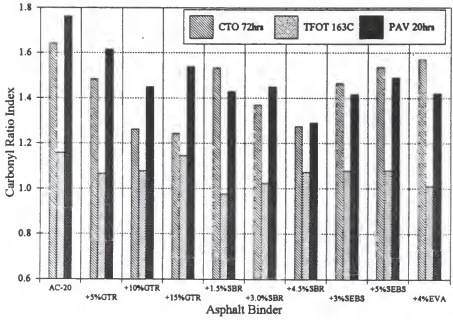

Figure 4.28 Comparison of Carbonyl Ratio Index for AC-20 Modified Binders

2. All modifiers increase the dynamic shear modulus (G*) and decrease the phase angle (δ) of the binder in comparison with the unmodified binders at high pavement service temperatures based on results of the dynamic shear rheometer tests.

3. For PAV-aged residues, the addition of SBR and GTR has the effect of decreasing the G* while the addition of gilsonite, SEBS and EVA has the effect of increasing the G* of the binders at intermediate pavement temperatures. All modifiers decrease the phase angle of the binders. However, the difference in the phase angle among the various aged binders is not as significant as their effect on the G* values.

4. The SBR and GTR modified binders exhibit a significantly lower Fraass breaking temperature than that of the unmodified base asphalts. On the other hand, the gilsonite modified binders show a higher Fraass breaking temperature than that of the base asphalts. The modification with the ground tire rubber and SBR tends to prevent the sudden rupture of the asphalt test specimen that usually happens in the other asphalt test specimens.

5. The addition of GTR and SBR lowers the creep stiffness of the PAV-aged asphalt binders at -12 and -24°C as measured by the bending beam rheometer test. However, the addition of gilsonite, SEBS and EVA increases the creep stiffness at these low temperatures. A lower creep stiffness of PAV-aged binders at a low pavement service temperature usually means a higher resistance to cracking for the pavement material. A high m-value means a relatively fast decrease in rate of

stiffness with time, which helps to relax thermal stresses. The ground tire rubber modified binders have the highest m-values among all modified binders, and are followed by the SBR modified binders.

6. The addition of SBR and GTR generally increases the failure strain of the PAV-aged asphalts at -12°C as measured by the direct tension test. However, the addition of gilsonite, EVA and SEBS generally reduces the failure strain at this low temperature.

7. All of the modified binders show a significantly lower temperature susceptibility as compared with the unmodified binders, and the temperature susceptibility decreases as the concentration of modifiers increases, based on the penetration viscosity number (PVN). AC-20 + 4.5% SBR is the least temperature susceptible binder while all four unmodified binders are among the most temperature susceptible group of binders. Among all modifiers, the SBR increases the PVN the most (i.e. lowers the temperature susceptibility the most).

8. The BTDC family of curves were used to show the effects of aging and modifier addition on the rheological properties of the binders over a wide temperature range. Based on the BTDC, the addition of GTR and SBR substantially reduces the temperature susceptibility of the binders. The addition of SEBS slightly decreases the temperature susceptibility of a binder. The temperature susceptibility of a binder is hardly changed with the addition of gilsonite. The temperature susceptibility of a binder generally decreases as it ages. However, the

temperature susceptibility of asphalts modified with a high level of ground tire rubber modified binder is hardly changed with aging.

9. The addition of all modifiers generally reduces the aging potential of the asphalt binders in terms of the viscosity aging indices. The ground tire rubber modified binders have the least severe aging potential, followed by SBR, EVA, SEBS and gilsonite modified binders.

10. All modifiers appear to reduce the aging potential of the asphalt binders in terms of caronyl ratio index. SBR shows the greatest effect on reducing the aging potential of the asphalts. However, the effect of modifier concentration does not show any consistent trend.

CHAPTER 5
RESULTS OF ASPHALT MIXTURE TESTS

5.1 Effects of Modifiers on High Temperature Characteristics

5.1.1 Results of Gyratory Testing Machine Test

The Gyratory Testing Machine (GTM) is a combination compaction and plane strain, simple shear testing machine for use on bituminous-type paving materials. Its controlled kneading in conjunction with cyclic loading provides an improved mechanical analog of a flexible pavement structure. This movement is intended to simulate the actual deformation of the pavement under traffic. Measurement of density, shearing resistance as well as rate and amount of consolidation of samples can be made.

The gyratory shear strength (Gs) value is a measure of the shear resistance of the asphalt concrete sample. Results of a previous study [5] indicated that a minimum gyratory shear value of 54 psi is needed for FDOT S-I mixtures subjected to light to medium traffic conditions. The air voids of the mixture at initial compaction should be within 5 and 7 percent. The results from the Gyratory Testing Machine for seven different types of mixtures are given in Appendix B.1. Figures 5.1 and 5.2 show the comparison of gyratory shear strength, and air void content at different compaction levels for seven unaged mixtures, respectively. It can be seen that all specimens after the initial compaction meet the minimum requirement of the gyratory shear value even though the

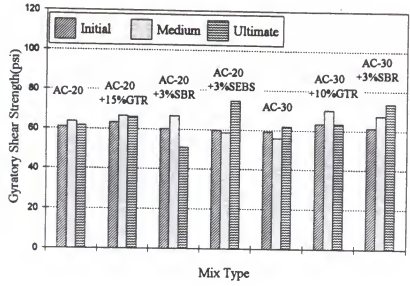

Figure 5.1 Comparison of Gyratory Shear Strength at Different Compaction Levels for Seven Unaged Mixtures

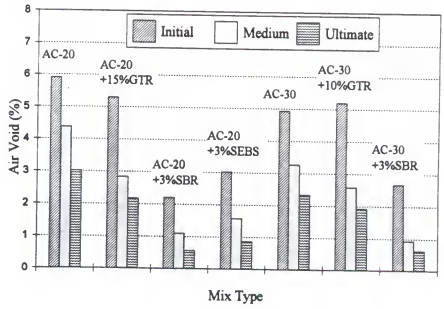

Figure 5.2 Comparison of Air Void at Different Compaction Levels for Seven Unaged Mixtures

air voids for some specimens are not in the target range. The GTR modified mixtures, such as AC-20 + 15% GTR and AC-30 + 10% GTR, have air voids close to those of the unmodified asphalt mixtures. The air voids of SEBS and SBR modified mixtures at initial compaction are much lower than those of the unmodified mixtures. There was no consistent trend in the gyratory shear strength with respect to the level of compaction.

Figures 5.3 and 5.4 display the comparison of gyratory shear strength during the medium and ultimate densification tests for the seven mixtures. It can be noted that the gyratory shear strength is not consistently related to the air void at a given level of densification. At the medium densification, the control AC-30 mix have the lowest Gs value with an air void of 3.27%. At medium densification, all of the modified mixes have a higher Gs value than that of the control AC-30 mix. The ranking of mixtures with respect to Gs values at medium densification is different from that at the ultimate densification. After the ultimate densification test, most of the modified mixes have a higher Gs value than that of the control AC-30 mix, except for that of AC-20 + 3%SBR.

The comparison of gyratory shear strength in ultimate densification test for seven SHRP long-term-oven-aging mixtures is illustrated in Figure 5.5. It can be noted that the air voids of all the aged mixtures are close to 4%. The AC-20, AC-30 and AC-20 + 3%SEBS mixtures have a Gs value of around 60 psi. The SBR modified mixtures have a Gs value of around 50 psi. The GTR modified mixes have the lowest Gs value of around 40 psi. The aged GTR modified mixtures have the most severe aging and least shear resistance among all mixes while the SEBS modified mix is the only one with a higher shear strength than that of the control AC-30 mix.

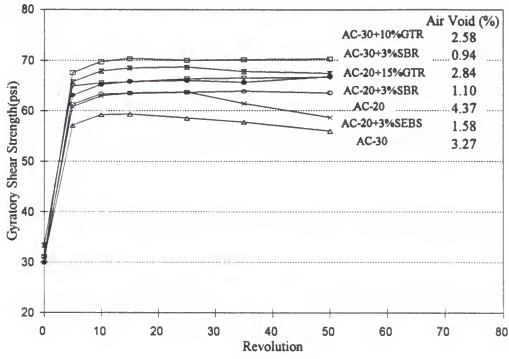

Figure 5.3 Comparison of Gyratory Shear Strength in Medium Densification Test for Seven Unaged Mixtures

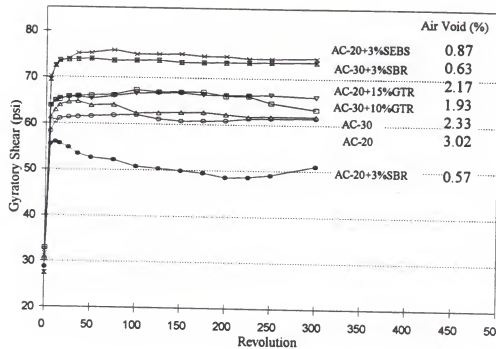

Figure 5.4 Comparison of Gyratory Shear Strength in Ultimate Densification Test for Seven Unaged Mixtures

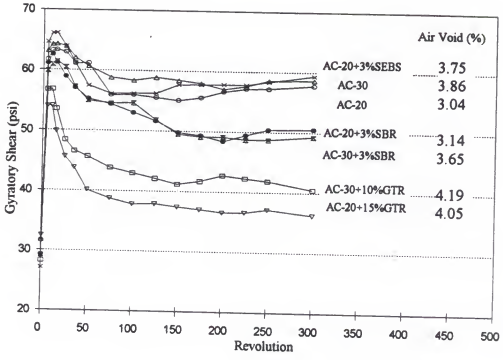

Figure 5.5 Comparison of Gyratory Shear Strength in Ultimate Densification Test for Seven SHRP Long-Term-Oven-Aging Mixtures

The Marshall-size samples were made at three different levels of compaction by using the GTM in this study. One group of three specimens were compacted with of 50 GTM's revolutions to simulate the pavement condition after one year of traffic. Another group of three specimens were compacted with 300 GTM's revolutions to simulate an ultimate condition in the pavement. Figure 5.6 shows the comparison of the properties of the two groups of samples at 50 GTM revolutions for the unaged mixtures. It can be seen that the difference in gyratory shear strength between the two groups of samples is substantial.

For a typical mixture, the gyratory shear strength generally increases and the air void decreases after an ultimate densification. Figure 5.7 displays the comparison of gyratory shear strength increase rate and air void decrease rate as compared with the control AC-30 mix after the ultimate densification for the unaged mixtures. It indicates that a higher gyratory shear increase rate corresponds with a higher air void decrease rate, for most of the mixes except for the AC-20 + 3% SBR mix. The GTR modified mixes have the lowest changes of air voids and Gs values among all mixes, while those of the SBR modified mixes have the highest.

5.1.2 Results of Loaded Wheel Test

The Loaded Wheel Tester (LWT) is intended to simulate the repeated applications of moving wheel loads on the asphalt mixtures tested. Rut depth measurements were made with a dial gauge at three different locations on the top of the beam at 0, 1000, 4000 and 8000 cycles. The results of the loaded wheel test for seven different types of mixtures are given in Appendix B.2. Figure 5.8 shows the relationship between rut depth

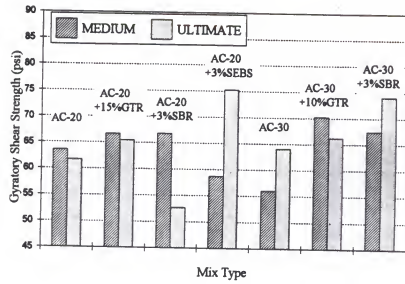

(A) Gyratory Shear Strength

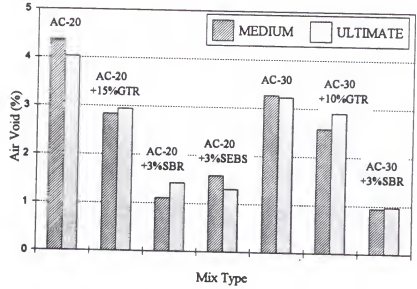

(B) Air Void

Figure 5.6 Comparison between the Samples Used in Medium and Ultimate Densifications at 50 GTM Revolutions for Seven Unaged Mixtures

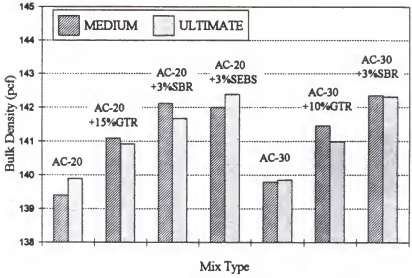

(C) Bulk Density

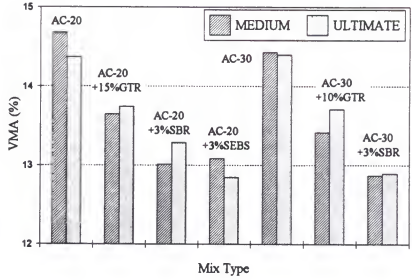

(D) VMA

Figure 5.6 Continued

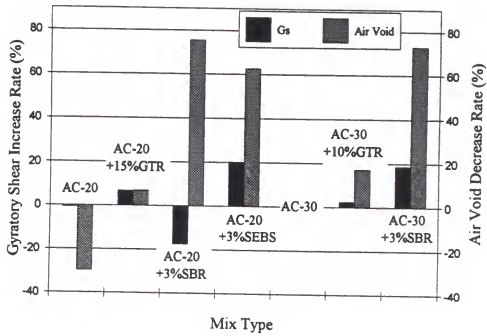

Figure 5.7 Comparison of Gyratory Shear Increase Rate and Air Void Decrease Rate with Control AC-30 Mix after Ultimate Densification for Unaged Mixtures

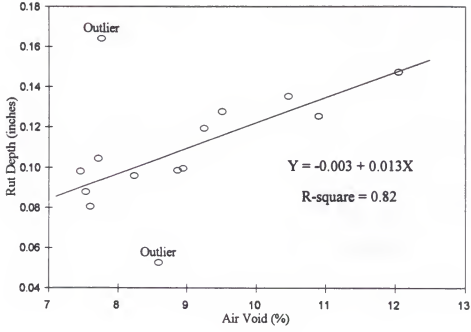

Figure 5.8 Relationship Between Rut Depth and Air Voids at 1000 Cycles in Loaded Wheel Test

and air voids at 1000 cycles in the loaded wheel test. It can be noted that the regression equation show a high goodness of fit as seen from the high R^2 value, except for two outliers. The relationship between rut depth and air voids after 1000 cycles for the mixtures is not as good as that within 1000 cycles. The air voids could be an indicator in association with rut depth to represent the performance characteristic of the mixture.

The relationship between rut depth and load application in the loaded wheel test for the mixtures is shown in Figure 5.9. It can be seen that the unmodified AC-20 and AC-30 mixes have higher rut depths than those of the modified mixes. Modified mixes all have improved rutting resistance in terms of lower rut depth. Figure 5.10 displays the comparison of increase rate of rut depth in the loaded wheel test. It can be seen that the SBR modified mixes have the highest reduction rate in rut depth of up to 32% and 38% as compared with the control AC-30 mix, while the GTR modified mixes have 13% and 21% reduction. The unmodified AC-20 mix has a 6% higher rut depth than that of the control AC-30 mix. However, SBR modified asphalt mixtures have a higher shear resistance with the highest rut reduction rate while the air void is least among them.

Figure 5.11 illustrates the relationship between rut depth in the loaded wheel test and air voids in the gyratory testing machine test for unaged mixtures. The representative parameters between the LWT's rut depth at 4000 and 8000 cycles, and the GTM's air void at a medium densification show similar relationships. The regression equations show a reasonable goodness of fit as seen from the high R^2 value. The evaluation of these relationships needs to be further investigated in order to make a decisive conclusion.

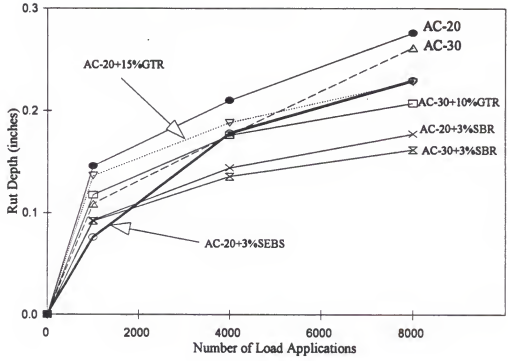

Figure 5.9 Relationship Between Rut Depth and Load Application in Loaded Wheel Test

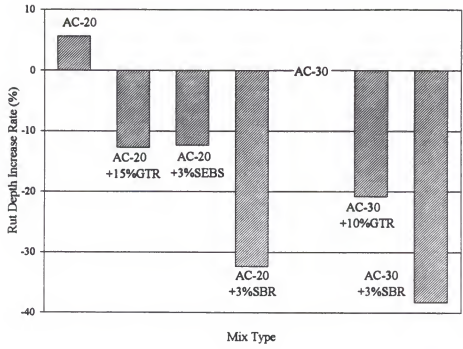

Figure 5.10 Comparison of Increase Rate of Rut Depth in Loaded Wheel Test

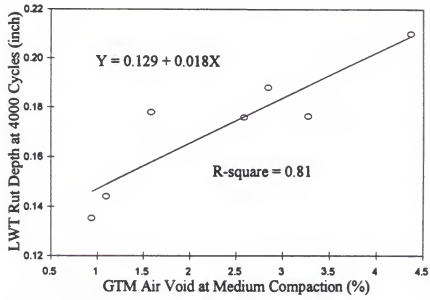

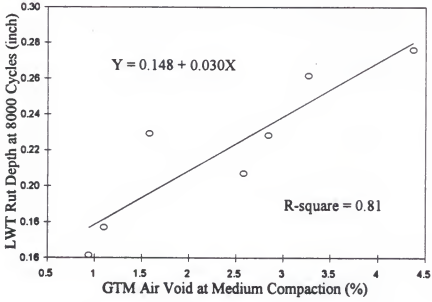

Figure 5.11 Relationship Between Rut Depth in Loaded Wheel Test and Air Voids in Gyratory Testing Machine Test for Unaged Mixtures

5.2 Effects of Modifiers on Low Temperature Characteristics

5.2.1 Results of Diametral Resilient Modulus Test

The results of diametral resilient modulus tests are given in Appendix B.3. Figure 5.12 shows the comparison of total diametral resilient modulus at 0°C for unaged and SHRP LTOA mixes under different levels of compaction. It can be seen that the total resilient modulus usually increases with the higher level of compaction for the unaged mixes.

Figure 5.13 displays the comparison of Poisson's ratio at three different temperatures for unaged mixes under the ultimate compaction condition. It can be noted that the Poisson's ratio generally does not vary much at the same compaction condition.

Mixtures with high resilient moduli at low temperatures are considered to be too brittle to resist the thermal and load associated cracking. At low temperatures, a low elastic modulus is beneficial to prevent a rapid accumulation of tensile stresses and strains during temperature drops. Figures 5.14 and 5.15 illustrate the relationship between total diametral resilient modulus and temperature for unaged initial and medium compacted mixtures, respectively. It indicates that the mixture with AC-20 + 15% GTR had the lowest total resilient modulus at all temperatures from 0 through -20°C. At 0°C, all of modified mixes had a lower modulus than that of the control AC-30 mix. At -20°C, some modified mixes have a higher modulus than that of the control AC-30 mix.

Figure 5.16 shows the relationship between total diametral resilient modulus and temperature for unaged ultimate compacted mixtures. The total resilient modulus of the GTR and SBR modified asphalt mixtures are lower than that of the base asphalt mixtures

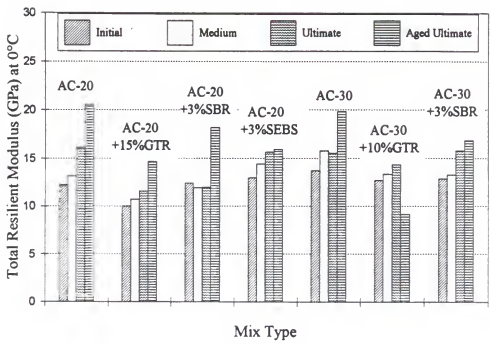

Figure 5.12 Comparison of Total Diametral Resilient Modulus at 0°C for Unaged and SHRP LTOA Mixes under Different Levels of Compactions

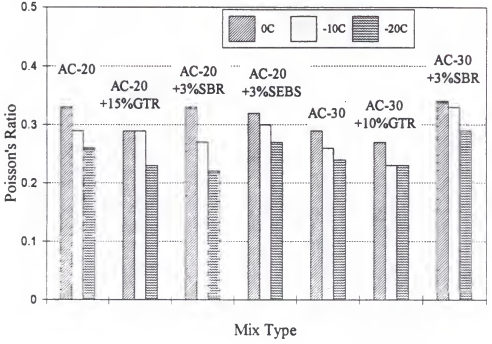

Figure 5.13 Comparison of Poisson's Ratio at Three Different Temperatures for Unaged Mixes under Ultimate Compaction

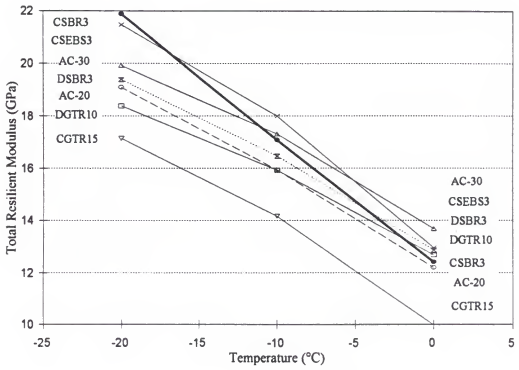

Note: CGTR15 : AC-20 + 15% GTR
CSBR3 : AC-20 + 3% SBR
CSEBS3 : AC-20 + 3% SEBS
DGTR10 : AC-30 + 10% GTR
DSBR3 : AC-30 + 3% SBR

Figure 5.14 Relationship Between Total Diametral Resilient Modulus and Temperature for Unaged Initial Compacted Mixtures

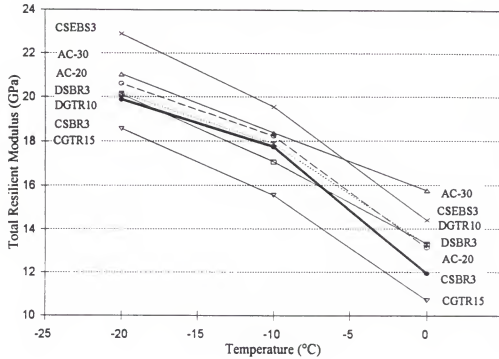

Note: CGTR15 : AC-20 + 15% GTR
CSBR3 : AC-20 + 3% SBR
CSEBS3 : AC-20 + 3% SEBS
DGTR10 : AC-30 + 10% GTR
DSBR3 : AC-30 + 3% SBR

Figure 5.15 Relationship Between Total Diametral Resilient Modulus and Temperature for Unaged Medium Compacted Mixtures

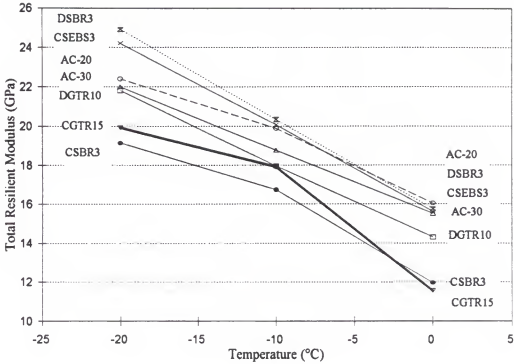

Note: CGTR15 : AC-20 + 15% GTR
CSBR3 : AC-20 + 3% SBR
CSEBS3 : AC-20 + 3% SEBS
DGTR10 : AC-30 + 10% GTR
DSBR3 : AC-30 + 3% SBR

Figure 5.16 Relationship Between Total Diametral Resilient Modulus and Temperature for Unaged Ultimate Compacted Mixtures

at the same test temperatures as seen from Figures 5.14 through 5.16. However, the SEBS modified asphalt mixtures have a higher resilient modulus as compared with the unmodified asphalt mixtures. The SEBS modifier does not appear to be a good additive for an asphalt mixture to resist the thermal and load associated cracking at low temperatures.

Figures 5.17 through 5.19 display the comparison of the % reduction in total diametral resilient modulus as compared with the AC-30 mix at 0°C, -10°C and -20°C, respectively. A higher reduction in resilient modulus provides greater potential resistance to low temperature cracking. It can be seen that GTR modified mixtures have the greatest reduction, especially for the AC-20 + 15% GTR mixture. The SEBS modified mixture has a very low value which dramatically drops as the test temperature decreases.

Figure 5.20 presents the comparison of % change in total diametral resilient modulus as compared with AC-30 mix at -20°C for unaged ultimate compacted mixes. It can be noted that AC-20 + 3% SBR and AC-20 + 15% GTR mixes have the first and second highest % reduction in modulus, respectively.

5.2.2 Results of Indirect Tensile Creep Test

The creep test was conducted in a load-control mode and involved applying a static load and then holding it constant throughout the test. The indirect tensile creep test is typically used for determination of low temperature cracking. In this study, this test was used to evaluate the effect of the ground tire rubber on the thermal cracking potential of asphalt mixtures. It is known that an asphalt mixture is a viscoelastic material. The viscoelastic deformation is a result of the combined elastic and viscous response of the

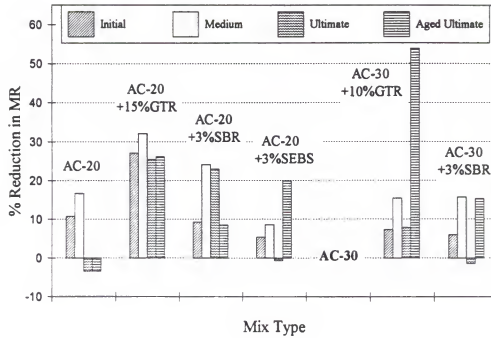

Figure 5.17 Comparison of % Reduction in Total Diametral Resilient Modulus as Compared with AC-30 Mix at 0°C

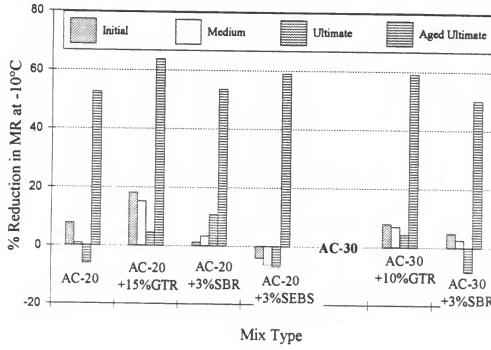

Figure 5.18 Comparison of % Reduction in Total Diametral Resilient Modulus as Compared with AC-30 Mix at -10°C

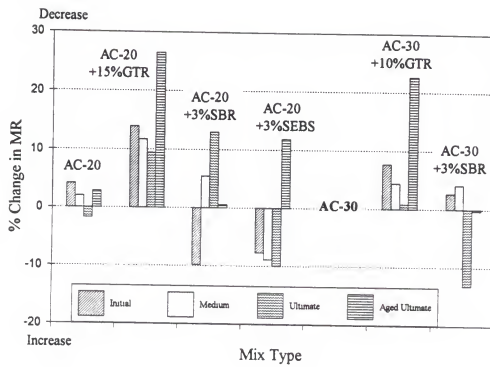

Figure 5.19 Comparison of % Change in Total Diametral Resilient Modulus as Compared with AC-30 Mix at -20°C

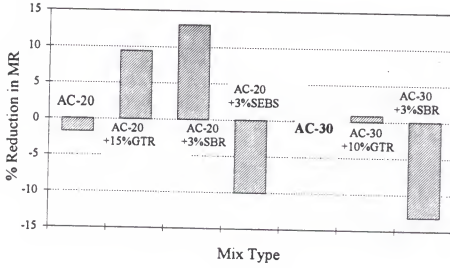

Figure 5.20 Comparison of % Reduction in Total Diametral Resilient Modulus Compared with AC-30 Mix at -20°C for Unaged Ultimate Compacted Mixes

mixture under an applied load. There have been many rheological models which used different combinations of Hookean springs and Newtonian dashpots to model the rheological behavior of asphalt mixtures, such as the Maxwell, Kelvin, Burgers, Kuhn and Rigden models. Among these models, the Burgers model is one of the simplest. The slope and intercept from the Burgers model, as illustrated in Figure 5.21, were used to evaluate the indirect tensile creep data in this study. The top spring models the pure elastic deformation, and the combined middle spring and dashpot model the delayed elastic deformation, and the lower dashpot models the pure viscous flow. The creep compliance from a creep test illustrates the strain caused by a unit stress and can be represented by the response of a Burgers model under a unit applied stress. The creep compliance can be expressed as: $1/E_0 + 1/E_1 \times (1-e^{-tE1/\eta 1}) + t/\eta_0$. It can be seen that the slope of the creep compliance plot approaches $1/\eta_0$ at large t. The intercept of the creep compliance plot at a vertical axis is equal to $(1/E_0 + 1/E_1)$, which can be considered to be equal to 1/(total elastic stiffness) of the mixture.

The results of indirect tensile creep tests are given in Appendix B.4. Figure 5.22 shows the relationship between creep compliance and time at different compaction levels and temperatures for unaged mixtures. It can be seen that the creep compliance usually increases with increasing temperature and with less compaction for unaged mixes. At a given compaction level and a fixed temperature, AC-20 + 15% GTR mix has the highest creep compliance followed by AC-30 + 10% GTR and the control AC-30 mixes. The GTR modified binder improves the low temperature cracking potential of the mix by increasing the creep compliance as compared with the unmodified mix.

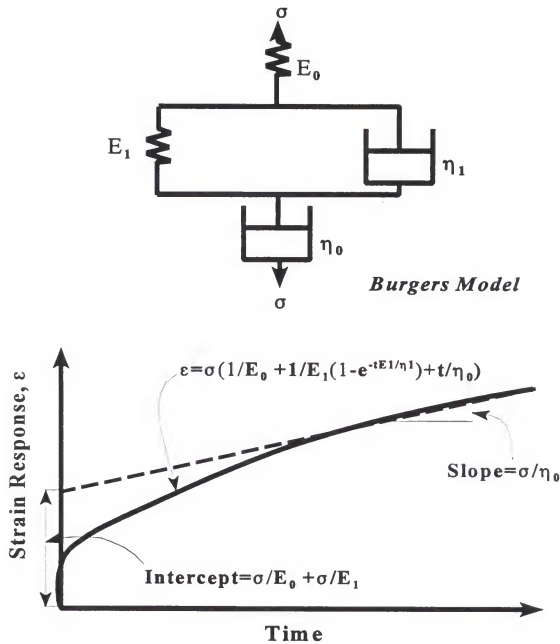

Figure 5.21 Response of a Burgers Model Subjected to a Unit Stress

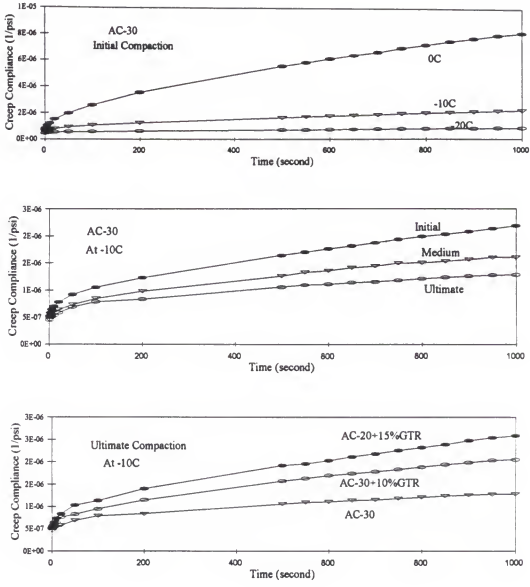

Figure 5.22 Relationship Between Creep Compliance and Time at Different Compaction Levels and Temperatures for Unaged Mixtures

It can be confirmed by computation that the slope of the creep curve did not reach a constant value until approximately halfway (500 sec) through the loading period. The steady state condition is reached when the slope of creep curve reaches a constant value. The creep compliance at a later time could be predicted by a linear extrapolation after it reaches a steady state. The slopes of the creep compliance curves are taken between 500 and 1000 seconds. The regression equations show high goodness of fit as seen from the high R^2 value close to 1 (Appendix B.4). Figure 5.23 displays the comparison of the creep compliance slope and intercept for three test temperatures for the unaged ultimate compacted mixes. It indicates that the GTR modified mixes have a higher creep compliance slopes and intercepts as compared with the control AC-30 mix at a given temperature, especially for the AC-20 + 15% GTR mix. A mixture with a higher creep compliance slope (i.e. low viscous stiffness) and intercept (i.e. low elastic stiffness) would strain more through viscous deformation and not build up tensile stresses at low temperatures.

Figure 5.24 shows the comparison of creep compliance at initial and ultimate compactions for unaged mixtures at -10°C. It can be noticed that there is no difference on the creep compliance among all mixtures. The effect of GTR addition for the mixture is not significant.

5.2.3 Results of Indirect Tensile Strength Test

This test is conducted by loading a cylindrical specimen along its length at -10°C to obtain a failure strength. The indirect tensile strength is the maximum tensile stress that a specimen can tolerate before fracture. It represents the failure resistance of the

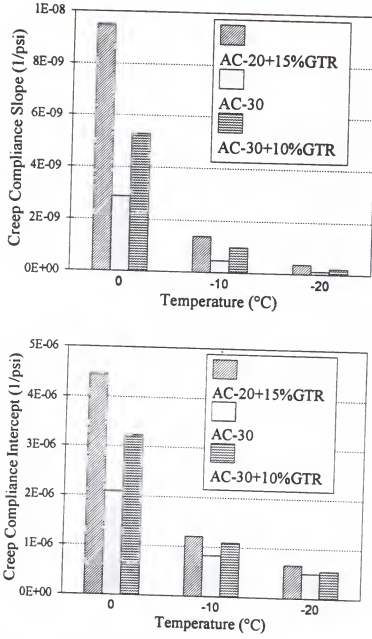

Figure 5.23 Comparison of Creep Compliance Slope / Intercept and Temperature for Unaged Ultimate Compacted Mixes

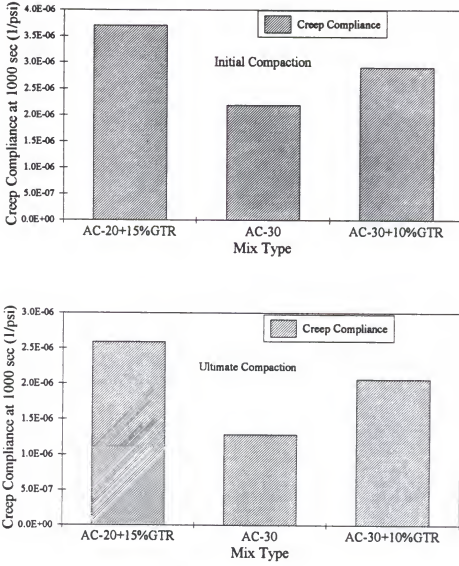

Figure 5.24 Comparison of Creep Compliance at Initial and Ultimate Compaction for Unaged Mixes at -10°C

asphalt concrete under tensile stresses that can be used to predict the thermal cracking potential of an asphalt concrete. The results of indirect tensile strength tests are given in Appendix B.5. Figure 5.25 shows the comparison of indirect tensile strength at -10°C under different levels of compaction. It can be noted that the indirect tensile strength generally increases with higher level of compaction for unaged mixtures. However, the strength of mixtures after SHRP LTOA process decreases substantially and is even lower than that of mixtures at the initial compaction. The reduction in strength may be due to the damage of the mixtures.

Figure 5.26 displays the comparison of indirect tensile strength at -10°C at initial and ultimate compaction for unaged mixtures. It can be seen that all these unmodified and modified mixtures do not differ much in strength.

5.3 Results of Tests on Recovered Asphalt Residues

The broken GTM specimens from indirect tensile strength test were extracted by using the reflux extraction and rotovap recovery methods. Seven types of recovered LTOA residues were evaluated by the penetration test at 25°C and the Brookfield viscosity tests. The results of tests on recovered binders are given in Appendix B.6. Test data could not be completely obtained due to the difficulty of recovery process on modified asphalts. It was observed that some of the modifiers are not soluble in trichloroethylene during the extraction process. It was found that only gilsonite and SEBS are completely recoverable in this study. A modified recovery process needs to be developed to completely extract the modifiers, such as GTR and SBR. Figures 5.27 and 5.28 show the Bitumen Test Data Chart for the unaged unmodified binders and LTOA

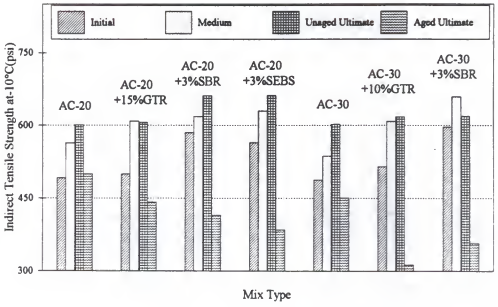

Figure 5.25 Comparison of Indirect Tensile Strength at -10°C under Different Levels of Compaction

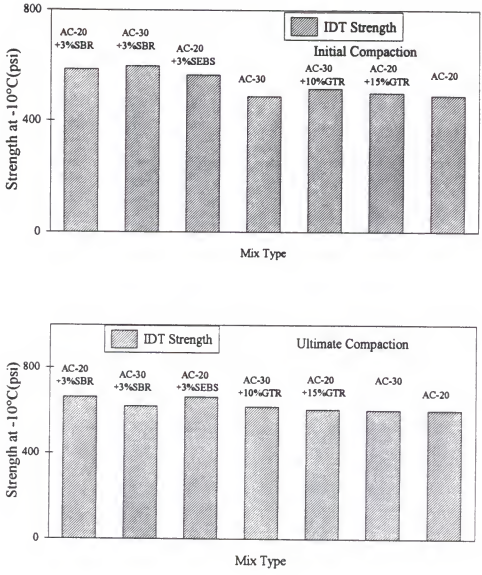

Figure 5.26 Comparison of Indirect Tensile Strength at -10°C at Initial and Ultimate Compaction for Unaged Mixtures

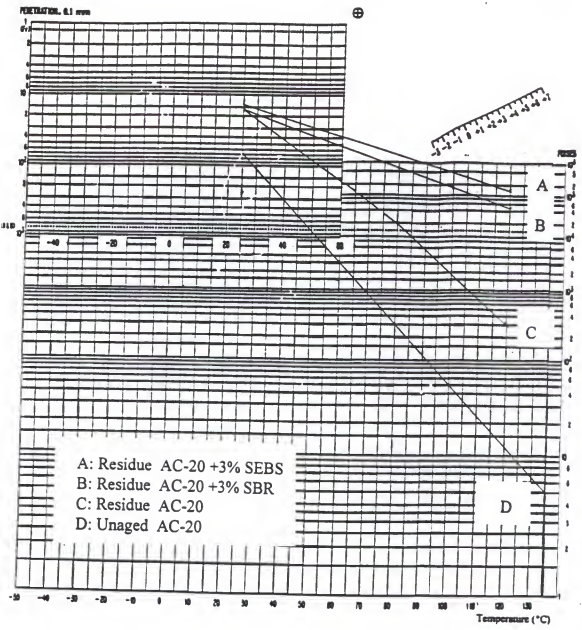

Figure 5.27 Bitumen Test Data Chart for Unaged AC-20 Binder and LTOA Recovered Modified AC-20 Residues

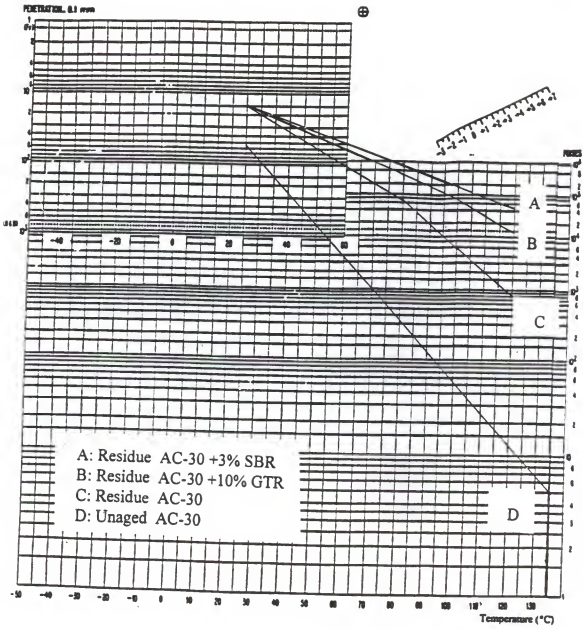

Figure 5.28 Bitumen Test Data Chart for Unaged AC-30 Binder and LTOA Recovered Modified AC-30 Residues

recovered residues. It can be seen that the recovered residues are much more severely aged as compared with the unaged binders. The recovered residues might be over-heated during the reflux extraction process. The aging indices for AC-20 and AC-30 residues are approximately 100 and 160, respectively. The recovered binders might not be representative of the modified binders.

5.4 Relationships Between Binder and Mixture Properties

The selected seven unmodified and modified binders were mixed with the specified aggregates to produce Marshall-size specimens. They were evaluated by the binder and mixture tests, whose results are shown in the previous sections. This section presents the relationships between binder and mixture properties.

Figures 5.29 and 5.30 show the relationships between the gyratory shear strength of LTOA mixtures and the Brookfield viscosity at 60°C of PAV-20 hour-aged binders, and the complex shear modulus at 60°C of TFOT-163°C-aged binders, respectively. It can be seen that the linear regression equations show a fair goodness of fit as seen from the high R^2 values of 0.83 and 0.81. The LTOA mixture's gyratory shear strength decreases with an increase in Brookfield viscosity and the complex shear modulus.

Figure 5.31 illustrates the relationship between rut depth at 8000 cycles of the loaded wheel test of the mixture and the Brookfield viscosity at 60°C of the unaged binder. It can be noted that the rut depth of the unaged mixture decreases as the Brookfield viscosity of the unaged binder increases.

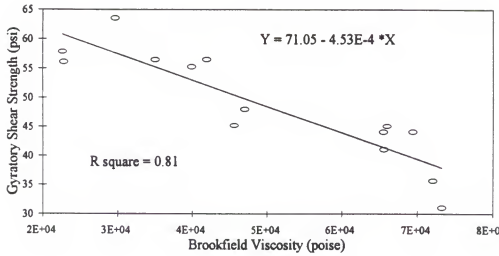

Figure 5.29 Relationship Between Gyratory Shear Strength after LTOA Process and Brookfield Viscosity at 60°C after PAV-20 hour-aging Process

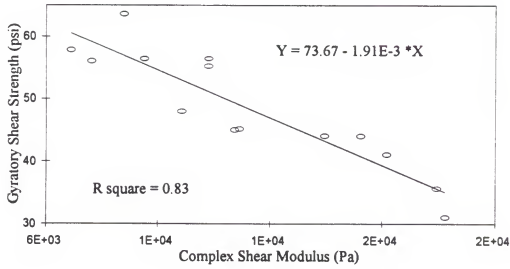

Figure 5.30 Relationship Between Gyratory Shear Strength after LTOA Process and Complex Shear Modulus at 60°C after TFOT-163°C-aging Process

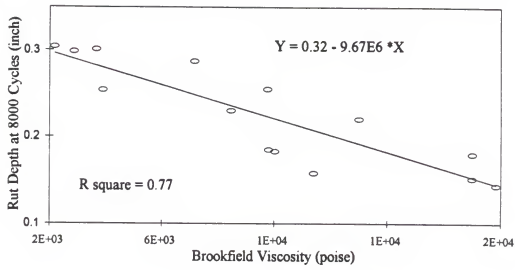

Figure 5.31 Relationship Between Rut Depth at 8000 Cycles and Brookfield Viscosity at 60°C

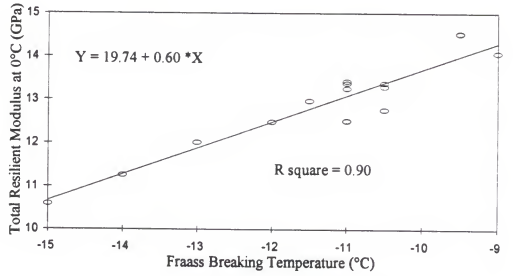

Figure 5.32 Relationship Between Total Resilient Modulus at 0°C & Initial Compaction and Fraass Breaking Temperature

Figures 5.32 through 5.34 show the relationships between the total resilient modulus and the Fraass breaking temperature. It can be observed that the total resilient modulus increases as the Fraass breaking temperature increases.

5.5 Summary of Findings

Based on the results of tests on asphalt mixtures in the testing program, the major findings are summarized as follows:

1. The GTR modified asphalt mixtures show higher air voids as compared with those of the SBR and SEBS modified asphalt mixtures as seen from the GTM test results. This might be attributed to the higher viscosity of the GTR-modified binders at the compaction temperature.
2. There is no relationship between the gyratory shear strength and the air voids of the compacted asphalt mixtures.
3. At ultimate compaction condition, most of the modified asphalt mixtures, with the exception of the mixture containing AC-20 + 3%SBR, show a higher gyratory shear strength than that of the control AC-30 mixture.
4. The rut depth at 4000 and 8000 cycles in the loaded wheel test is related to the air voids of the unaged mixtures at a medium densification in the gyratory testing machine test. Lower air voids correspond to lower rut depths.
5. All modified mixtures show greater rutting resistance in terms of lower rut depth as compared with the control mix. The SBR modified asphalt mixtures have the highest shear strength, the lowest rut depth and the lowest % air voids.

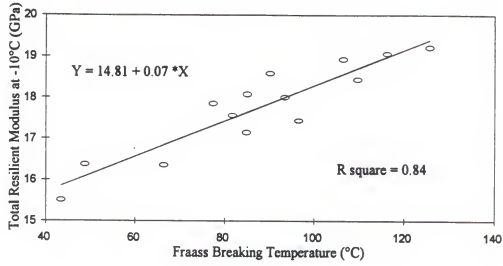

Figure 5.33 Relationship Between Total Resilient Modulus at -10°C & Initial Compaction and Fraass Breaking Temperature

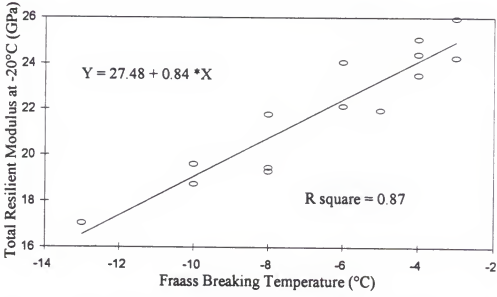

Figure 5.34 Relationship Between Total Resilient Modulus at -20°C After LTOA Process and Fraass Breaking Temperature of CTO-72 hour-aging Binder

6. The AC-20 + 15% GTR mixture has the lowest total resilient modulus at 0, -10°C and -20°C. The total resilient modulus of the GTR and SBR modified asphalt mixtures are lower than that of the unmodified asphalt mixtures at the same test temperatures, except for the SEBS modified asphalt mixtures.
7. The GTR modified asphalt mixtures show a higher creep compliance at low temperatures as compared with that of the unmodified mixtures.
8. The indirect tensile strength of the unaged mixtures does not vary much with the different levels of compaction. However, the strength of mixtures which were aged by the SHRP LTOA process decreases slightly with additional densification.
9. Some modifiers are not soluble in trichloroethylene as observed during the extraction process. Only gilsonite and SEBS were completely recoverable in this study.
10. The rut depth of the unaged mixture at 8000 cycles of the loaded wheel test decreases as the Brookfield viscosity of the unaged binder at 60°C increases.
11. The total resilient modulus of the mixtures increases as the Fraass breaking temperature of the binders increase.

CHAPTER 6
CONCLUSIONS AND RECOMMENDATIONS

6.1 Conclusions

A research study has been conducted to investigate the effects of modifier types, modifier concentration and mixture types on rutting and cracking resistance of pavements under Florida conditions. The main findings from this study are summarized as follows:

1. The addition of SBR, SEBS, EVA, GTR and gilsonite increase the viscosity of the binder at high pavement temperatures (50 - 70°C). This effect increases as the level of modifier addition increases. An increase in viscosity of the binders at a high pavement temperature usually means a higher resistance to rutting for the pavement material.
2. The addition of these modifiers increases the dynamic shear modulus (G*) and decreases the phase angle (δ) of the binder at high pavement service temperatures. This effect is beneficial for the improvement of rutting resistance of the pavement.
3. The addition of SBR and GTR has the effect of decreasing, while the addition of gilsonite, SEBS and EVA has the effect of increasing the dynamic shear modulus at intermediate pavement temperatures of between 10°C and 40°C.

4. The addition of SBR and GTR has the effect of lowering the Fraass breaking temperature of the aged asphalt binders, while the addition of gilsonite has the effect of raising it. The addition of SEBS and EVA has no significant effect on the Fraass breaking temperature of an asphalt.
5. The addition of GTR and SBR lowers the creep stiffness of the PAV-aged asphalt binders at -12 and -24°C, as measured by the bending beam rheometer test. However, the addition of gilsonite, SEBS and EVA increases the creep stiffness at these low temperatures. A lower creep stiffness of PAV-aged binders at a low pavement service temperature usually means a higher resistance to cracking for the pavement material.
6. All of the modified binders show a significantly lower temperature susceptibility as compared with the unmodified binders, and the temperature susceptibility decreases as the concentration of modifiers increases. Among all modifiers, the SBR lowers the temperature susceptibility the most.
7. The gilsonite modified binders have the most severe aging potential among all. The ground tire rubber modified binders have the least severe aging potential, followed by SBR, EVA and then SEBS.
8. The GTR-modified asphalt mixtures have a higher % air voids as compared with the SBR- and SEBS-modified mixtures under the same compactive effort with the GTM.

9. The GTR, SBR and SEBS modified mixes have a higher gyratory shear strength as compared with that of the control AC-30 at ultimate densification condition, except for that of AC-20 + 3%SBR.

10. The SBR, GTR and SEBS modified mixtures all improve the rutting resistance as seen from the lower rut depths in the loaded wheel test. The SBR modified asphalt mixtures show the lowest rut depth while the % air voids at ultimate densification is the least among all the mixtures.

11. The mixture of AC-20 + 15% GTR have the lowest total resilient modulus among all mixtures at 0, -10°C and -20°C. The total resilient modulus of the GTR and SBR modified asphalt mixtures are lower than that of the unmodified asphalt mixtures at the same test temperatures, except for the SEBS modified asphalt mixtures.

12. The GTR modified asphalt mixtures have a higher creep compliance than that of the unmodified mixtures at low temperatures.

13. The indirect tensile strength of mixtures aged by the SHRP LTOA process is lower than that of mixtures at the initial compaction condition (without this aging process).

14. The modified asphalt mixtures have about the same indirect tensile strengths as those of the unmodified mixtures at low temperatures.

15. The rut depth of the asphalt mixtures in the loaded wheel test decreases as the viscosity of the binder increases. The lower viscosity of the binder

used in the mixture gives a higher potential for rutting problem at high pavement temperatures.

16. Among the five asphalt additives investigated in this study, the most effective additives for improved rutting and cracking resistance of asphalt mixtures are GTR and SBR. The two modified binders with the best high- and low-temperature properties are AC-20 + 15% GTR and AC-30 + 3% SBR.

6.2 Recommendations

Based on the findings of this study, the following recommendations are made:

1. The family curves of the BTDC could be used to show the effects of aging and modifier added on the consistency and temperature susceptibility of an asphalt binder over a wide temperature range.
2. The present binder extraction method is not adequate for recovery of the modified binders from the mixtures. An improved method is needed for this purpose.
3. The evaluation of the relationship between the properties of the binders and the mixtures needs to be further investigated using a broader data base in order to obtain more reliable and comprehensive results.

Table A.1 Brookfield Viscosity (poises) at 60° C

Asphalt Type	Original Binder	CTO-Aged 72 hrs	CTO-Aged 168 hrs	TFO-Aged 163° C	TFO-Aged 185° C	PAV-Aged 20 hrs	PAV-Aged 40 hrs
A	646 495	11512 11443	51145 42344	1814 1591	3583 3805	5413 6006	15251 13377
AGI5	1515 1839	25811 22778	86963 59984	5023 4806	14327 12990	18147 15875	43645 41756
AGI10	3794 3237	44505 54485	94537 129867	12030 11017	29441 26927	47748 50179	127992 117211
AGI15	9673 6995	109542 110766	1447576 123295	28791 26419	65787 79344	141097 142809	365520 335407
B	1361 1001	18608 17138	37294 48260	3253 3113	5520 6161	11408 11790	26717 25563
BGI5	2777 3568	24443 23661	71782 73201	9898 9648	15284 11242	40214 39075	75565 73659
BGI10	8259 8069	31658 40958	98371 101629	23137 20746	42458 41588	97589 103522	213824 191729
BGI15	26460 21164	25520 65339	128626 143372	61255 50732	143887 141988	247923 234795	602439 498945
BEV4	3414 7491	70191 81059	96689 125095	12320 9228	37426 48421	41332 47667	121127 90724
C	2872 2180	24607 22583	32986 41421	6057 5814	11803 11895	22611 22824	65114 67045
CGT5	5083 5008	33307 26465	43212 41972	8050 8640	21622 19844	27436 29610	109413 100413
CGT10	7732 7634	30015 32184	48541 48666	14646 14962	40776 32399	43606 46288	183541 145838
CGT15	19858 21352	25507 39219	53575 68198	24933 25772	62219 55676	72052 73226	239283 271082
CSB15	6024 6085	31748 57588	58960 72743	7938 8582	16554 30028	28749 25929	138457 127069
CSB30	11400 10019	55110 52429	94254 58698	15408 13275	45210 46012	47036 39928	228095 231918

Table A.1 - Continued

Asphalt Type	Original Binder	CTO-Aged 72 hrs	CTO-Aged 168 hrs	TFO-Aged 163° C	TFO-Aged 185° C	PAV-Aged 20 hrs	PAV-Aged 40 hrs
CSB45	23885 21001	88397 40977	82346 82735	21163 35612	106229 49244	59223 55993	457664 420020
CSE3	7162 8463	41661 40883	66658 66997	22322 20486	27326 26816	65932 69421	234987 234701
CSE5	18455 18558	67325 59195	142843 66216	21852 21955	20483 34469	126861 131651	586460 538223
CEV4	15878 16522	93119 97817	129226 112152	20393 19753	80678 94599	86415 85527	231238 271139
D	3902 3669	35082 36462	75956 84908	8112 8390	15287 16096	34997 29678	82280 84158
DGT5	4940 4655	31648 25723	59296 92080	11717 12624	26960 31612	49870 51319	135122 158438
DGT10	9762 9796	34180 37927	82799 82282	19988 20860	51022 52370	65521 65567	249879 261210
DGT15	16414 16961	34892 40913	95261 98975	31067 32185	88592 103878	101140 107498	427294 401024
DSB3	16985 17829	46805 51070	73736 84683	16001 16852	46263 54245	41922 454630	83876 80933

Table A.2 G*(Pa) at 1.59 Hz (10 rad/sec)

Asphalt Type	10°C	20°C	30°C	40°C	50°C
	PAV20	PAV20	PAV20	PAV20	Unaged
A	6.52E+06 5.82E+06	1.50E+06 1.47E+06	3.32E+05 3.25E+05	7.48E+04 7.78E+04	4.08E+03 4.20E+03
AGI5	1.15E+07 1.16E+07	3.53E+06 3.54E+06	9.52E+05 9.54E+05	2.23E+05 2.25E+05	1.07E+04 1.11E+04
AGI10	1.98E+07 1.95E+07	6.05E+06 5.98E+06	1.78E+06 1.73E+06	4.28E+05 4.29E+05	2.19E+04 2.14E+04
AGI15	3.05E+07 3.04E+07	1.02E+07 1.01E+07	3.04E+06 3.05E+06	6.79E+05 7.23E+05	5.75E+04 4.25E+04
B	1.12E+07 8.25E+06	3.24E+06 3.20E+06	8.28E+05 6.12E+05	1.71E+05 1.71E+05	1.06E+04 1.12E+04
BGI5	1.92E+07 1.93E+07	5.73E+06 5.70E+06	1.57E+05 1.60E+05	3.77E+05 3.76E+05	2.47E+04 2.58E+04
BGI10	2.60E+07 2.59E+07	8.74E+06 8.71E+06	2.63E+05 2.68E+05	6.79E+05 6.97E+05	3.02E+04 2.98E+04
BGI15	3.93E+07 3.89E+07	1.42E+07 1.41E+07	4.62E+05 4.72E+05	1.15E+06 1.19E+06	1.09E+05 1.15E+05
BEV4	1.28E+07 1.28E+07	3.64E+06 3.58E+06	8.94E+05 8.73E+05	2.40E+05 2.27E+05	2.05E+04 2.30E+04
C	1.10E+07 1.09E+07	3.02E+06 2.99E+06	8.54E+05 7.70E+05	2.33E+05 2.28E+05	1.38E+04 1.39E+04
CGT5	1.12E+07 8.25E+06	3.11E+06 2.30E+06	8.40E+05 6.21E+05	1.89E+05 1.82E+05	1.38E+04 1.42E+04
CGT10	8.04E+06 8.15E+06	2.27E+06 2.27E+06	6.78E+05 5.93E+05	1.87E+05 1.60E+05	2.36E+04 2.39E+04
CSB30	8.05E+06 5.95E+06	2.19E+06 1.62E+06	6.90E+05 5.10E+05	1.20E+05 1.22E+05	3.15E+04 3.00E+04
CSB45	6.44E+06 4.76E+06	1.96E+06 1.45E+06	5.98E+05 4.42E+05	1.44E+05 1.06E+05	3.73E+04 3.46E+04
CSE3	1.02E+07 1.61E+07	3.21E+06 4.84E+06	9.31E+05 1.49E+06	2.42E+05 3.89E+05	3.32E+04 2.47E+04
CSE5	2.61E+07 2.64E+07	8.27E+06 9.34E+06	2.46E+06 2.66E+06	6.02E+05 6.16E+05	4.15E+04 4.29E+04

Table A.2 Continued

Asphalt Type	50°C	60°C	60°C	70°C	70°C
	TFO163°C	Unaged	TFO163°C	Unaged	TFO163°C
A	8.12E+03 8.20E+03	1.35E+03 1.33E+03	1.96E+03 2.06E+03	3.21E+02 3.14E+02	5.29E+02 5.64E+02
AGI5	2.11E+04 2.12E+04	2.76E+03 2.75E+03	5.52E+03 5.50E+03	7.54E+02 7.78E+02	1.41E+03 1.49E+03
AGI10	4.78E+04 4.97E+04	6.12E+03 5.52E+03	1.22E+04 1.20E+04	1.49E+03 1.51E+03	3.08E+03 3.09E+03
AGI15	8.58E+04 8.38E+04	1.50E+04 1.11E+04	2.22E+04 2.29E+04	3.85E+03 2.85E+03	5.75E+03 5.77E+03
B	1.40E+04 1.50E+04	2.79E+03 2.72E+03	3.71E+03 3.69E+03	7.22E+02 7.13E+02	9.51E+02 9.60E+02
BGI5	3.89E+04 4.19E+04	6.02E+03 6.01E+03	1.02E+04 1.03E+04	1.44E+03 1.41E+03	2.60E+03 2.56E+03
BGI10	9.45E+04 9.32E+04	7.53E+03 8.31E+03	2.48E+04 2.62E+04	1.86E+03 2.01E+03	6.35E+03 6.72E+03
BGI15	1.74E+04 1.81E+04	2.71E+04 2.57E+04	4.65E+04 4.77E+04	6.32E+03 6.83E+03	1.21E+04 1.22E+04
BEV4	4.63E+05 4.74E+05	6.69E+03 7.10E+03	1.48E+04 1.37E+04	3.08E+03 2.80E+03	5.29E+03 4.91E+03
C	2.84E+04 2.89E+04	3.53E+03 3.52E+03	6.89E+03 7.63E+03	9.43E+02 9.64E+02	1.54E+03 1.69E+03
CGT5	3.97E+04 3.83E+04	4.56E+03 4.09E+03	1.07E+04 1.15E+04	1.13E+03 1.18E+03	3.00E+03 2.76E+03
CGT10	5.01E+04 4.82E+04	6.94E+03 7.87E+03	1.56E+04 1.58E+04	2.68E+03 2.81E+03	4.70E+03 4.46E+03
CSB30	4.29E+04 3.80E+04	8.82E+03 8.95E+03	1.09E+04 1.18E+04	2.62E+03 2.66E+03	3.19E+03 3.05E+03
CSB45	7.07E+04 7.07E+04	1.19E+04 1.23E+04	2.10E+04 2.16E+04	3.92E+03 4.08E+03	6.35E+03 5.73E+03
CSE3	5.75E+04 4.25E+04	6.75E+03 6.88E+03	1.73E+04 1.28E+04	1.97E+03 1.84E+03	3.80E+03 2.81E+03
CSE5	1.00E+05 7.40E+04	1.32E+04 1.33E+04	3.11E+04 2.30E+04	3.77E+03 3.80E+03	7.48E+03 5.53E+03

Table A.2 Continued

Asphalt Type	10°C	20°C	30°C	40°C	50°C
	PAV20	PAV20	PAV20	PAV20	Unaged
CEV4	1.84E+07 1.36E+07	4.84E+06 3.57E+06	1.27E+06 9.35E+05	3.91E+05 2.89E+05	2.96E+04 2.64E+04
D	1.71E+07 1.72E+07	5.04E+06 4.96E+06	1.25E+06 1.25E+06	3.44E+05 2.90E+05	1.84E+04 1.90E+04
DGT5	1.78E+07 1.32E+07	4.95E+06 3.66E+06	1.38E+06 1.02E+06	3.05E+05 3.01E+05	3.49E+04 3.51E+04
DGT10	1.21E+07 1.23E+07	3.36E+06 3.41E+06	1.12E+06 8.25E+05	3.22E+05 2.38E+05	3.42E+04 3.41E+04
DGT15	1.10E+07 9.55E+06	3.13E+06 3.18E+06	8.99E+05 8.85E+05	2.49E+05 2.35E+05	4.75E+04 4.45E+04
DSB3	1.48E+07 1.47E+07	3.99E+06 3.97E+06	1.08E+06 1.01E+06	2.80E+05 2.57E+05	2.63E+04 2.65E+04

Asphalt Type	50°C	60°C	60°C	70°C	70°C
	TFO163°C	Unaged	TFO163°C	Unaged	TFO163°C
CEV4	1.06E+05 7.83E+04	9.73E+03 8.67E+03	3.28E+04 2.42E+04	4.44E+03 3.96E+03	1.09E+04 8.04E+03
D	3.47E+04 3.48E+04	4.63E+03 4.68E+03	9.52E+03 8.80E+03	1.27E+03 1.19E+03	2.35E+03 2.48E+03
DGT5	4.71E+04 4.75E+04	9.02E+03 9.23E+03	1.40E+04 1.42E+04	2.28E+03 2.39E+03	3.89E+03 3.79E+03
DGT10	5.83E+04 5.39E+04	1.04E+04 1.05E+04	1.60E+04 1.82E+04	3.00E+03 3.06E+03	4.79E+03 4.68E+03
DGT15	6.32E+04 6.80E+04	1.49E+04 1.54E+04	2.12E+04 2.12E+04	4.59E+03 5.12E+03	7.31E+03 7.28E+03
DSB3	4.12E+04 4.32E+04	6.48E+03 6.46E+03	1.29E+04 1.18E+04	1.73E+03 1.78E+03	3.32E+03 3.36E+03

Table A.3 Phase Angle(Degree) at 1.59 Hz(10 rad/sec)

Asphalt Type	10°C	20°C	30°C	40°C
	PAV20	PAV20	PAV20	PAV20
A	43 43	51 51	57 58	65 65
AGI5	37 37	45 45	52 52	59 59
AGI10	33 33	41 41	48 49	56 56
AGI15	29 29	37 37	44 44	52 51
B	39 39	48 48	56 51	64 63
BGI5	34 34	42 42	50 49	58 58
BGI10	31 30	39 38	46 46	54 54
BGI15	27 27	35 35	42 42	50 50
BEV4	35 35	42 42	50 50	57 57
C	37 37	46 47	55 55	63 63
CGT5	37 37	46 46	55 55	62 62
CGT10	38 34	47 42	54 54	59 60
CGT15	38 34	46 41	52 53	56 56
CSB15	36 36	45 45	54 55	65 59
CSB30	37 34	46 42	56 50	63 57

Table A.3 Continued

Asphalt Type	10°C	20°C	30°C	40°C
	PAV20	PAV20	PAV20	PAV20
CSB45	37 33	45 40	51 52	58 59
CSE3	33 34	42 43	49 51	55 58
CSE5	31 32	39 39	47 47	54 53
CEV4	36 32	43 39	55 49	57 56
D	36 35	44 44	53 53	62 63
DGT5	37 33	43 43	52 52	60 60
DGT10	36 33	44 40	54 48	58 59
DGT15	36 32	43 39	50 51	55 55
DSB3	36 36	45 45	54 54	61 61

Table A.3 Continued

Asphalt Type	50°C		60°C		70°C	
	Unaged	TFO163°C	Unaged	TFO163°C	Unaged	TFO163°C
A	83 83	80 79	86 86	84 84	90 90	88 88
AGI5	79 78	73 73	84 83	79 79	87 87	84 84
AGI10	75 73	67 67	79 79	74 73	84 84	80 79
AGI15	74 66	63 63	80 72	69 69	85 77	76 76
B	80 80	77 77	84 84	82 82	88 88	86 86
BGI5	76 74	70 70	81 81	76 76	85 85	82 82
BGI10	74 67	63 62	79 71	70 69	85 77	76 76
BGI15	65 66	58 57	71 71	65 64	78 78	72 71
BEV4	66 65	65 63	70 70	68 68	78 78	76 76
C	80 80	73 74	84 84	79 80	88 88	85 85
CGT5	75 74	67 68	79 80	73 73	84 84	79 79
CGT10	67 68	60 63	74 74	67 67	79 79	74 74
CGT15	60 60	57 57	65 65	62 62	70 70	69 69
CSB15	74 73	70 70	79 78	76 75	84 84	81 81
CSB30	68 69	69 63	73 73	74 67	83 76	81 73

Table A.3 Continued

Asphalt Type	50°C		60°C		70°C	
	Unaged	TFO 163°C	Unaged	TFO 163°C	Unaged	TFO 163°C
CSB45	64 64	63 62	67 67	69 62	79 72	77 69
CSE3	70 71	65 64	78 78	74 72	82 82	80 78
CSE5	64 62	57 56	70 69	66 65	73 73	71 69
CEV4	66 65	70 52	70 69	69 61	79 77	79 70
D	79 78	73 73	83 84	79 79	87 87	83 84
DGT5	72 69	67 66	76 77	73 72	82 82	79 79
DGT10	65 66	61 62	71 72	67 68	78 78	74 74
DGT15	60 60	58 60	65 66	61 61	72 72	67 67
DSB3	74 74	68 69	79 79	73 74	84 84	79 79

Table A.4 Penetration at 25°C

Asphalt Type	Original Binder	CTO-Aged 72 hrs	CTO-Aged 168 hrs	TFO-Aged 163 °C	TFO-Aged 185 °C	PAV-Aged 20 hr	PAV-Aged 40 hrs
A	162 161	42 48	34 38	99 87	79 82	50 49	42 44
AGI5	97 96	30 36	24.5 28.5	53 48	44 48	33 33	26 31.5
AGI10	61 58	24 26	23.5 16.5	36 34	31 34	22 23	22 17
AGI15	37 35	22 23	15 21.5	27 24	23 26	18 16	17 12.5
B	111 109	33 36	33 25	62 58	51 56	33 34	29 25
BGI5	65 59	29 28	27 21	41 38	34.5 39	26 24	22 18
BGI10	41 38	20 22	19 16.5	28 26	28.5 22.5	18 20	18 12.5
BGI15	29 26	18 18	13.5 17	20 18	15.5 22	13 14	8 13.5
BEV4	69 71	31 35	31 24.5	59 58	54.5 49	30 31	28 21
C	74 71	27 26	19.5 26.5	44 40	36 40	26 26	23 19
CGT5	64 58	28 27	28 19.5	43 40	34.5 41	24 26	26 20
CGT10	60 55	35 30.5	30.5 24.5	44 40	41.5 38.5	27 27	28 21
CGT15	53 50	34 38	29 33.5	39 39	42 34.5	27 26	28 23
CSB15	60 65	27 33	29.5 23	41 40	40 35.5	26 26	25 18
CSB30	57 60	28 35	22 33.5	60 57	47 56	27 26	20 24.5

Table A.4 - Continued

Asphalt Type	Original Binder	CTO-Aged 72 hrs	CTO-Aged 168 hrs	TFO-Aged 163 °C	TFO-Aged 185 °C	PAV-Aged 20 hrs	PAV-Aged 40 hrs
CSB45	73 76	33 36	34 26	59 53	56 45	45 41	28 18.5
CSE3	52 53	27 27	18 26	43 42	38 39	29 31	21 24
CSE5	35 40	24 22	23.5 16	33 35	35 27.5	28 28	26 17.5
CEV4	50 51	28 27	20 28	36 54	42.5 38.5	25 20	21 15
D	56 54	24 26	22 22	38 34	35.5 31	23 22	22 21
DGT5	50 48	29 30	28 20	33 33	35 29	24 25	25 22
DGT10	49 46	29 30	28 24	36 33	30 36.5	26 26	27.5 22
DGT15	46 42	32 33	32 25	39 35	41 30.5	26 28	30 22
DSB3	54 59	32 29	27 23	45 49	40.5 45	24 23	19 26

Table A.5 Schweyer Constant Power Viscosity at 5°C

Asphalt Type	Original Binder	CTO-Aged 72 hrs	CTO-Aged 168 hrs
A	3.417E+04 2.583E+04	8.828E+05 6.672E+05	1.002E+06 7.576E+05
AGI5	1.746E+05 1.054E+05	3.152E+06 1.902E+06	3.787E+06 2.286E+06
AGI10	6.928E+05 4.272E+05	4.627E+06 2.853E+06	7.246E+06 4.468E+06
AGI15	2.092E+06 1.628E+06	6.748E+06 5.252E+06	1.495E+07 1.163E+07
B	7.621E+04 7.379E+04	1.118E+06 1.082E+06	1.377E+06 1.333E+06
BGI5	3.767E+05 3.133E+05	2.359E+06 1.961E+06	3.691E+06 3.069E+06
BGI10	1.392E+06 6.381E+05	5.184E+06 2.376E+06	1.029E+07 4.719E+06
BGI15	4.232E+06 2.478E+06	1.198E+07 7.018E+06	2.810E+07 1.646E+07
BEV4	6.088E+05 5.312E+05	2.606E+06 2.274E+06	4.738E+06 4.134E+06
C	3.812E+05 3.188E+05	1.901E+06 1.590E+06	3.159E+06 2.642E+06
CGT5	7.415E+05 5.083E+05	3.559E+06 2.441E+06	5.982E+06 4.102E+06
CGT10	1.432E+06 9.880E+05	5.917E+06 4.083E+06	1.055E+07 7.278E+06
CGT15	2.140E+06 1.200E+06	1.153E+07 6.468E+06	1.838E+07 1.031E+07
CSB15	7.636E+05 4.364E+05	5.091E+06 2.909E+06	7.586E+06 4.335E+06
CSB30	1.077E+06 8.429E+05	6.732E+06 5.268E+06	1.021E+07 7.994E+06

Table A.5 Continued

Asphalt Type	TFO-Aged 163 °C	TFO-Aged 185 °C	PAV-Aged 20 hr	PAV-Aged 40 hrs
A	2.815E+05 2.128E+05	3.670E+05 2.774E+05	8.884E+05 6.716E+05	1.777E+06 1.343E+06
AGI5	9.931E+05 5.994E+05	1.447E+06 8.734E+05	4.604E+06 2.779E+06	5.670E+06 9.393E+06
AGI10	3.071E+06 1.894E+06	4.941E+06 3.047E+06	2.508E+07 1.547E+07	5.216E+07 3.217E+07
AGI15	3.874E+06 3.016E+06	9.731E+06 7.547E+06	9.261E+07 7.208E+07	1.963E+08 1.528E+08
B	2.713E+05 2.627E+05	4.542E+05 4.398E+05	1.943E+06 1.882E+06	3.812E+06 3.691E+06
BGI5	9.227E+05 7.673E+05	1.863E+06 1.549E+06	9.917E+06 8.247E+06	1.984E+07 1.650E+07
BGI10	3.648E+06 1.672E+06	7.256E+06 3.326E+06	4.467E+07 2.048E+07	9.113E+07 4.178E+07
BGI15	9.459E+06 5.541E+06	2.083E+07 1.220E+07	1.373E+08 8.044E+07	2.856E+08 1.673E+08
BEV4	1.025E+06 8.946E+05	2.530E+06 2.208E+06	1.290E+07 1.126E+07	2.607E+07 2.275E+07
C	1.071E+06 8.954E+05	1.947E+06 1.629E+06	8.920E+06 7.460E+06	1.606E+07 1.343E+07
CGT5	1.981E+06 1.359E+06	3.670E+06 2.516E+06	1.129E+07 7.739E+06	2.011E+07 1.379E+07
CGT10	3.077E+06 2.123E+06	6.305E+06 4.350E+06	2.106E+07 1.453E+07	3.677E+07 2.537E+07
CGT15	6.150E+06 3.450E+06	1.092E+07 6.128E+06	3.041E+07 1.706E+07	5.200E+07 2.917E+07
CSB15	3.415E+06 1.951E+06	5.154E+06 2945E+06	8.971E+06 5.126E+06	1.599E+07 9.135E+06
CSB30	4.313E+06 3.376E+06	6.741E+06 5.275E+06	1.138E+07 8.904E+06	2.007E+07 1.571E+07

Table A.5 Continued

Asphalt Type	Original Binder	CTO-Aged 72 hrs	CTO-Aged 168 hrs
CSB45	2.078E+06 1.202E+06	1.786E+07 1.034E+07	2.452E+07 1.418E+07
CSE3	1.640E+06 1.240E+06	5.012E+06 3.788E+06	1.053E+07 7.961E+06
CSE5	2.744E+06 1.656E+06	8.730E+06 5.270E+06	1.815E+07 1.095E+07
CEV4	2.437E+06 1.503E+06	1.052E+07 6.485E+06	1.880E+07 1.159E+07
D	4.499E+05 3.501E+05	5.252E+06 4.088E+06	6.737E+06 5.243E+06
DGT5	6.605E+05 6.395E+05	6.097E+06 5.903E+06	8.254E+06 7.993E+06
DGT10	1.267E+06 1.053E+06	8.735E+06 7.265E+06	1.283E+07 1.067E+07
DGT15	2.729E+06 1.251E+06	1.426E+07 6.538E+06	2.300E+07 1.054E+07
DSB3	6.937E+05 4.063E+05	7.025E+05 4.115E+06	9.292E+06 5.442E+06

Table A.5 Continued

Asphalt Type	TFO-Aged 163 °C	TFO-Aged 185 °C	PAV-Aged 20 hrs	PAV-Aged 40 hrs
CSB45	1.014E+07 5.864E+06	1.477E+07 8.546E+06	1.388E+07 8.027E+06	2.398E+07 1.387E+07
CSE3	2.677E+06 2.023E+06	6.525E+06 4.932E+06	2.980E+07 2.253E+07	5.472E+07 4.136E+07
CSE5	4.428E+06 2.672E+06	1.099E+07 6.634E+06	6.184E+07 3.732E+07	1.158E+08 6.987E+07
CEV4	5.567E+06 3.433E+06	1.134E+07 6.993E+06	3.365E+07 2.075E+07	6.178E+07 3.809E+07
D	1.687E+06 1.313E+06	2.713E+06 2.111E+06	9.987E+06 7.773E+06	1.705E+07 1.327E+07
DGT5	2.479E+06 2.401E+06	3.970E+06 3.844E+06	1.246E+07 1.207E+07	2.107E+07 2.040E+07
DGT10	4.619E+06 3.841E+06	7.449E+06 6.195E+06	1.968E+07 1.637E+07	3.260E+07 2.712E+07
DGT15	7.597E+06 3.483E+06	1.363E+07 6.250E+06	3.635E+07 1.666E+07	5.897E+07 2.703E+07
DSB3	2.561E+06 1.500E+06	4.127E+06 3.677E+06	2.153E+06 2.153E+06	6.153E+06 3.604E+06

Table A.6 Schweyer Constant Power Viscosity (Pa.sec) at 25°C

Asphalt Type	Original Binder	CTO-Aged 72 hrs	CTO-Aged 168 hrs
A	1.089E+07 6.109E+06	2.289E+08 1.411E+08	3.546E+08 2.949E+08
AGI5	8.655E+07 4.945E+07	4.834E+8 3.763E+08	8.369E+08 8.104E+08
AGI10	2.749E+08 2.151E+08	9.769E+08 7.384E+08	2.632E+09 2.189E+09
AGI15	4.878E+08 2.822E+08	1.977E+09 1.193E+09	9.985E+09 4.577E+09
B	2.335E+07 1.765E+07	4.813E+08 2.968E+08	9.861E+08 5.776E+08
BGI5	1.228E+08 7.415E+07	1.125E+09 8.754E+08	3.971E+09 1.821E+09
BGI10	3.216E+08 1.984E+08	1.966E+09 1.904E+09	1.005E+10 5.889E+09
BGI15	2.463E+09 2.057E+09	4.026E+09 3.348E+09	2.015 E10 1.758E+10
BEV4	9.055E+07 6.845E+07	9.126E+08 8.836E+08	3.473E+09 2.904E+09
C	1.933E+08 1.167E+08	1.140E+09 9.485E+08	3.968E+09 2.721E+09
CGT5	2.796E+08 1.724E+08	2.439E+09 1.118E+09	6.864E+09 4.736E+09
CGT10	3.915E+08 3.047E+08	3.638E+09 2.131E+09	1.314E+10 7.369E+09
CGT15	5.081E+08 4.919E+08	6.365E+09 2.918E+09	1.786E+10 1.020E+10
CSB15	2.341E+08 1.947E+08	2.243E+09 1.314E+09	5.401E+09 4.227E+09
CSB30	3.005E+08 2.909E+08	3.080E+09 2.688E+09	1.023E+10 5.917E+09

Table A.6 Continued

Asphalt Type	Original Binder	CTO-Aged 72 hrs	CTO-Aged 168 hrs
CSB45	4.389E+08 3.650E+08	5.055E+09 4.228E+09	1.277E+10 9.651E+09
CSE3	3.684E+08 1.689E+08	2.566E+09 1.753E+09	1.197E+10 7.226E+09
CSE5	5.854E+08 3.429E+08	5.087E+09 3.510E+09	2.369E+10 1.461E+10
CEV4	3.154E+08 1.446E+08	6.422E+09 3.602E+09	2.020E+10 1.572E+10
D	2.018E+08 1.182E+08	1.964E+09 1.122E+09	3.808E+09 2.878E+09
DGT5	3.845E+08 3.355E+08	4.137E+09 3.237E+09	1.105E+10 6.670E+09
DGT10	5.990E+08 5.010E+08	6.158E+09 3.563E+09	1.629E+10 1.004E+10
DGT15	1.097E+09 7.525E+80	7.526E+09 5.688E+09	2.310E+10 1.798E+10
DSB3	2.130E+08 1.470E+08	2.218E+09 1.339E+09	4.090E+09 3.961E+09

Table A.6 Continued

Asphalt Type	TFO-Aged 163 °C	TFO-Aged 185 °C	PAV-Aged 20 hr	PAV-Aged 40 hrs
A	2.563E+07 2.143E+07	5.446E+07 4.116E+07	2.411E+08 1.823E+08	1.044E+09 6.435E+08
AGI5	2.673E+08 1.833E+08	7.108E+08 4.291E+08	6.251E+08 3.773E+08	2.205E+09 1.716E+09
AGI10	4.199E+08 2.897E+08	1.245E+09 7.677E+08	1.384E+09 8.532E+08	4.347E+09 4.210E+09
AGI15	8.457E+08 4.743E+08	3.957E+09 3.080E+09	2.825E+09 2.199E+09	1.051E+10 8.738E+09
B	4.754E+07 2.717E+07	1.256E+08 9.491E+07	6.641E+08 5.020E+08	2.314E+09 2.241E+09
BGI5	3.646E+09 2.854E+08	1.679E+09 1.013E+09	1.677E+09 1.012E+09	5.654E+09 4.702E+09
BGI10	1.324E+09 7.660E+08	5.242E+09 3.233E+09	3.544E+09 2.186E+09	1.517E+10 6.954E+09
BGI15	7.404E+09 5.596E+09	3.626E+10 2.822E+10	6.821E+09 5.309E+09	2.979E+10 1.745E+10
BEV4	1.996E+08 1.204E+08	8.393E+08 8.127E+08	1.731E+09 1.676E+09	9.105E+09 4.174E+09
C	9.827E+07 6.060E+07	2.790E+08 2.320E+08	1.836E+09 1.527E+09	7.219E+09 4.229E+09
CGT5	5.061E+08 3.939E+08	1.633E+09 1.581E+09	2.726E+09 2.639E+09	2.807E+09 8.557E+09
CGT10	7.187E+08 5.432E+08	2.819E+09 2.344E+09	4.798E+09 3.990E+09	1.589E+10 1.329E+10
CGT15	1.137E+09 6.866E+08	4.146E+09 1.901E+09	9.740E+09 4.465E+09	2.755E+10 1.889E+10
CSB15	1.918E+08 1.182E+08	4.867E+08 2.850E+08	3.274E+09 1.918E+09	1.065E+10 7.352E+09
CSB30	3.093E+08 2.407E+08	9.972E+08 4.571E+08	5.792E+09 2.655E+09	1.868E+10 1.048E+10

Table A.6 Continued

Asphalt Type	TFO-Aged 163 °C	TFO-Aged 185 °C	PAV-Aged 20 hrs	PAV-Aged 40 hrs
CSB45	7.265E+08 7.035E+08	2.219E+09 1.300E+09	8.388E+09 4.913E+09	2.898E+10 1.656E+10
CSE3	5.472E+08 4.551E+08	2.764E+09 2.412E+09	3.777E+09 3.296E+09	1.368E+10 1.070E+10
CSE5	1.648E+09 1.596E+09	9.944E+09 8.317E+09	7.838E+09 6.556E+09	3.257E+10 1.884E+10
CEV4	6.388E+08 5.312E+08	2.704E+09 1.854E+09	8.483E+09 5.817E+09	2.915E+10 2.203E+10
D	3.445E+08 1.579E+08	8.495E+08 5.837E+08	2.693E+09 1.858E+09	9.109E+09 5.498E+09
DGT5	4.730E+08 2.770E+08	1.359E+09 7.621E+08	5.742E+09 3.221E+09	1.793E+10 1.106E+10
DGT10	8.653E+08 3.967E+08	2.301E+09 1.315E+09	7.619E+09 4.354E+09	2.113E+10 1.645E+10
DGT15	1.261E+09 7.387E+08	3.764E+09 2.946E+09	1.092E+10 8.546E+09	3.411E+10 2.579E+10
DSB3	4.166E+08 3.634E+08	1.424E+09 8.238E+08	2.170E+09 1.256E+09	6.921E+09 4.178E+09

Table A.7 Fraass Breaking Point Temperature (°C)

Asphalt Type	Original Binder	CTO-Aged 72 hrs	CTO-Aged 168 hrs	TFO-Aged 163 °C	TFO-Aged 185 °C	PAV-Aged 20 hr	PAV-Aged 40 hrs
A	-15.5 -15.0	-10.0 -11.0	-4.0 -8.0	-14.0 -12.0	-12.0 -10.0	-11.0 -9.0	-7.0 -4.0
AGI5	-13.0 -13.0	-7.5 -5.5	-3.0 -5.0	-8.0 -10.0	-7.0 -6.0	-8.0 -8.0	-5.0 -3.0
AGI10	-10.0 -12.0	-4.0 -4.0	-1.0 -4.0	-6.0 -8.0	-5.0 -3.0	-8.0 -6.0	-3.0 -1.0
AGI15	-9.0 -8.5	-2.0 -2.0	-2.0 0.0	-4.0 -6.0	-4.0 0.0	-6.0 -2.0	-1.0 0.0
B	-12.5 -13.5	-4.0 -4.0	-3.0 -1.0	-12.0 -13.0	-10.0 -9.0	-8.0 -10.0	-5.0 -3.0
BGI5	-12.5 -10.5	-3.0 -4.0	-3.5 -0.5	-8.0 -8.0	-6.0 -5.0	-7.0 -7.0	-2.0 -4.0
BGI10	-9.5 -10.0	-1.0 -4.0	-2.0 0.0	-8.0 -4.0	-4.0 -2.0	-4.0 -6.0	-2.0 0.0
BGI15	-6.0 -5.0	0.0 -3.0	-1.0 1.0	-2.0 -5.0	-3.0 0.0	-4.0 -2.0	0.0 1.0
BEV4	-13.5 -13.0	-6.0 -6.0	-4.0 -1.0	-10.0 -10.0	-9.0 -5.0	-9.0 -8.0	-4.0 -2.0
C	-11.5 -10.5	-4.0 -4.0	-1.0 -2.0	-8.0 -8.0	-7.0 -5.0	-4.0 -2.0	0.0 -2.0
CGT5	-12.0 -11.5	-8.0 -7.0	-5.0 -2.0	-10.0 -8.0	-9.0 -5.0	-5.0 -5.0	-5.0 -1.0
CGT10	-15.0 -11.0	-10.0 -8.0	-7.0 -4.0	-9.0 -11.0	-10.0 -7.0	-9.0 -5.0	-6.0 -3.0
CGT15	-15.0 -14.0	-10.0 -13.0	-6.0 -8.0	-12.0 -10.0	-8.0 -12.0	-8.0 -8.0	-5.0 -7.0
CSB15	-10.5 -11.5	-8.0 -8.0	-6.0 -3.0	-8.0 -8.0	-8.0 -5.0	-4.0 -6.0	-5.5 -0.5
CSB30	-13.0 -11.0	-11.0 -8.0	-7.0 -5.0	-8.0 -10.0	-8.0 -10.0	-6.0 -8.0	-3.0 -7.0

Table A.7 - Continued

Asphalt Type	Original Binder	CTO-Aged 72 hrs	CTO-Aged 168 hrs	TFO-Aged 163 °C	TFO-Aged 185 °C	PAV-Aged 20 hr	PAV-Aged 40 hrs
CSB45	-21.5 -20.5	-10.0 -13.0	-12.0 -6.0	-14.0 -12.0	-14.0 -10.0	-11.0 -8.0	-9.0 -5.0
CSE3	-9.0 -11.0	-6.0 -8.0	-4.0 -6.0	-8.0 -8.0	-7.0 -5.0	-3.0 -5.0	-4.0 -2.0
CSE5	-7.0 -11.0	-7.0 -4.0	-4.0 -1.0	-8.0 -4.0	-6.0 -4.0	-4.0 -2.0	-3.0 0.0
CEV4	-11.5 -10.0	-4.0 -4.0	1.0 -3.0	-8.0 -6.0	-6.0 -4.0	-5.0 -4.0	-4.0 -1.0
D	-9.5 -11.0	-4.0 -3.0	0.0 -2.0	-4.0 -8.0	-2.0 -6.0	-2.0 -2.0	1.0 -1.0
DGT5	-11.0 -10.0	-8.0 -5.0	-5.0 -3.0	-10.0 -6.0	-8.0 -5.0	-4.0 -2.0	-4.0 0.0
DGT10	-11.0 -12.0	-8.0 -10.0	-6.0 -8.0	-8.0 -12.0	-6.0 -10.0	-7.0 -6.0	-2.0 -6.0
DGT15	-11.0 -14.0	-12.0 -9.0	-10.0 -6.0	-14.0 -10.0	-12.0 -8.0	-7.0 -9.0	-8.0 -3.0
DSB3	-10.5 -10.5	-5.0 -3.0	-1.0 -3.0	-8.0 -6.0	-4.0 -6.0	-5.0 -1.0	0.0 -2.0

Table A.8 Creep Stiffness (MPa) of PAV 20 Hours Residue at -12°C and -24°C

Asphalt Type	At -12°C	At -24°C	Asphalt Type	At -12°C	At -24°C
A	39.73 39.38	247.20 211.10	CGT15	48.69 43.44	215.10 231.50
AGI5	61.53 55.63	314.60 303.40	CSB15	92.79 84.21	389.00 349.10
AGI10	88.40 82.33	389.60 369.20	CSB30	85.07 81.73	370.10 368.60
AGI15	120.50 122.20	461.60 463.80	CSB45	63.58 57.13	300.10 295.90
B	59.59 57.14	308.30 312.40	CSE3	116.20 106.50	393.02 407.52
BGI5	89.63 107.10	397.30 325.8	CSE5	109.90 117.10	500.72 528.31
BGI10	128.60 132.20	534.40 523.90	CEV4	118.40 108.70	438.30 430.00
BGI15	186.10 166.80	622.10 581.10	D	125.60 109.70	490.00 510.70
BEV4	70.51 71.26	316.10 337.80	DGT5	78.12 78.54	378.10 429.00
C	90.14 84.92	449.60 439.20	DGT10	77.44 66.43	366.20 337.00
CGT5	79.43 72.94	323.00 351.50	DGT15	62.81 56.03	274.30 299.80
CGT10	61.67 61.93	277.70 253.20	DSB3	96.54 93.47	505.70 464.10

Table A.9 The m-Value of PAV 20 Hours Residue at -12°C and -24°C

Asphalt Type	At -12°C	At -24°C	Asphalt Type	At -12°C	At -24°C
A	0.444 0.439	0.327 0.320	CGT15	0.385 0.394	0.303 0.300
AGI5	0.399 0.403	0.295 0.304	CSB15	0.370 0.376	0.263 0.232
AGI10	0.360 0.374	0.267 0.264	CSB30	0.368 0.378	0.250 0.249
AGI15	0.332 0.330	0.235 0.242	CSB45	0.370 0.375	0.255 0.256
B	0.413 0.399	0.294 0.291	CSE3	0.356 0.366	0.249 0.255
BGI5	0.370 0.369	0.261 0.214	CSE5	0.335 0.331	0.215 0.229
BGI10	0.336 0.343	0.230 0.242	CEV4	0.334 0.338	0.251 0.258
BGI15	0.303 0.310	0.226 0.216	D	0.357 0.362	0.237 0.252
BEV4	0.370 0.365	0.279 0.286	DGT5	0.378 0.354	0.276 0.258
C	0.377 0.377	0.266 0.270	DGT10	0.363 0.385	0.277 0.272
CGT5	0.371 0.380	0.296 0.285	DGT15	0.375 0.394	0.287 0.278
CGT10	0.380 0.385	0.288 0.285	DSB3	0.376 0.383	0.288 0.260

Table A.10 Results of Direct Tension Test at -12°C on PAV-20 hour-aged Asphalt Binders

Asphalt Type	Failure Strain (%)				Asphalt Type	Failure Strain (%)			
A	>5	>5	>5	>5	CGT15	>5	>5	>5	>5
AGI5	>5	>5	>5	>5	CSB15	>5	>5	>5	>5
AGI10	3.39	3.56	3.85	3.90	CSB30	>5	>5	>5	>5
AGI15	0.44	0.46	0.50	0.51	CSB45	>5	>5	>5	>5
B	>5	>5	>5	>5	CSE3	0.85	0.89	1.01	1.09
BGI5	1.39	1.46	1.58	1.60	CSE5	0.52	0.59	0.70	0.76
BGI10	0.32	0.34	0.37	0.37	CEV4	0.68	0.62	0.52	0.46
BGI15	0.3	0.3	0.3	0.3	D	1.34	1.32	1.30	1.29
BEV4	>5	>5	>5	>5	DGT5	1.66	1.57	1.47	1.45
C	2.52	2.41	2.23	2.20	DGT10	>5	>5	>5	>5
CGT5	>5	>5	>5	>5	DGT15	>5	>5	>5	>5
CGT10	>5	>5	>5	>5	DSB3	>5	>5	>5	>5

Table A.11 Penetration Viscosity Number [$PAV_{(25-60)}$]

Asphalt Type	UNAGED	CTO-Aged 72hrs	TFO-Aged 163°C	PAV-Aged 20 hr
A	-0.31 -0.91	0.33 0.54	-0.14 -0.50	-0.12 -0.05
AGI5	-0.34 -0.21	0.57 0.73	-0.10 -0.30	0.65 0.76
AGI10	-0.04 -0.54	0.72 1.02	0.14 -0.03	0.65 0.76
AGI15	-0.02 -0.40	1.37 1.45	0.51 0.26	1.28 1.11
B	-0.20 -0.69	0.41 0.47	-0.29 -0.44	-0.04 0.04
BGI5	-0.38 -0.28	0.47 0.38	0.15 0.02	0.75 0.60
BGI10	-0.02 -0.16	0.16 0.52	0.36 0.16	0.97 1.17
BGI15	0.54 0.18	-0.17 0.63	0.72 0.41	1.27 1.33
BEV4	-0.08 0.78	1.52 1.86	0.96 0.64	0.99 1.17
C	-0.07 -0.55	0.37 0.23	-0.21 -0.38	0.24 0.24
CGT5	0.21 0.03	0.96 0.43	0.03 -0.01	0.29 0.47
CGT10	0.52 0.37	0.85 1.01	0.64 0.51	0.88 0.93
CGT15	1.24 1.21	0.75 1.33	0.94 0.98	1.32 1.28
CSB15	0.24 0.44	0.59 1.45	-0.05 -0.02	0.45 0.36
CSB30	0.82 0.78	1.14 1.46	1.21 0.97	0.94 0.74

Table A.11 Continued

Asphalt Type	UNAGED	CTO-Aged 72hrs	TFO-Aged 163°C	PAV-Aged 20 hr
CSB45	1.68 2.25	1.84 1.28	1.50 1.81	2.01 1.79
CSE3	0.21 0.41	0.84 0.82	1.00 0.88	1.36 1.51
CSE5	0.49 0.71	1.08 0.84	0.56 0.65	1.89 1.92
CEV4	0.92 1.00	1.61 1.60	0.63 1.27	1.36 1.01
D	-0.27 -0.38	0.51 0.66	-0.15 -0.28	0.44 0.24
DGT5	-0.18 -0.36	0.70 0.56	-0.01 0.06	0.82 0.90
DGT10	0.52 0.22	0.77 0.91	0.61 0.52	1.15 1.18
DGT15	0.82 0.70	0.94 1.13	1.15 1.01	1.57 1.74
DSB3	0.81 1.58	1.21 1.13	0.76 0.95	0.66 0.67

Table A.12 Brookfield Viscosity Aging Index at 60°C

Asphalt Type	CTO-Aged 72 hrs	CTO-Aged 168 hrs	TFOT-Aged 163 °C	TFOT-Aged 185 °C	PAV-Aged 20 hr	PAV-Aged 40 hrs
A	17.81 23.11	79.12 85.53	2.81 3.21	5.54 7.69	8.37 12.13	23.59 27.02
AGI5	17.04 12.39	57.41 32.62	3.32 2.61	9.46 7.06	11.98 8.63	28.81 22.71
AGI10	11.73 16.83	24.92 40.12	3.17 3.40	7.76 8.32	12.59 15.50	33.74 36.21
AGI15	11.32 15.84	14.97 17.63	2.98 3.78	6.80 11.34	14.59 20.42	37.79 47.95
B	13.67 17.11	27.40 48.19	2.39 3.11	4.05 6.15	8.38 11.77	19.63 25.53
BGI5	8.80 6.63	25.85 20.51	3.56 2.70	5.50 3.15	14.48 10.95	27.22 20.64
BGI10	3.83 5.11	11.91 12.68	2.80 2.59	5.14 5.19	11.82 12.91	25.89 23.92
BGI15	0.96 3.09	4.86 6.77	2.31 3.40	5.44 6.71	9.37 11.09	22.77 23.58
BEV4	20.56 10.82	28.32 16.70	3.61 1.23	10.96 6.46	12.11 6.36	35.48 12.11
C	8.57 10.36	11.49 19.00	2.11 2.67	4.11 5.46	7.87 10.47	22.67 30.76
CGT5	6.55 5.28	8.50 8.38	1.58 1.73	4.25 3.96	5.40 5.91	21.53 20.05
CGT10	3.88 4.22	6.28 6.37	1.89 1.96	5.27 4.24	5.64 6.06	23.74 19.10
CGT15	1.28 1.84	2.70 3.19	1.26 1.21	3.13 2.61	3.63 3.43	12.05 12.70
CSB15	5.27 9.46	9.79 11.95	1.32 1.41	2.75 4.93	4.77 4.26	22.98 20.88
CSB30	4.83 5.23	8.27 5.86	1.35 1.32	3.97 4.29	4.13 3.99	20.01 23.15

Table A.12 Continued

Asphalt Type	CTO-Aged 72 hrs	CTO-Aged 168 hrs	TFO-Aged 163 °C	TFO-Aged 185 °C	PAV-Aged 20 hrs	PAV-Aged 40 hrs
CSB45	3.70 1.95	3.45 3.94	0.89 1.70	4.45 2.34	2.48 2.67	19.16 20.00
CSE3	5.82 4.83	9.31 7.92	3.12 2.42	3.82 3.17	9.21 8.20	32.81 27.73
CSE5	3.65 3.19	7.74 3.57	1.18 1.18	1.11 1.86	6.87 7.09	31.78 29.00
CEV4	5.86 5.92	8.14 6.79	1.28 1.20	5.08 5.73	5.44 5.18	14.56 16.41
D	8.99 9.94	19.47 23.14	2.08 2.29	3.92 4.39	8.97 8.09	21.09 22.94
DGT5	6.41 5.53	12.00 19.78	2.37 2.71	5.46 6.79	10.09 11.02	27.35 34.03
DGT10	3.50 3.87	8.48 8.40	2.05 2.13	5.23 5.35	6.71 6.69	25.60 26.66
DGT15	2.13 2.41	5.80 5.84	1.89 1.90	5.40 6.12	6.16 6.34	26.03 29.54
DSB3	2.76 2.86	4.34 4.75	0.94 0.95	2.72 3.04	2.47 2.56	4.94 4.54

Table A.13 Results of Infarared Spectral Analysis

Asphalt Type	Carbony1 Ratio			
	Original	CTO 72 hrs	TFO 163°C	PAV 20 hrs
A	0.3300 0.3377	0.6359 0.6195	0.4046 0.4027	0.5267 0.5128
AGI5	0.3650 0.3514	0.5951 0.5913	0.4212 0.4132	0.4999 0.4936
AGI10	0.3930 0.3947	0.5483 0.5525	0.4481 0.4151	0.4894 0.4886
AGI15	0.3964 0.3732	0.4748 0.4907	0.4273 0.4312	0.5021 0.4990
B	0.3072 0.3947	0.5483 0.5525	0.4481 0.4151	0.4894 0.4886
BGI5	0.3882 0.3604	0.5372 0.5467	0.4019 0.4093	0.4446 0.4435
BGI10	0.3707 0.3899	0.5373 0.5130	0.3954 0.4021	0.5523 0.5560
BGI15	0.3939 0.3855	0.4578 0.4305	0.4159 0.3958	0.5379 0.5342
BEV4	0.3482 0.3499	0.5202 0.5145	0.4068 0.3896	0.5792 0.6009
C	0.3363 0.3134	0.5353 0.5304	0.3734 0.3773	0.5814 0.5623
CGT5	0.3687 0.3171	0.5062 0.5057	0.3723 0.3560	0.5546 0.5474
CGT10	0.4184 0.3047	0.4502 0.4414	0.3820 0.3787	0.5135 0.5091

Table A.13 Continued

Asphalt Type	Carbonyl Ratio			
	Original	CTO 72 hrs	TFO 163°C	PAV 20 hrs
CGT15	0.3558 0.3011	0.3975 0.4120	0.3815 0.3659	0.5013 0.5022
CSB15	0.3611 0.3423	0.5532 0.5252	0.3401 0.3449	0.5037 0.5015
CSB30	0.3702 0.3774	0.5184 0.5049	0.3662 0.3981	0.5436 0.5395
CSB45	0.3813 0.3929	0.5463 0.4383	0.3955 0.4346	0.5031 0.4963
CSE3	0.3446 0.3697	0.5202 0.5250	0.3860 0.3820	0.4967 0.5136
CSE5	0.3716 0.3989	0.5884 0.5938	0.4173 0.4129	0.5639 0.5830
CEV4	0.3895 0.3695	0.5953 0.5947	0.3953 0.3707	0.5412 0.5364
D	0.3561 0.3224	0.4613 0.4641	0.3930 0.3902	0.5412 0.5292
DGT5	0.3671 0.3423	0.5517 0.6171	0.3804 0.3860	0.5112 0.5076
DGT10	0.3599 0.3224	0.5264 0.4888	0.3960 0.3924	0.4881 0.4787
DGT15	0.3487 0.3165	0.4489 0.4989	0.3990 0.4121	0.5100 0.4985
DSB3	0.3527 0.3430	0.5062 0.6240	0.3777 0.4036	0.5135 0.5075

Table B.1 Results of Gyratory Testing Machine

Unaged Mixes	Initial Compaction			
	Gyratory Shear (psi)	Bulk Density (pcf)	Air Void (%)	VMA (%)
AC-20	63.59	137.0	6.03	16.16
	58.42	137.8	5.49	15.68
	60.99	136.8	6.17	16.28
C-20+15%GTR	61.77	137.6	5.20	15.75
	64.73	137.6	5.23	15.77
	65.89	137.3	5.46	15.97
AC-20+3%SBR	56.55	140.5	2.23	14.00
	61.47	140.2	2.47	14.21
	62.55	141.0	1.91	13.72
AC-20+3%SEBS	61.94	139.4	3.37	14.67
	59.36	140.2	2.85	14.21
	57.92	140.2	2.83	14.19
AC-30	58.69	138.0	4.52	15.54
	59.51	136.9	5.24	16.18
	59.90	137.3	5.02	15.98
AC-30+10%GTR	63.05	137.0	5.63	16.12
	63.55	137.8	5.11	15.66
	63.55	138.1	4.87	15.45
AC-30+3%SBR	62.45	140.2	2.44	14.18
	58.83	139.4	3.01	14.69
	62.48	140.0	2.60	14.33

Table B.1 Continued

Unaged Mixes	Medium Compaction			
	Gyratory Shear (psi)	Bulk Density (pcf)	Air Void (%)	VMA (%)
AC-20	62.85	139.6	4.12	14.54
	68.48	139.4	4.34	14.65
	59.29	139.1	4.55	14.84
AC-20+15%GTR	69.44	141.6	2.51	13.35
	64.48	140.5	3.23	13.99
	65.89	141.2	2.78	13.59
AC-20+3%SBR	68.82	142.2	1.03	12.95
	64.38	141.7	1.38	13.25
	67.08	142.4	0.90	12.83
AC-20+3%SEBS	66.20	141.4	1.99	13.46
	54.62	141.9	1.62	13.12
	55.13	142.7	1.12	12.68
AC-30	48.28	139.5	3.45	14.59
	58.24	139.5	3.45	14.59
	61.42	140.3	2.91	14.11
AC-30+10%GTR	70.83	141.7	2.44	13.29
	69.41	141.6	2.48	13.33
	70.60	141.1	2.81	13.62
AC-30+3%SBR	68.65	142.1	1.15	13.05
	59.62	142.6	0.75	12.70
	73.96	142.4	0.93	12.86

Table B.1 Continued

Unaged Mixes	Ultimate Compaction			
	Gyratory Shear (psi)	Bulk Density (pcf)	Air Void (%)	VMA (%)
AC-20	56.15	141.5	2.94	13.40
	63.61	141.5	2.93	13.39
	64.89	141.1	3.18	13.62
AC-20+15%GTR	67.52	142.2	2.07	12.96
	63.88	141.8	2.37	13.23
	66.87	142.2	2.08	12.97
AC-20+3%SBR	48.53	142.6	0.78	12.73
	56.44	142.7	0.68	12.64
	48.22	143.3	0.26	12.27
AC-20+3%SEBS	70.00	142.9	0.98	12.56
	75.90	143.2	0.75	12.36
	77.39	143.0	0.87	12.46
AC-30	67.99	141.7	1.93	13.25
	63.00	140.3	2.92	14.12
	54.80	141.4	2.15	13.44
AC-30+10%GTR	54.86	142.2	2.07	12.96
	65.60	142.4	1.92	12.83
	69.78	142.6	1.80	12.73
AC-30+3%SBR	76.45	142.8	0.66	12.62
	71.66	143.0	0.47	12.45
	72.68	142.6	0.74	12.69

Table B.1 Continued

SHRP Long Term Oven Aging Mixes	Ultimate Compaction			
	Gyratory Shear (psi)	Bulk Density (pcf)	Air Void (%)	VMA (%)
AC-20	59.41	141.6	2.89	13.36
	56.06	141.0	3.27	13.70
	57.82	141.5	2.95	13.41
AC-20+15%GTR	35.65	140.1	3.49	14.22
	31.07	139.5	3.94	14.62
	42.02	138.3	4.72	15.32
AC-20+3%SBR	48.24	139.2	3.11	14.77
	47.97	138.9	3.37	15.00
	55.25	139.5	2.94	14.63
AC-20+3%SEBS	57.67	139.4	3.40	14.69
	60.16	138.0	4.31	15.50
	60.34	139.1	3.56	14.83
AC-30	56.42	141.3	3.86	14.50
	63.58	141.7	3.63	14.30
	55.99	141.0	4.08	14.70
AC-30+10%GTR	36.49	138.2	4.81	15.40
	44.00	141.0	3.61	14.30
	41.03	139.2	4.14	14.70
AC-30+3%SBR	46.26	138.0	3.97	15.53
	56.46	138.9	3.35	14.99
	45.17	138.5	3.63	15.23

Table B.2 Results of Loaded Wheel Test

Mix Type	Rut Depth (inch)			Bulk Density (pcf)	Air Void (%)
	At 1000 Cycles	At 4000 Cycles	At 8000 Cycles		
AC-20	0.146	0.238	0.304	131.9	9.51
	0.123	0.187	0.250		
	0.114	0.176	0.236		
	0.160	0.226	0.299	134.5	7.76
	0.159	0.197	0.259		
	0.174	0.236	0.311		
AC-20+15%GTR	0.129	0.182	0.220	127.7	12.04
	0.151	0.202	0.232		
	0.162	0.259	0.324		
	0.119	0.153	0.180	129.4	10.90
	0.120	0.150	0.188		
	0.137	0.183	0.226		
AC-20+3%SBR	0.106	0.163	0.183	132.6	7.72
	0.103	0.143	0.169		
	0.105	0.172	0.206		
	0.077	0.120	0.158	132.8	7.60
	0.074	0.112	0.142		
	0.091	0.154	0.204		
AC-20+3%SEBS	0.100	0.217	0.287	131.5	8.87
	0.100	0.187	0.224		
	0.096	0.186	0.231		
	0.068	0.186	0.230	131.9	8.59
	0.044	0.141	0.179		
	0.046	0.151	0.225		
AC-30	0.109	0.175	0.245	131.2	9.24
	0.123	0.208	0.260		
	0.126	0.200	0.283		
	0.093	0.170	0.301	133.7	7.45
	0.095	0.145	0.234		
	0.107	0.161	0.238		
AC-30+10%GTR	0.110	0.161	0.185	132.2	8.94
	0.092	0.142	0.159		
	0.097	0.167	0.209		
	0.151	0.208	0.255	130.0	10.46
	0.128	0.190	0.222		
	0.127	0.188	0.213		
AC-30+3%SBR	0.093	0.133	0.152	131.9	8.24
	0.091	0.128	0.149		
	0.104	0.151	0.209		
	0.091	0.131	0.144	132.9	7.54
	0.093	0.133	0.153		
	0.080	0.136	0.162		

Table B.3 Results of Diametral Resilient Modulus Tests

Unaged Initial Compaction	Total Diametral Resilient Modulus (GPa)			Poisson's Ratio		
	0°C	-10°C	-20°C	0°C	-10°C	-20°C
AC-20	10.91	13.82	20.22	0.22	0.22	0.27
	12.97	17.96	17.62	0.32	0.33	0.21
	12.76	16.09	19.47	0.30	0.30	0.26
AC-20+15%GTR	10.59	14.00	17.35	0.40	0.30	0.24
	11.26	15.64	18.15	0.35	0.32	0.26
	8.10	12.86	15.97	0.23	0.26	0.20
AC-20+3%SBR	8.28	15.74	23.17	0.29	0.42	0.37
	13.26	17.11	20.19	0.29	0.29	0.29
	15.73	18.39	22.31	0.46	0.32	0.36
AC-20+3%SEBS	12.30	19.06	22.72	0.24	0.35	0.35
	14.07	16.61	19.80	0.26	0.27	0.27
	12.51	18.35	21.88	0.29	0.33	0.34
AC-30	14.53	16.86	20.38	0.34	0.27	0.22
	13.42	17.20	18.71	0.34	0.27	0.21
	13.12	17.88	20.70	0.30	0.27	0.26
AC-30+10%GTR	12.21	14.86	17.74	0.38	0.27	0.24
	12.49	16.56	19.95	0.40	0.32	0.34
	13.38	16.38	17.47	0.34	0.30	0.19
AC-30+3%SBR	11.95	15.92	20.52	0.28	0.26	0.25
	13.38	17.25	17.88	0.26	0.23	0.20
	13.30	16.25	19.76	0.32	0.23	0.24

Table B.3 Continued

Unaged Medium Compaction	Total Diametral Resilient Modulus (GPa)			Poisson's Ratio		
	0°C	-10°C	-20°C	0°C	-10°C	-20°C
AC-20	13.11	18.58	20.38	0.23	0.29	0.49
	13.17	18.94	21.83	0.28	0.26	0.44
	13.10	17.15	19.60	0.24	0.21	0.48
AC-20+15%GTR	10.63	16.37	18.34	0.26	0.29	0.19
	10.33	15.50	19.17	0.26	0.24	0.18
	11.15	14.77	18.16	0.30	0.21	0.15
AC-20+3%SBR	11.70	18.77	21.05	0.33	0.34	0.29
	11.95	16.36	18.34	0.31	0.26	0.22
	12.23	18.08	20.26	0.28	0.33	0.28
AC-20+3%SEBS	14.86	19.06	24.29	0.37	0.29	0.32
	14.39	18.93	21.17	0.31	0.27	0.25
	13.98	20.66	23.39	0.33	0.37	0.31
AC-30	16.19	17.48	22.26	0.32	0.23	0.24
	15.68	18.43	19.40	0.41	0.26	0.19
	15.43	19.21	21.43	0.38	0.27	0.23
AC-30+10%GTR	14.57	16.96	20.53	0.30	0.22	0.21
	13.70	17.85	21.29	0.30	0.27	0.26
	11.73	16.36	18.49	0.21	0.29	0.19
AC-30+3%SBR	13.59	19.16	21.09	0.19	0.20	0.20
	13.16	17.04	20.10	0.25	0.23	0.23
	13.12	17.44	19.26	0.24	0.20	0.17

Table B.3 Continued

Unaged Ultimate Compaction	Total Diametral Resilient Modulus (GPa)			Poisson's Ratio		
	0°C	-10°C	-20°C	0°C	-10°C	-20°C
AC-20	16.99	21.06	23.72	0.36	0.32	0.28
	14.80	18.36	20.67	0.28	0.25	0.22
	16.36	20.28	22.83	0.34	0.31	0.27
AC-20+15%GTR	12.25	18.61	19.81	0.32	0.28	0.21
	10.68	17.42	19.79	0.25	0.31	0.24
	11.80	17.74	20.22	0.31	0.29	0.23
AC-20+3%SBR	11.91	16.31	20.27	0.37	0.30	0.24
	10.10	16.46	17.66	0.36	0.34	0.19
	13.90	17.48	19.52	0.26	0.18	0.23
AC-20+3%SEBS	16.54	20.72	25.63	0.35	0.31	0.30
	14.41	20.15	22.34	0.27	0.33	0.23
	15.93	19.38	24.68	0.34	0.28	0.29
AC-30	15.67	18.92	23.31	0.30	0.25	0.27
	14.68	18.11	20.31	0.26	0.25	0.21
	16.21	19.31	22.44	0.31	0.27	0.26
AC-30+10%GTR	14.22	16.96	20.29	0.29	0.24	0.23
	13.15	17.52	22.38	0.23	0.21	0.21
	15.55	19.43	22.83	0.30	0.24	0.25
AC-30+3%SBR	14.54	18.01	21.26	0.28	0.24	0.20
	15.58	19.75	23.54	0.44	0.33	0.26
	17.13	23.28	29.95	0.29	0.42	0.41

Table B.3 Continued

LTOA Ultimate Compaction	Total Diametral Resilient Modulus (GPa)			Poisson's Ratio		
	0°C	-10°C	-20°C	0°C	-10°C	-20°C
AC-20	17.11	20.41	24.42	0.24	0.25	0.26
	21.02	20.99	21.28	0.41	0.30	0.20
	23.35	22.95	23.51	0.45	0.35	0.25
AC-20+15%GTR	15.90	18.57	19.62	0.29	0.29	0.28
	15.30	16.22	17.03	0.31	0.30	0.18
	12.67	14.45	15.76	0.39	0.37	0.31
AC-20+3%SBR	19.19	22.29	25.00	0.37	0.39	0.38
	16.72	19.42	21.79	0.28	0.31	0.30
	18.47	21.46	24.07	0.35	0.38	0.37
AC-20+3%SEBS	18.16	19.62	22.15	0.35	0.40	0.36
	12.57	17.09	19.30	0.22	0.31	0.28
	16.93	18.89	21.32	0.37	0.39	0.35
AC-30	23.22	47.88	25.06	0.44	0.50	0.28
	18.33	41.73	25.96	0.30	0.50	0.28
	17.90	46.10	20.23	0.30	0.50	0.15
AC-30+10%GTR	9.66	19.57	19.46	0.41	0.23	0.19
	8.42	17.05	16.96	0.32	0.18	0.15
	9.30	18.84	18.74	0.39	0.22	0.18
AC-30+3%SBR	17.78	23.87	25.20	0.33	0.49	0.50
	15.49	20.80	21.96	0.26	0.38	0.50
	17.12	22.98	24.26	0.32	0.47	0.50

Table B.4 Results of Indirect Tensile Creep Tests

Mix Type	Compaction Condition	Test Temp (°C)	Poisson's Ratio	Creep Compliance at 1000 sec (1/psi)	Intercept (1/psi)	Slope (1/psi)	R^2
AC-20+ 15%GTR	Initial	0	0.46	1.77E-5	7.01E-6	1.08E-8	0.999
		-10	0.36	3.71E-6	1.85E-6	1.92E-9	0.996
		-20	0.20	1.41E-6	8.68E-7	5.69E-10	0.991
	Medium	0	0.20	1.71E-5	6.36E-6	1.09E-8	0.999
		-10	0.33	2.83E-6	1.48E-6	1.36E-9	0.999
		-20	0.16	1.19E-6	8.06E-7	3.97E-10	0.995
	Ultimate	0	0.15	1.40E-5	4.45E-6	9.51E-9	0.999
		-10	0.28	2.59E-6	1.22E-6	1.39E-9	0.999
		-20	0.22	1.02E-6	6.62E-7	3.66E-10	0.996
AC-30	Initial	0	0.31	8.13E-6	2.96E-6	5.26E-9	0.999
		-10	0.28	2.19E-6	1.10E-6	1.09E-9	0.999
		-20	0.17	8.33E-7	5.77E-7	2.63E-10	0.995
	Medium	0	0.40	4.87E-6	2.02E-6	2.86E-9	0.999
		-10	0.22	1.60E-6	9.54E-7	6.79E-10	0.987
		-20	0.30	7.08E-7	4.75E-7	2.35E-10	0.997
	Ultimate	0	0.23	4.94E-6	2.09E-6	2.88E-9	0.999
		-10	0.35	1.28E-6	8.30E-7	4.70E-10	0.996
		-20	0.30	6.23E-7	5.04E-7	1.18E-10	0.978
AC-30+ 10%GTR	Initial	0	0.47	1.07E-5	3.93E-6	6.74E-9	1.000
		-10	0.24	2.90E-6	1.53E-6	1.41E-9	0.996
		-20	0.23	8.78E-7	6.37E-7	2.52E-10	0.968
	Medium	0	0.27	9.91E-6	3.72E-6	6.25E-9	0.997
		-10	0.20	2.08E-6	1.28E-6	8.06E-10	0.994
		-20	0.23	8.13E-7	5.82E-7	2.38E-10	0.995
	Ultimate	0	0.32	8.47E-6	3.23E-6	5.28E-9	1.000
		-10	0.24	2.06E-6	1.10E-6	9.87E-10	0.998
		-20	0.14	7.65E-7	5.53E-7	2.18E-10	0.989

Table B.5 Results of Indirect Tensile Strength Test at -10°C

Mix Type	Initial Compaction				Medium Compaction			
	Strength (psi)		Air Void (%)		Strength (psi)		Air Void (%)	
AC-20	500 482 492		6.03 5.49 6.17		528 583 580		4.21 4.34 4.55	
AC-20+15%GTR	485 520 495		5.20 5.23 5.46		626 593 607		2.51 3.23 2.78	
AC-20+3%SBR	543 566 648		2.23 2.47 1.91		615 599 640		1.03 1.38 0.90	
AC-20+3%SEBS	568 605 520		3.37 2.85 2.83		639 634 618		1.99 1.62 1.12	
AC-30	524 527 412		4.52 5.24 5.02		546 551 514		3.45 3.45 2.91	
AC-30+10%GTR	503 498 546		5.63 5.11 4.87		611 602 611		2.44 2.48 2.81	
AC-30+3%SBR	596 570 624		2.44 3.01 2.60		614 688 677		1.15 0.75 0.93	

Mix Type	Unaged Ultimate Compaction				LTOA Ultimate Compaction			
	Strength (psi)		Air Void (%)		Strength (psi)		Air Void (%)	
AC-20	607 601 595		2.94 2.93 3.18		500 500 498		2.89 3.27 2.95	
AC-20+15%GTR	595 605 618		2.07 2.37 2.08		501 455 371		3.49 3.94 4.72	
AC-20+3%SBR	641 637 707		0.78 0.68 0.26		382 418 444		3.11 3.37 2.94	
AC-20+3%SEBS	695 635 658		0.98 0.75 0.87		417 324 415		3.40 4.31 3.56	
AC-30	589 601 616		1.93 2.92 2.15		519 515 316		3.86 3.63 4.08	
AC-30+10%GTR	645 606 602		2.07 1.92 1.80		202 433 304		4.81 3.61 4.14	
AC-30+3%SBR	589 652 616		0.66 0.47 0.74		281 436 355		3.97 3.35 3.63	

Table B.6 Results of Tests on Recovered Binders

Asphalt Residue	Penetration at 25°C (0.1mm)	Brookfield Viscosity (poise)			
		60°C	80°C	100°C	120°C
AC-20	17	339883	20172	2029	312
AC-20+15%GTR	10	---	---	---	---
AC-20+3%SBR	17	---	---	182932	4660
AC-20+3%SEBS	14	---	---	---	130836
AC-30	16	---	87309	6879	839
AC-30+10%GTR	15	---	---	79722	15424
AC-30+3%SBR	15	---	---	184497	44983

REFERENCES

1. Paterson, W.D.O., "Road Deterioration and Maintenance Effects: Models for Planning and Management," The Highway Design and Maintenance Standards Series, A World Bank Publication, The Johns Hopkins University Press, Baltimore and London, 1987.

2. OECD Scientific Expert Group, "Heavy Trucks, Climate and Pavement Damage," Road Transport Research, Organization for Economic Cooperation and Development, Paris, 1988.

3. Vinson, T. S., Janoo, V. C., and Haas, R. C.G., "Summary Report: Low Temperature and Thermal Fatigue Cracking," SHRP - A/IR - 90 -001, SR-OSU-A-003A-89-1, June 1989.

4. Sugaware, T., and Moriyoshi, A., "Thermal Fracture of Bituminous Mixtures," Proceedings, Paving in Cold Areas Mini-Workshop, Lexington, Kentucky, 1984.

5. Ruth, B.E., Scherocman, J.A., and Carroll, J.J., "Evaluation of FDOT Specifications and Procedures for Asphalt Mixtures in Relation to Pavement Rutting under Heavy Traffic Conditions," Final Report to FDOT, State Project No.99700-7405-010, UF Project No. 4910450421412, Department of Civil Engineering, University of Florida, Gainesville, March 1989.

6. Hofstra, A., and Klomp, A.J.G., "Permanent Deformation of Flexible Pavements Under Simulated Road Traffic Conditions," Proceedings, Third International Conference on the Structural Design of Asphalt Pavements, Vol. I, London, 1972, pp. 613-621.

7. Eisenmann, J., and Hilmer, A., "Influence of Wheel Load and Inflation Pressure on the Rutting Effect at Asphalt-Pavements - Experiments and Theoretical Investigations," Proceedings, Sixth International Conference on the Structural Design of Asphalt Pavements, Vol. I, Ann Arbor, 1987, pp. 392-403.

8. Highway Research Board, "The AASHO Road Test," Special Report 73, Publication No. 1012, Washington, D.C., 1962.

9. Committee on Characteristics of Bituminous Materials, "Low Temperature Properties of Paving Asphalt Cements," State-of -the -Art Report 7, Transportation Research Board, Washington, D.C., 1988.

10. Brown, S.F., and Pell, P.S., "Repeated Loading of Bituminous Materials," CAPSA 74, National Institute for Road Research, Republic of South Africa, Durban, 1974.

11. Uge, P. and van de Loo, P.J., "Permanent Deformation of Asphalt Mixes," Koninklijke / Shell-Laboratorium, Amsterdam, November 1974.

12. Davis, R., "Large Stone Mixes: An Historical Insight," IS-103, National Asphalt Paving Association, 1988.

13. Mahboub, K. and Little, D.N., " Improved Asphalt Concrete Design Procedure," Research Report 474-1F, Texas Transportation Institute, 1988.

14. Monismith, C.L., Epps, J.A. and Finn, F.N., "Improved Asphalt Mix Design," Proceedings, The Association of Asphalt Paving Technologists, Vol. 54, 1985, pp. 347-406.

15. Monismith, C.L. and Tayebali, A.A., "Permanent Deformation (Rutting) Considerations in Asphalt Concrete Pavement Sections," Proceedings, The Association of Asphalt Paving Technologists, Vol. 57, 1988, pp. 414-463.

16. Cooper, K.E., Brown, S.F. and Pooley, G.R., "The Design of Aggregate Gradings for Asphalt Basecourses," Proceedings, The Association of Asphalt Paving Technologists, Vol. 54, 1985, pp. 324-346.

17. Linden, F. and Van der Heide, J., "Some Aspects of the Compaction of Asphalt Mixes and Its Influence on Mix Properties," Proceedings, The Association of Asphalt Paving Technologists, Vol. 56, 1987, pp. 408-426.

18. Von Quintus, H.L., Scherocman, J.A., Hunghes, C.S. and Kennedy, T.W., "Development of Asphalt-Aggregate Mixture Analysis System: AAMAS, Phase II - Volume I," Preliminary Draft Final Report, Brent Rauhut Engineering Inc., Austin, TX, 1988.

19. Vallerga, B.A. and Zube, E., "An Investigation of Design Methods for Asphaltic Paving Mixtures," Proceedings, American Society for Testing Materials, Vol. 53, 1953, pp. 1079-1102.

20. Bonnot, J., "Asphalt Aggregate Mixtures," Transportation Research Record 1096, Transportation Research Board, 1986, pp. 42-51.

21. Vallerga, B.A., Monismith, C.L. and Tayebali, A.A., "Early Rutting of Asphalt Concrete in a Hot Desert Environment - A Case History," 68th Annual Meeting of the Transportation Research Board, Washington, D.C., January 1989.

22. King, G.N., King, H.W., Harders, O., Chavenot, P. and Planche, J., "Influence of Asphalt Grade and Polymer Concentration on the High Temperature Performance of Polymer Modified Aspahlt," Proceedings, The Association of Asphalt Paving Technologists, Vol. 61, 1992, pp. 29-66.

23. Haas, R., Thompson, E., Meyer, F. and Tessier, G.R., "The Role of Additives in Asphalt Paving Technology," Proceedings, The Association of Asphalt Paving Technologists, Vol. 52, 1983, pp. 324-345.

24. Button, J.W., "Summary of Asphalt Additive Performance at Selected Sites," 71st Annual Meeting of Transportation Research Board, Washington, D.C., January 1992.

25. Brule, B., Brion, Y. and Tanguy, A., "Paving Asphalt Polymer Blends: Relationships between Composition, Structure and Properties," Proceedings, The Association of Asphalt Paving Technologists, Vol. 57, 1988, pp. 41-64.

26. Huang, S.C., "Development of Criteria for Durability of Modified Asphalts," Ph.D. Dissertation, University of Florida, 1994

27. Kinloch, A.J. and Young, R.J., "Fracture Behaviour of Polymers," Elsevier Applied Science Publishers Ltd., Washington, D.C., 1983.

28. Charrier, J., "Polymeric Materials and Processing - Plastics, Elastomers and Composites," Hanser Publishers, New York, 1991.

29. Verhaeghe, B.M.J.A., Rust, F.C., Vos, R.M. and Visser, A.T., "Properties of Polymer- and Fibre-Modified Porous Asphalt Mixes," 6th Conference on Asphalt Pavements for Southern Africa - Proceedings, Volume 1,Cape Town, South Africa, October 1994, pp. III-262-280.

30. Collins, J.H. and Mikols, W.J., "Block Copolymer Modification of Asphalt Intended for Surface Dressing Application," Proceedings, The Association of Asphalt Paving Technologists, Vol. 54, 1985, pp. 1-17.

31. Rempp, P. and Merrill, E.W., "Polymer Synthesis," Basel Heidelberg, New York, 1986.

32. Collins, J.H., Bouldin, M.G., Gellens, R. and Berker, A., "Improved Performance of Paving Asphalts by Polymer Modification," Proceedings, The Association of Asphalt Paving Technologists, Vol. 60, 1991, pp. 43-79.

33. Armijo, J.D., "Assessing the Effects of Commerical Modifiers on Montana Asphalts by Conventional Testing Methods," 72st Annual Meeting of Transportation Research Board, Washington D.C., January 1993.

34. Chehovits, J.G., Dunning, R.L. and Morris G.R., "Characteristics of Asphalt-Rubber by the Sliding Plate Microviscometer," Proceedings, The Association of Asphalt Paving Technologists, Vol. 51, 1982, pp. 240-261.

35. Kortschot, M. and Woodhams, R.T., "Torsional Braid Analysis of Bitumen-Liquid Rubbber Mixtures," Polymer Engineering and Science, March 1984, pp. 252-258.

36. Scofield, L.A., " The History, Development, and Performance of Asphalt Rubber at ADOT," Special Report, Report Number AZ-SP-8902, Arizona Department of Transportation, Materials Section, Phoenix, AZ, December 1989.

37. Huffman, J.E., " The Use of Ground Vulcanized Rubber in Asphalt, Asphalt Pavement Construction: New Materials and Techniques," American Society for Testing and Materials, Special Technical Publication 724, 1980, pp. 3-12.

38. Vallerga, B.A. and Bagley, J.R., "Design of Asphalt-Rubber Single Surface Treatments with Multilayered Aggregate Structure," American Society for Testing and Materials, Special Technical Publication 724, 1980, pp. 22-38.

39. Lalwani, S., Abushihada, A. and Halasa, A., "Reclaimed Rubber-Asphalt Blends Measurement of Rheological Properties to Assess Toughness, Resiliency, Consistency and Temperature Sensitivity," Proceedings, The Association of Asphalt Paving Technologists, Vol. 51, 1982, pp. 562-579.

40. "More Solution to Sticky Problems - A Guide to Getting More from your Brookfield Viscometer," Brookfield Engineering Laboratories, INC., New York, 1988.

41. Tia, M. and B.E. Ruth, "Basic Rheology and Rheological Concepts Established by H.E. Schweyer," Asphalt Rheology: Relationship to Mixture, ASTM STP 941, O.E. Briscoe, Ed., American Society for Testing and Materials, Philadelphia, PA, 1987, pp.118-145.

42. Thenoux, G., Lees, G. and Bell, C.A., "Laboratory Investigation of the Fraass Brittle Test," Journal of the Association of Asphalt Paving Technologists, Vol. 54, 1985, pp.529-550.

43. "Standard Test Method for Determining the Flexural Creep Stiffness of Asphalt Binder Using the Bending Beam Rheometer (BBR)," AASHTO Designation: TP1 - Edition 1A, American Association of State Highway and Transportation Officials Provisional Standard, August 1993.

44. "Background of SHRP Asphalt Binder Test Methods - Lecture Notes," National Asphalt Training Center, Demonstration Project 101, Asphalt Institute Research Center, Lexington ,KY, September 1993, pp.1-35.

45. "Standard Test Method for Determining the Rheological Properties of Asphalt Binder Using a Dynamic Shear Rheometer (DSR)," AASHTO Designation: TP5 - Edition 1A, American Association of State Highway and Transportation Officials Provisional Standard, August 1993.

46. "Standard Test Method for Determining the Fracture Properties of Asphalt Binder in Direct Tension (DT)," AASHTO Designation: TP3 - Edition 1A, American Association of State Highway and Transportation Officials Provisional Standard, August 1993.

47. "Users Manual - Model 1600 FT-IR," Perkin Elmer, April 1989, Norwalk, CT.

48. "Method for Determining Asphalt Durability Using the California Tilt-Oven Durability Test," California Test 374, November 1983.

49. "Standard Practice for Accelerated Aging of Asphalt Binder Using a Pressurized Aging Vessel (PAV)," AASHTO Designation: PP1 - Edition 1A, American Association of State Highway and Transportation Officials Provisional Standard, August 1993.

50. Bell, C. A., Sosnovske, D. and Kliewer, J. E., "Relating Asphalt and Aggregate Properties and Their Laboratory Aging to Field Performance of Asphalt Mixtures," 73rd Annual Meeting of Transportation Research Board, Washington, D.C., January 1994.

51. Roque, R. and W. G. Buttlar, "The Development of a Measurement and Analysis System to Accurately Determine Asphalt Concrete Properties Using the Indirect Tensile Mode," Journal of the Association of Asphalt Paving Technologists, Vol. 61, 1992, pp.304-332.

52. Buttlar, W. G. and R. Roque,"Experimental Development and Evaluation of the New SHRP Measurement and Analysis System for Indirect Tensile Testing at Low Temperatures," Transportation Research Record, No. 1454, pp.163-171, 1994.

53. Buttlar, W. G, "Relationships Between Asphalt Binder and Mixture Stiffness at Low Temperatures for the Control of Thermal Cracking Pavement Performance," Ph.D. Dissertation, The Pennsylvania State University, University Park, PA, 1996.

54. "Test Method for Determining the Creep Compliance and Strength of Hot Mix Asphalt (HMA) Using the Indirect Tensile Test Device," AASHTO Designation: TP9-94 Edition 1B, American Association of State Highway and Transportation Officials Provisional Standard, March 1995.

55. Lai, J. S., "Development of a Laboratory Rutting Resistance Testing Method for Asphalt Mixes," Final Report, Materials and Research, Georgia Department of Transportation, August 1989.

56. Lai, J. S., "User's Manual, Georgia Loader Wheel Tester and Rolling Compactor," School of Civil Engineering, Georgia Institute of Technology, Atlanta, GA, October 1994.

57. "Standard Test Method for Quantitative Extraction of Bitumen from Bituminous Paving Mixtures," ASTM D2172-81, Annual Book of ASTM Standards, Vol. 04.03, 1990.

58. "Standard Test Method for Recovery of Asphalt from Solution by Abson Method," ASTM D1856-79, Annual Book of ASTM Standards, Vol. 04.03, 1990.

59. "Standard Test Method for Recovery of Asphalt from Solution by Using the Rotavapor Apparatus," Florida Department of Transportation, Draft 9, January 24, 1992.

BIOGRAPHICAL SKETCH

Chuang-Tsair Shih was born on June 22, 1963, in Kaohsiung, Taiwan, where he attended elemental, secondary and high schools. He received his high school diploma in June 1981. In June 1986, he received a Bachelor of Science degree in civil engineering from Fengchia University, Taichung, Taiwan. He started his graduate study at the University of Florida in January 1988. He received his Master of Science degree in civil engineering in August 1989. He started his Ph.D. program in the field of civil engineering materials in 1990.

I certify that I have read this study and that in my opinion it conforms to acceptable standards of scholarly presentation and is fully adequate, in scope and quality, as a dissertation for the degree of Doctor of Philosophy.

Mang Tia

Mang Tia, Chairman
Professor of Civil Engineering

I certify that I have read this study and that in my opinion it conforms to acceptable standards of scholarly presentation and is fully adequate, in scope and quality, as a dissertation for the degree of Doctor of Philosophy.

Byron E. Ruth

Byron E. Ruth, Cochairman
Professor of Civil Engineering

I certify that I have read this study and that in my opinion it conforms to acceptable standards of scholarly presentation and is fully adequate, in scope and quality, as a dissertation for the degree of Doctor of Philosophy.

Reynaldo Roque

Reynaldo Roque
Associate Professor of Civil Engineering

I certify that I have read this study and that in my opinion it conforms to acceptable standards of scholarly presentation and is fully adequate, in scope and quality, as a dissertation for the degree of Doctor of Philosophy.

David Bloomquist
Associate Professor of Civil Engineering

I certify that I have read this study and that in my opinion it conforms to acceptable standards of scholarly presentation and is fully adequate, in scope and quality, as a dissertation for the degree of Doctor of Philosophy.

Mark C. K. Yang
Professor of Statistics

This dissertation was submitted to the Graduate Faculty of the College of Engineering and to the Graduate School and was accepted as partial fulfillment of the requirements for the degree of Doctor of Philosophy.

December, 1996

Winfred M. Phillips
Dean, College of Engineering

Karen A. Holbrook
Dean, Graduate School